

# The role of the Arg1/eNOS/sGC pathway in red blood cells *in vivo*

Inaugural-Dissertation

zur Erlangung des Doktorgrades  
der Mathematisch-Naturwissenschaftlichen Fakultät  
der Heinrich-Heine-Universität Düsseldorf

vorgelegt von

**Sophia Katharina Heuser**

aus Bonn, Deutschland

Düsseldorf, Januar 2024

aus dem Labor für experimentelle Herzinfarktforschung, Klinik für Kardiologie, Pneumologie und Angiologie der Heinrich-Heine-Universität Düsseldorf

druckt mit der Genehmigung der  
Mathematisch-Naturwissenschaftlichen Fakultät der  
Heinrich-Heine-Universität Düsseldorf

Berichterstatter:

1. Univ.-Prof. Dr. Dr. rer. nat. Miriam M. Cortese-Krott
2. Univ.-Prof. Dr. rer. nat. Axel Gödecke

Tag der mündlichen Prüfung: 29.02.2024

Ich versichere an Eides Statt, dass die Dissertation von mir selbständig und ohne unzulässige fremde Hilfe unter Beachtung der „Grundsätze zur Sicherung guter wissenschaftlicher Praxis an der Heinrich-Heine-Universität Düsseldorf“ erstellt worden ist.

Diese Dissertation wurde in gleicher oder ähnlicher Form in keinem anderen Prüfungsverfahren eingereicht.

Düsseldorf den

Sophia Katharina Heuser



To my family

## Zusammenfassung

**Hintergrund und Hypothese:** Die endotheliale Stickstoffmonoxid-Synthase (eNOS) exprimiert in Endothelzellen (EC) reguliert den Gefäßtonus und Blutdruck (BP) durch die Synthese von Stickstoffmonoxid (NO) und die nachfolgende Aktivierung von der löslichen Guanylatzyklase (sGC) und Proteinkinase G. Desweiteren ist das Enzym Arginase 1 (Arg1) in ECs exprimiert und nutzt L-Arginin als Substrat, wie eNOS. Vor Kurzem wurde entdeckt, dass Erythrozyten (RBCs) auch eNOS exprimieren und zur BP-Regulierung beiträgt. Auch Arg1 und sGC ist in RBCs exprimiert. Diese Studie stellte die Hypothese auf, dass der Arg1/eNOS/sGC Stoffwechselweg in RBCs eine essenzielle Rolle in RBCs *in vivo* spielt.

**Ziel der Studie:** Ziel dieser Studie war es, die Arg1/eNOS/sGC-Signalweg in RBCs *in vivo* mit Hilfe von transgenen Mausmodellen zu untersuchen. Die drei Hauptziele dieser Studie waren (1) die Analyse der NO-Signalübertragung in den ECs von EC-spezifischen Arg1 knock-out (KO)-Mäusen, (2) die Untersuchung der Rolle von RBC Arg1 durch die Erzeugung von RBC Arg1 KO-Mäusen und (3) die Untersuchung der Rolle der sGC in RBCs mittels RBC sGC KO-Mäusen.

**Methoden:** Mithilfe des Cre/LoxP-Systems wurden EC- und RBC-spezifische Arg1 KO und RBC sGC KO-Modelle erstellt. Die Spezifität des Gen-Targetings wurde bestätigt durch Messung von mRNA-Expression und der Proteinlevel. Gefäßfunktion, systemische Hämodynamik und NO-Metaboliten wurden untersucht, und es wurden Blutbilder erstellt. Differenzierung von erythroide Vorläuferzellen und der Prozentuale Anteil von Retikulozyten wurde analysiert. *Colony Forming Unit*-Assays wurden in Knochenmark und Milz ausgeführt.

**Ergebnisse:** Die zellspezifische Deletion des Zielgens wurde in allen drei Mauslinien erreicht. EC Arg1 KO-Mäuse zeigten eine reduzierte eNOS-Expression in der Aorta, welche weder die vaskuläre Funktion, den BP noch NO Metabolite beeinflusste. RBC Arg1 KO-Mäuse zeigten keine Veränderung der Gefäßfunktion, BP und der Erythropoese. RBC sGC KO-Mäuse hingegen zeigten eine verminderte Erythropoese im Knochenmark, Stress-Erythropoese in der Milz jedoch ein unverändertes Blutbild.

**Zusammenfassung und Schlussfolgerung:** Die Studie zeigte, dass die Beziehung zwischen eNOS und Arg1 sowohl in EC wie auch in RBCs anderes ist als erwartet. Das Entfernen von Arg1 in EC oder RBCs hatte keinen positiven Effekt auf den Gefäßtonus oder den BP, auch die L-Arginin Bioverfügbarkeit wurde nicht verbessert. Jedoch beeinflusst Arg1 aus RBCs die Konzentration von NO-Metaboliten in RBC und Plasma. Arg1 exprimiert in erythroide Vorläuferzellen beeinflusst nicht die Erythropoese. Jedoch zeigte die Studie, dass sGC in RBCs eine essenzielle Rolle in Erythropoese im Knochenmark, aber nicht in der Milz spielt.

## Summary

**Background and hypothesis:** Endothelial nitric oxide synthase (eNOS), expressed in endothelial cells (ECs), regulates vascular tone and blood pressure (BP) through the synthesis of nitric oxide (NO) and the subsequent activation of soluble guanylate cyclase (sGC) and downstream enzymes. Furthermore, the enzyme arginase 1 (Arg1) is expressed in ECs and uses L-arginine as a substrate, like eNOS. Recently, it was discovered that red blood cells (RBCs) also express eNOS, which contributes to the regulation of BP. RBCs also express Arg1 and sGC. This study hypothesized that the Arg1/eNOS/sGC pathway plays an essential role in RBCs *in vivo*.

**Aim of the study:** The aim of this study was to investigate Arg1/eNOS/sGC in RBCs *in vivo* using transgenic mouse models. The three main goals of this study were (1) to analyze NO signaling in the ECs of EC-specific Arg1 knock-out (KO) mice, (2) to investigate the role of RBC Arg1 by generating RBC Arg1 KO mice, and (3) to investigate the role of sGC in RBCs using RBC sGC KO mice.

**Methods:** EC- or RBC-specific Arg1 KO and RBC sGC KO mice models were generated using the Cre/LoxP system. The specificity of gene targeting was confirmed by measurement of mRNA expression of protein levels. Vascular function, systemic hemodynamics, NO metabolites, and blood counts were measured. The differentiation of erythroid progenitor cells and the percentage of reticulocytes were analyzed. Colony-forming unit assays were performed in the bone marrow and spleen of the mice.

**Results:** Cell-specific deletion of the target gene was achieved in all three mouse lines. EC Arg1 KO mice showed reduced eNOS expression in the aorta and preserved vascular function, BP, or NO metabolites. RBC Arg1 KO mice showed no changes in vascular function, BP, or erythropoiesis. In contrast, RBC sGC KO mice showed decreased erythropoiesis in the bone marrow, stress erythropoiesis in the spleen, and preserved hematocrit.

**Summary and conclusion:** This study showed that the relationship between eNOS and Arg1 is different than expected in both EC and RBCs. Removing Arg1 in EC or RBCs had no positive effect on vascular tone or BP, nor did it improve L-arginine bioavailability or cardioprotection. However, Arg1 from RBCs affects the levels of NO metabolites in RBCs and plasma. Arg1 expression in erythroid progenitor cells does not affect erythropoiesis. Finally, the study showed that sGC in RBCs plays an essential role in erythropoiesis in the bone marrow, but not in the spleen.

## Table of contents

<b>Zusammenfassung</b> .....	<b>V</b>
<b>Summary</b> .....	<b>VI</b>
<b>List of all figures</b> .....	<b>XI</b>
<b>List of all tables</b> .....	<b>XII</b>
<b>Abbreviations</b> .....	<b>XIV</b>
<b>1 Introduction</b> .....	<b>1</b>
<b>1.1 Nitric oxide and its metabolism</b> .....	<b>1</b>
1.1.1 The role of the eNOS/sGC pathway in the regulation of vascular function and systemic hemodynamics.....	1
1.1.2 The role of arginase as a counterpart of NOS enzymes.....	3
<b>1.2 The RBC</b> .....	<b>3</b>
1.2.1 Erythropoiesis.....	4
1.2.2 Stress erythropoiesis.....	5
1.2.3 The discovery of the Arg1/eNOS/sGC pathway in RBCs.....	7
1.2.4 The role of the eNOS/sGC pathway in erythropoiesis and globin expression.....	7
<b>2 Aim of the study</b> .....	<b>9</b>
<b>3 Materials and Methods</b> .....	<b>11</b>
<b>3.1 Material</b> .....	<b>11</b>
<b>3.2 Animals</b> .....	<b>15</b>
3.2.1 Generation of EC Arg1 KO mice.....	15
3.2.2 Generation of RBC Arg1 KO mice.....	15
3.2.3 Generation of RBC sGC KO mice.....	15
<b>3.3 Collection of mouse tissues, blood, and cells</b> .....	<b>16</b>
3.3.1 Tissue collection.....	16
3.3.2 Blood collection and isolation of RBCs.....	16
3.3.3 Purification of RBC suspension.....	16
3.3.4 Bone marrow cells collection.....	17
3.3.5 Isolation of ECs from the heart and the lung.....	17
3.3.6 Isolation of erythroid cells (Ter119 <sup>+</sup> ) from bone marrow cells.....	18
<b>3.4 Molecular characterization of transgenic mice</b> .....	<b>18</b>
3.4.1 Analysis of DNA recombination.....	18
3.4.2 Analysis of mRNA expression in targeted and non-targeted tissues by real-time RT-PCR.....	20



## Summary

3.4.3	Reaction for the enrichment of low abundant yield .....	20
3.4.4	qPCR carried out with TaqMan-assay.....	20
3.4.5	Analysis of targeted protein levels via Western blot and ELISA .....	21
3.4.6	Determination of Arg1 protein levels in the aorta .....	21
3.4.7	Determination of Agr1 expression by immunotransmission electronic microscopy .....	22
3.4.8	Urea assay for determination of arginase activity in targeted tissues. ....	22
<b>3.5</b>	<b>Characterization of systemic hemodynamics and vascular function.....</b>	<b>22</b>
3.5.1	Blood pressure measurements by Millar catheterization.....	22
3.5.2	Measurement of vascular function <i>in vivo</i> .....	22
3.5.3	Measurement of endothelial function <i>ex vivo</i> .....	23
3.5.4	Induction of acute myocardial infarction (AMI) and measurement of infarct size and left ventricular function .....	23
<b>3.6</b>	<b>Hematological analysis.....</b>	<b>24</b>
3.6.1	Blood count and reticulocyte count.....	24
3.6.2	Measurement of transferrin levels in plasma.....	24
3.6.3	Measurement of ferritin levels in plasma .....	24
3.6.4	Measurement of EPO levels in plasma .....	24
3.6.5	Measurement of free hemoglobin in plasma .....	25
3.6.6	Quantitative analysis of erythroid differentiation in bone marrow and spleen.....	25
3.6.7	Pappenheim-staining of bone marrow cells .....	25
3.6.8	Semisolid colony forming assay for bone marrow and spleen cells.....	25
<b>3.7</b>	<b>Measurement of metabolites in tissue, cells, and plasma.....</b>	<b>26</b>
3.7.1	Measurement of NO metabolites in blood and organs .....	26
3.7.2	Measurement of L-arginine, L-ornithine, and L-citrulline concentrations in plasma by LC-MS .....	26
<b>3.8</b>	<b>Statistical analysis .....</b>	<b>27</b>
<b>4</b>	<b>Results.....</b>	<b>28</b>
<b>4.1</b>	<b>The role of EC Arg1 in the regulation of vascular function <i>in vivo</i>.....</b>	<b>28</b>
4.1.1	Generation of EC Arg1 KO mice .....	28
4.1.2	Reduced mRNA expression of Arg1 but increased arginase activity in the aorta.....	30
4.1.3	Endothelial function is preserved in EC Arg1 KO mice. ....	32
4.1.4	Downregulation of eNOS expression but preserved systemic NO metabolites and L-arginine bioavailability. ....	33
4.1.5	Summary of results in EC Arg1 KO mice .....	36
<b>4.2</b>	<b>The role of Arg1 in RBC erythroid cells <i>in vivo</i>.....</b>	<b>37</b>
4.2.1	Generation of RBC-specific KO mice .....	37
4.2.2	Arginase activity in other blood compartments is higher than in RBCs.....	38
4.2.3	Hematological analysis showed no changes in blood count and EPO levels. ....	39

## Summary

4.2.4	No changes in erythropoietic activity in bone marrow and spleen .....	40
4.2.5	Preserved vascular function and systemic hemodynamics in RBC Arg1 KO mice .....	41
4.2.6	Lack of Arg1 in RBC is not affecting infarct size or LV- dysfunction after AMI .....	42
4.2.7	Preserved global L-arginine bioavailability and increased nitrate levels in plasma but reduced nitrite levels in RBCs .....	44
4.2.8	Summary of results on RBC Arg1 KO mice .....	47
<b>4.3</b>	<b>The role of red cell sGC in hematopoiesis <i>in vivo</i> .....</b>	<b>48</b>
4.3.1	Generation of RBC-specific sGC KO mice .....	48
4.3.2	The bone marrow of RBC sGC KO mice showed reduced erythropoiesis. ....	49
4.3.3	The lack of sGC in RBCs causes splenomegaly and stress erythropoiesis in the spleen .....	52
4.3.4	Preserved spleen size and no stress-erythropoiesis in global sGC KO mice .....	53
4.3.5	Preserved blood count in RBC sGC KO mice .....	54
4.3.6	Global KO of sGC leads to changes in WBC count .....	55
4.3.7	Preserved iron status in RBC sGC KO mice .....	56
4.3.8	Preserved circulating NO metabolites in RBC sGC KO mice .....	56
4.3.9	Summary of results on RBC sGC KO mice .....	58
<b>4.4</b>	<b>Analysis of hematological phenotype of Hbb-Cre<sup>pos</sup> mice .....</b>	<b>59</b>
4.4.1	Preserved blood count of Hbb-Cre <sup>pos</sup> mice .....	59
4.4.2	No changes in erythropoietic activity in Hbb-Cre <sup>pos</sup> mice .....	60
4.4.3	Hbb-Cre <sup>pos</sup> mice do not show stress-erythropoiesis .....	61
4.4.4	Summary of results on Hbb-Cre <sup>pos/neg</sup> mice .....	62
<b>5</b>	<b>Discussion .....</b>	<b>63</b>
<b>5.1</b>	<b>Lack of Arg1 in ECs leads to downregulation of eNOS but preserved vascular function .....</b>	<b>65</b>
5.1.1	Lack of Arg1 does not affect vascular function under basal conditions .....	66
5.1.2	Preserved NO-metabolites and L-arginine bioavailability in EC Arg1 KO mice .....	67
5.1.3	Conclusion .....	68
<b>5.2</b>	<b>The lack of red cell Arg1 contributes to circulating NO metabolites in plasma but does not improve vascular function or contribute to cardioprotection after I/R .69</b>	
5.2.1	Low Arg1 activity RBCs as compared to WBC and platelets .....	70
5.2.2	L-arginine bioavailability is unchanged but NO metabolites in plasma are changed ....	71
5.2.3	The lack of Arg1 in RBCs does not affect systemic hemodynamics or vascular function. ....	72
5.2.4	Deletion of Arg1 from RBC is not cardioprotective after AMI .....	72
5.2.5	Arg1 does not play a role in erythroid differentiation .....	73
5.2.6	Conclusion .....	74

<b>5.3</b>	<b>Lack of sGC in erythroid cells leads to disrupted erythropoiesis in the bone marrow, which is fully rescued by stress erythropoiesis in the spleen.....</b>	<b>75</b>
5.3.1	sGC in erythroid cells is involved in RBC maturation .....	76
5.3.2	Stress erythropoiesis compensates for disrupted erythropoiesis in the bone marrow ..	77
5.3.3	The levels of NO metabolites did not change in RBCs and plasma.....	78
5.3.4	Conclusion .....	78
<b>6</b>	<b>Summary &amp; perspective.....</b>	<b>80</b>
<b>7</b>	<b>References.....</b>	<b>82</b>
<b>8</b>	<b>Acknowledgment.....</b>	<b>96</b>
<b>9</b>	<b>Publication &amp; Manuscripts .....</b>	<b>98</b>
<b>10</b>	<b>Curriculum Vitae.....</b>	<b>100</b>

## List of all figures

<b>Figure 1 eNOS-signaling in the vessel wall.</b> .....	2
<b>Figure 2 - Steady-state erythropoiesis.</b> .....	5
<b>Figure 3 - Stress-erythropoiesis occurs in the spleen.</b> .....	6
<b>Figure 4 - Graphical abstract.</b> .....	10
<b>Figure 5 Table of instruments</b> .....	14
<b>Figure 6 - Genetic characterization of EC Arg1 KO mice.</b> .....	29
<b>Figure 7 - Decreased Arg1 expression in aorta but preserved protein levels</b> .....	31
<b>Figure 8 - Preserved vascular response to ACh in resistance and conductance arteries of EC Arg1 KO mice.</b> .....	32
<b>Figure 9 - Downregulation of eNOS in the endothelium.</b> .....	34
<b>Figure 10 - Preserved NO metabolites and L-arginine bioavailability.</b> .....	36
<b>Figure 11 - Genetic characterization of RBC Arg1 KO mice.</b> .....	37
<b>Figure 12 - Arginase activity in different blood compartments.</b> .....	38
<b>Figure 13 - Vascular function is preserved in Arg1 KO mice.</b> .....	41
<b>Figure 14 - LV dysfunction after acute myocardial infarction is not affected by the lack of Arg1 in RBCs.</b> .....	42
<b>Figure 15 - Area of risk and infarct size of RBC Arg1 KO mice.</b> .....	44
<b>Figure 16 - L-arginine-metabolites in plasma and NO metabolites in RBCs of RBC Arg1 KO mice.</b> .....	45
<b>Figure 17 - Genetic characterization of RBC sGC KO mice.</b> .....	49
<b>Figure 18 - Steady-state-erythropoiesis in RBC sGC KO mice.</b> .....	50
<b>Figure 19 - Characterization of Spleen of RBC sGC KO mice.</b> .....	52
<b>Figure 20 - Pappenheim-staining of bone marrow cells of Hbb-Cre mice.</b> .....	61
<b>Figure 21 Arg1/eNOS/sGC pathway in RBCs in vivo.</b> .....	63
<b>Figure 22 Lack of Arg1 in ECs leads to downregulation of eNOS in the vessel wall but preserved vascular function.</b> .....	65
<b>Figure 23 The lack of red cell Arg1 contributes to circulating nitrate in plasma, but does not improve vascular function or contribute to cardioprotection after I/R.</b> .....	69
<b>Figure 24 Lack of sGC in erythroid cells leads to disrupted erythropoiesis in the bone marrow, which is fully rescued by stress erythropoiesis in the spleen.</b> .....	75

## List of all tables

<b>Table 1 Chemicals</b> .....	11
<b>Table 2 Commercial Kits</b> .....	12
<b>Table 3 Antibodies used for flow cytometry</b> .....	13
<b>Table 4 Antibodies used for western blot</b> .....	13
<b>Table 5 Composition of solutions</b> .....	13
<b>Table 6 Table of softwares</b> .....	15
<b>Table 7 Primers for DNA recombination</b> .....	19
<b>Table 8 Primer used for mRNA expression</b> .....	21
<b>Table 9 Parameters for arginase assay</b> .....	22
<b>Table 10 Results of blood count of EC Arg1 KO mice and WT littermate controls</b> .....	30
<b>Table 11 Parameters of systemic hemodynamics and cardiac function in EC Arg1 KO mice and WT littermate controls</b> .....	33
<b>Table 12 Distribution of NO metabolites in blood and organs of EC Arg1 KO mice and corresponding WT littermate controls</b> .....	35
<b>Table 13 Results of blood count of RBC Arg1 KO mice</b> .....	39
<b>Table 14 Quantification of terminal erythroid differentiation in bone marrow and spleen of RBC Arg1 KO mice</b> .....	40
<b>Table 15 Parameters of systemic hemodynamics in RBC Arg1 KO mice and WT littermate control</b> .....	42
<b>Table 16 Echocardiographic parameters were assessed in RBC Arg1 KO mice by high-resolution ultrasound before and after AMI</b> .....	43
<b>Table 17 Distribution of NO metabolites in blood and organs of RBC Arg1 KO mice and corresponding WT littermate controls</b> .....	46
<b>Table 18 Results of Pappenheim-staining of RBC sGC KO and global sGC KO mice</b> .....	49
<b>Table 19 CFU-Assay in bone marrow of RBC sGC KO and global sGC KO mice and their controls</b> .....	51
<b>Table 20 Quantification of terminal erythroid differentiation in bone marrow of RBC sGC KO mice and global sGC KO mice and their littermate controls</b> .....	51
<b>Table 21 CFU-Assay in the spleen of RBC-sGC KO and global sGC KO mice</b> .....	53
<b>Table 22 Quantification of terminal erythroid differentiation in the spleen of RBC sGC KO mice and global sGC KO mice</b> .....	53
<b>Table 23 Results of blood count of RBC sGC KO mice and WT littermate control</b> .....	54
<b>Table 24 Results of blood count of global sGC KO mice and WT littermate control</b> .....	55
<b>Table 25 Distribution of NO metabolites in blood and organs of RBC sGC KO mice and corresponding WT littermate controls</b> .....	57
<b>Table 26 Results of blood count of Hbb-Cre<sup>pos</sup> mice and WT littermate control</b> .....	59
<b>Table 27 Quantification of terminal erythroid differentiation in the bone marrow of Hbb-Cre<sup>pos</sup> mice and WT control</b> .....	60
<b>Table 28 CFU-Assay in the bone marrow of Hbb-Cre<sup>pos</sup> mice and WT littermate control</b> .....	60

List of all tables

<b>Table 29 CFU-Assay in the spleen of <i>Hbb-Cre<sup>pos</sup></i> mice and WT.....</b>	<b>61</b>
<b>Table 30 Quantification of terminal erythroid differentiation in the spleen of <i>Hbb-Cre<sup>pos</sup></i> mice and WT control .....</b>	<b>62</b>

## Abbreviations

ACh	acetylcholine
AMI	acute myocardial infarction
Arg	arginase
Arg1	arginase 1
Arg2	arginase 2
BFU-E	burst-forming units-erythroid
BMP4	bone morphogenetic protein 4
BP	blood pressure
BSA	bovine serum albumin
CFU	colony forming units
cGMP	cyclic guanosine monophosphate
CLD	chemiluminescence detector
CO	cardiac output
deoxy-Hb	deoxygenated hemoglobin
DNA	deoxyribonucleic acid
EC	endothelial cell
EDTA	ethylenediaminetetraacetic acid
eNOS	endothelial nitric oxide synthase
EPO	erythropoietin
FMD	flow-mediated dilation
FSC	forward scatter
gKO	global knockout
GTP	guanosine triphosphate
Hb F	fetal hemoglobin
Hbb	hemoglobin beta chain
HCT	hematocrit
HGB	hemoglobin
HR	hear rate
HSC	hematopoietic stem cells
I/R	ischemia-reperfusion
iNOS	inducible nitric oxide synthase
KO	knockout
LV	left ventricular
Lym	lymphocytes
MAP	mean arterial pressure
MCH	mean corpuscular hemoglobin
MCHC	mean corpuscular hemoglobin concentration
MCV	mean corpuscular volume
Mo	monocytes
NEM	N-ethylmaleimide
nNOS	neuronal nitric oxide synthase
NO	nitric oxide
NO-heme	nitrosyl heme
NOS	nitric oxide synthase
PBS	phosphate-buffered saline
PE	phenylephrine
PKG	protein kinase G
PSC	pluripotent stem cells
qPCR	quantitative polymerase chain reaction
RBC	red blood cell

## Abbreviations

RDW	red blood cell distribution
RNA	ribonucleic acid
RT	reverse transcriptase
RXNO	total nitrosated species
SBP	systolic blood pressure
SCD	sickle cell anemia
SDS	sodium dodecyl sulfate
sGC	soluble guanyl cyclase
SMCs	smooth muscle cells
SNP	sodium nitroprussid
TAM	tamoxifen
TBS	tris-buffered saline
TTC	triphenyl tetrazolium chloride
T-TBS	tris buffered saline plus tween 20
WBC	white blood cell
WT	wildtype



# 1 Introduction

## 1.1 Nitric oxide and its metabolism

Nitric oxide (NO) is a free radical molecule produced in the body by the nitric oxide synthase (NOS) (EC: 1.14.13.39). For a long time, it was assumed that NO has harmful effects on the body, but with the discovery of the NOS enzymes, the importance of NO signaling was found (Lundberg et al., 2022). In 1980, Furchgott and Zawadzki introduced the concept of endothelium-dependent relaxation (Furchgott et al., 1980). Following studies identified an endothelium-derived relaxation factor that causes vasodilation through the activation of soluble guanylate cyclase (sGC) in the endothelium (Furchgott et al., 1984). Until it was shown that the endothelium-derived relaxation factor was NO (Ignarro et al., 1987).

The NOS enzymes convert L-arginine into L-citrulline and NO. There are three isoforms of NOS: the inducible NOS (NOS1/iNOS), which is constitutively expressed in macrophages (Hevel et al., 1991), nNOS (NOS2) in the neuronal system (Mayer et al., 1990), and endothelial NOS (NOS3/eNOS) in endothelial cells (ECs), which is also expressed in other cell types, such as red blood cells (RBCs) (Pollock et al., 1991; Kleinbongard et al., 2006).

### 1.1.1 *The role of the eNOS/sGC pathway in the regulation of vascular function and systemic hemodynamics*

eNOS plays a crucial role in maintaining vascular homeostasis through NO production. NO regulates blood pressure (BP), organ perfusion, platelet aggregation, and vascular tone (Moncada et al., 1991; Farah et al., 2018). Reduced eNOS activity and NO levels are associated with endothelial dysfunction, hypertension, and metabolic syndrome (Mohan et al., 2008; Y. M. Yang et al., 2009). In mouse models, the lack of eNOS in all tissues or ECs leads to endothelial dysfunction and hypertension (Godecke et al., 1998; Stauss et al., 1999; Leo et al., 2021).

NO produced in the endothelium by eNOS diffuses into the vascular smooth muscle cells, where it binds to the heme group of sGC (EC:4.6.1.2) and induces vasodilation by activating downstream signaling (Arnold et al., 1977; Miki et al., 1977; Ignarro et al., 1987). sGC, a direct target of eNOS-derived NO, is a heterodimer consisting of two subunits,  $\alpha$  and  $\beta$ . Two functional isoforms of sGC are known in the body:  $\alpha1\beta1$  and  $\alpha2\beta1$ . The  $\alpha1\beta1$ -subunit is expressed in vascular smooth muscle cells, platelets, brain, and RBCs (Mergia et al., 2006; Nimmegeers et al., 2007; Cortese-Krott et al., 2018), whereas the  $\alpha2\beta1$ -subunit is expressed in the brain, uterus, and placenta (Russwurm et al., 1998; Mergia et al., 2003).

## Introduction

sGC is involved in various functions in the body, such as the regulation of platelet aggregation, neurotransmission, cardiac function, and vascular relaxation. The  $\alpha 1\beta 1$  isoform is the most important isoform in the regulation of vascular function (Nimmegeers et al., 2007). The conversion of GTP to cGMP is catalyzed by the activation of sGC by NO. This increase in cGMP levels causes further downstream reactions by activating protein kinase G (PKG), leading to vasodilation by phosphorylation. Thus, sGC/PKG pathway, plays a key role in the regulation of vascular function, BP, and vascular remodeling (Mergia et al., 2006; Frankenreiter et al., 2017).

sGC-signaling plays a significant role in myocardial infarction, sepsis-induced myocardial dysfunction, and stroke (Buys et al., 2008; Atochin et al., 2010; Nagasaka et al., 2011; Frankenreiter et al., 2017) and is already used as a therapeutic target for the treatment of heart failure and pulmonary arterial hypertension (Ghofrani et al., 2013; Butler et al., 2022).

The importance of sGC in vascular function and cardioprotection has been explored using various knockout (KO) approaches. The lack of the  $\beta_1$ -unit results in a loss of the expression of the  $\alpha 1\beta$ -subunit of sGC in all tissues and leads to a significant reduction in lifespan (Friebe et al., 2007). Global  $\alpha 1$  or  $\alpha 2$  KO did not affect the lifespan of mice but showed other dysfunctions (Mergia et al., 2006; Buys et al., 2008). The lack of the  $\alpha 1$ -subunit leads to vascular dysfunction, hypertension, and kidney dysfunction (Mergia et al., 2018).

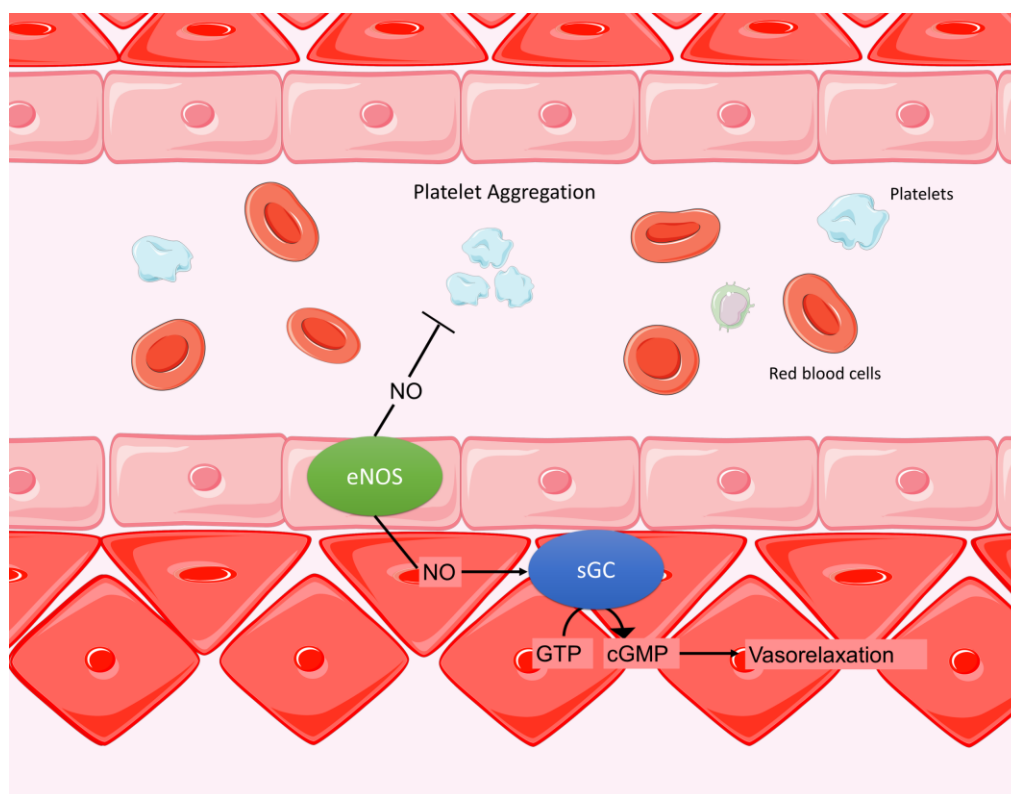


**Figure 1 eNOS-signaling in the vessel wall.** eNOS produces NO, which diffuses in the vascular smooth muscle cells where it causes vasorelaxation by activation of sGC and downstream enzymes.

## Introduction

### *1.1.2 The role of arginase as a counterpart of NOS enzymes*

In the endothelium not only eNOS use L-arginine as a substrate but also arginase (EC:3.5.3.1). Arginase converts L-arginine into L-ornithine and urea. Two functional arginase isoforms are expressed in the body. Arginase 1 (Arg1) is located in the cytoplasm of cells and is highly expressed in hepatocytes, but also in vascular smooth muscle cells, white blood cells (WBCs), ECs, and RBCs (Ignarro et al., 2001; Munder et al., 2005; Monticelli et al., 2016). Arginase 2 (Arg2), also known as kidney Arg, is expressed in the mitochondria of the cell (Beaulieu et al., 1997).

A role attributed to arginase in both the immune system and the cardiovascular system is as a “counterpart” of iNOS, as these two classes of enzymes can compete for the same substrate, L-arginine (Cinelli et al., 2020). iNOS is activated to produce high levels of NO, which kills intracellular pathogens and bacteria. Macrophages can also be activated to express high levels of arginase, which is involved in tissue repair and wound healing. In mouse macrophages, it was demonstrated that Arg1 could “steal” L-arginine from iNOS, limiting high-output NO formation and its damaging effects (Chang et al., 1998). The contra-regulation of both enzymes is important for the regulation of the immune response and for preventing excessive inflammation.

Based on this knowledge, a similar relationship has been proposed for the endothelium. Previous studies have shown that Arg1 expressed in the endothelium is involved in vascular dysfunction by limiting the bioavailability of L-arginine (C. Zhang et al., 2001; Toque et al., 2013) resulting in endothelial dysfunction and hypertension (Mahdi et al., 2020). Studies have demonstrated that inhibiting arginase improves vascular function, increases NO bioavailability, and lowers BP in rats with endothelial dysfunction (J. H. Kim et al., 2009; Bagnost et al., 2010). Additionally, it has been shown that a lack of Arg1 in the endothelium protects mice fed a high-fat high-salt diet from endothelial dysfunction (Yao et al., 2017). In contrast, deletion of Arg1 in ECs did not improve vasomotor function in diabetic mice (Chennupati et al., 2018).

The expression of eNOS in ECs plays a crucial role in vascular function and hemodynamics. Arg1, as a counterpart, is also expressed in ECs, but its role in EC eNOS-signaling still needs to be investigated.

## **1.2 The RBC**

RBCs have a simple structure with no organelles or nuclei. They are characterized by a biconcave shape, and the main feature of RBCs is their reversal deformability to circulate through narrow capillaries with diameters smaller than their own. RBCs play an important role in the transport of oxygen to tissues and various physiological processes. The lifespan of RBCs

## Introduction

is approximately 55 days in mice and 120 days in humans (H. D. Zhang et al., 2018; Zimring, 2020).

RBCs can transport oxygen because of their high hemoglobin expression. Hemoglobin is a hetero-tetramer, where each subunit consists of a globin chain and a heme group (Perutz, 1960). Globins are a family of proteins that are important for oxygen binding and transport by hemoglobin (Gotting et al., 2015). They are divided into  $\alpha$ ,  $\beta$ ,  $\gamma$ ,  $\delta$ ,  $\epsilon$  and  $\zeta$ -globins.  $\zeta$  and  $\delta$  is mostly expressed in embryonic erythrocytes. Fetal hemoglobin (Hb F), which consists of  $\alpha_2\gamma_2$ , is found in a high percentage of hemoglobin in newborns but decreases rapidly (Old, 2013). During the perinatal phase, another switch from  $\gamma$ - to  $\beta$ -globin occurs in the human body.

### 1.2.1 Erythropoiesis

Erythropoiesis is a process by which RBCs are continuously produced to maintain sufficient oxygen transport in the body. This process leads to a production of  $2.5 \times 10^6$  RBCs per second and is mainly taking place in the bone marrow (Palis, 2014).

The bone marrow, spleen, and liver are the major erythropoietic tissues in mammals. During the developmental stages, erythropoiesis moves from the yolk sac to the fetal liver prenatally. In adults, it shifts towards the spleen and finally to the bone marrow (Palis et al., 1999; Chen et al., 2021).

Erythropoiesis starts with hematopoietic stem cells (HSCs) proliferating and differentiating into common myeloid progenitors (Akashi et al., 2000). These progenitors develop into erythroid burst-forming units (BFU-E) then into erythroid colony-forming units (CFU-Es) and finally into erythroblasts (Stephenson et al., 1971). Erythroblasts mature into RBCs through “terminal erythropoiesis” in erythroblastic islands. These islands consist of a central macrophage surrounded by erythroblasts at various differentiation stages (W. Li et al., 2020). The proerythroblast, the first identifiable erythroblast, divides 3-4 times to form reticulocytes (Liu et al., 2013). A proerythroblast divides into two basophilic erythroblasts. Four polychromic erythroblasts are generated. The four polychromic erythroblasts then develop into eight orthochromatic erythroblasts (Hu et al., 2013). During this development, they shrink in size and the hemoglobin concentration increases (Waugh et al., 1997). Orthochromatic erythroblasts mature into reticulocytes, young RBCs without a nucleus, but with residual ribosomal RNA. This is the last stage before entering the bloodstream.

Erythropoietin (EPO) is a hormone mainly produced in the kidney. Its production is regulated by the Hb-concentration, Hb-O<sub>2</sub> affinity, and tissue oxygen tension (Jelkmann, 2016; Suresh et al., 2019). After EPO production in the adult kidney is activated, it is released into the plasma and stimulates the bone marrow erythroid progenitor cells through the EPO-R receptor (Tsiftoglou, 2021).

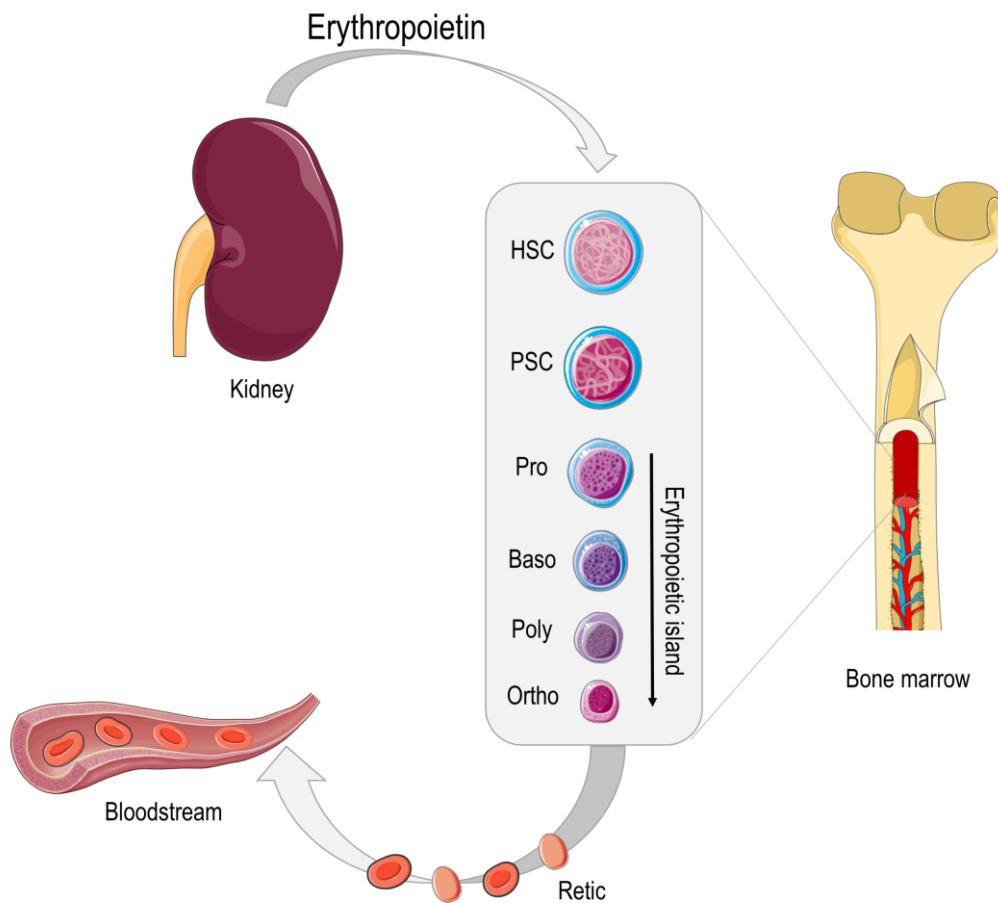


**Figure 2 - Steady-state erythropoiesis.** Erythropoiesis is induced by erythropoietin (EPO), a renal hormone. EPO stimulates HSC to differentiate into erythroblasts until reticulocytes are released into the bloodstream. Erythroblasts are generated in erythropoietic islands in the bone marrow.

### 1.2.2 Stress erythropoiesis

When tissue hypoxia occurs due to anemia or other causes, it triggers a physiological stress response that leads to stress erythropoiesis. This process is capable of producing a large number of RBCs to address hypoxic conditions (Lenox et al., 2005). Erythropoiesis moves back to the liver and spleen (Lenox et al., 2009; Liao et al., 2018).

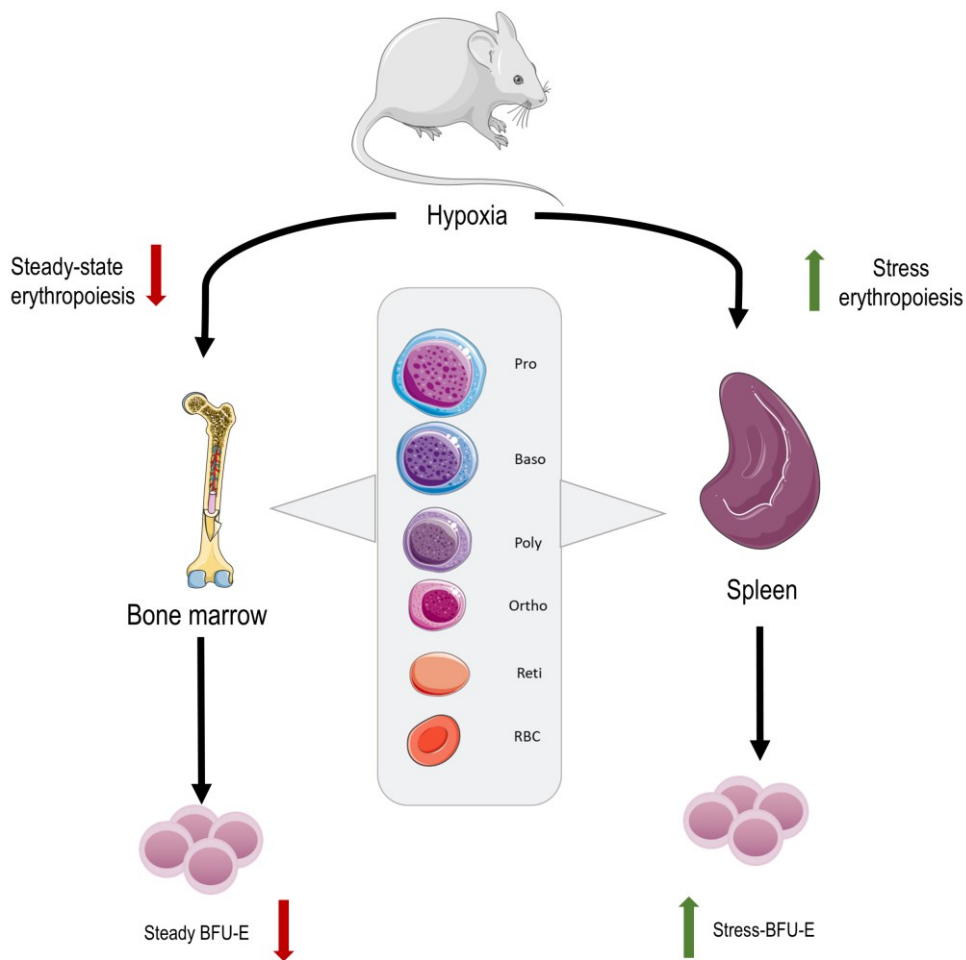


**Figure 3 - Stress-erythropoiesis occurs in the spleen.** In acute anemia, the bone marrow is not capable of producing enough RBCs. A stress response leads to the activation of spleen erythropoiesis via BMP4/hedgehog signaling.

Stress erythropoiesis, in contrast with steady-state erythropoiesis, is not induced by EPO but by the bone morphogenetic protein 4 (BMP4) pathway (Perry et al., 2007). Increased EPO levels lead to increased steady-state erythropoiesis (Singh et al., 2018; Paulson et al., 2020). On the other hand, stress erythropoiesis is induced by BMP4 to overtake defective bone marrow erythropoiesis until it can resume producing RBCs. Indeed, it was shown that special BMP4<sup>R</sup> cells are located in the spleen, which differentiate into BFU-Es after exposure to BMP4. This increase in stress BFU-Es occurs only in the spleen and not in the bone marrow (Lenox et al., 2005). Interestingly, it was shown that progenitor cells from the bone marrow can respond to BMP4 by hedgehog signaling in the spleen microenvironment (Perry et al., 2009).

This stress-erythropoiesis pathway has been found only in mice until now. Human stress-erythropoiesis is more similar to fetal erythropoiesis, which is defined by fetal hemoglobin, antigens, and fetal erythrocyte characteristics.

## Introduction

### 1.2.3 *The discovery of the Arg1/eNOS/sGC pathway in RBCs*

For a long time, it was thought that RBCs are just gas transporters that deliver oxygen to all organs and tissues. Recently, it was shown that RBCs carry functional eNOS and its downstream enzymes sGC and PKG (Kleinbongard et al., 2006; Cortese-Krott et al., 2018).

Wood et al. (2013) used bone marrow transplantation to study red cell eNOS function. Bone marrow cells from global eNOS KO mice were transplanted into WT and global eNOS KO mice. WT mice without eNOS in their blood cells showed higher BP and lower nitrite levels than WT controls. (Wood et al., 2013). In contrast, global eNOS KO mice transplanted with WT bone marrow showed lower BP than global KO mice transplanted with global eNOS KO bone marrow. This suggests that eNOS in blood cells affects BP regulation and NO metabolites. This study removed eNOS from all blood cells; however, its role in RBCs was not examined. In a recent study, RBC-specific eNOS KO and knock-in mice were generated (Leo et al., 2021). This study showed that the absence of eNOS in RBCs leads to hypertension, but not vascular dysfunction. Reintroducing eNOS into RBCs reduced the BP of global KO mice but could not fully restore the phenotype (Leo et al., 2021). In an additional study, eNOS expression in RBCs was shown to be cardioprotective (Cortese-Krott et al., 2022). EC eNOS likely affects BP by controlling vascular function, whereas RBC eNOS likely regulates BP by controlling NO metabolites.

Furthermore, RBCs express Arg1 (P. S. Kim et al., 2002). Yang et. al investigated the role of red cell Arg1 (J. Yang et al., 2013). They showed that inhibiting Arg in the blood and suspension of RBCs increased the export of NO metabolites from RBCs and proposed that the inhibition of Arg1 is cardioprotective by increasing the export of NO metabolites.

The first approach for identifying the role of Arg1 in RBC *in vivo* was performed using a cell-specific KO model using the EpoR-promoter (Gogiraju et al., 2022). This study showed that reduced expression of Arg1 in erythrocytes promotes vascular calcification in atherosclerosis-prone mice. Notably, the EpoR promoter is not specific to erythroid cells but is also found in different tissue macrophages and hematopoietic cells (H. Zhang et al., 2021).

It has been shown that eNOS in RBCs plays an important role in the regulation of BP and circulating NO metabolites. The role of its up- and downstream enzymes, Arg1 and sGC, in the *in vivo* regulation of eNOS remains unknown.

### 1.2.4 *The role of the eNOS/sGC pathway in erythropoiesis and globin expression*

There is accumulating evidence that the Arg1/eNOS/sGC pathway plays a role in erythroid differentiation.

## Introduction

NO is known to play a role in the differentiation and survival of different cell types (Bloch et al., 1999; Tejedro et al., 2010; Beltran-Povea et al., 2015). The first studies investigating the role of NO signaling in erythroid differentiation revealed the potential role of eNOS in erythroid cell differentiation and survival (Kucukkaya et al., 2006; Cokic et al., 2008). Furthermore, it was shown that the activation of the NO/sGC pathway in erythroleukemic cells (K562) by hydroxyurea leads to an increase in  $\gamma$ -globin expression (Cokic et al., 2003). A recent study demonstrated that nNOS, but not eNOS, is crucial for EPO-dependent erythroid differentiation (Lee et al., 2023). These findings are in line with the preserved blood count in RBC eNOS KO and EC eNOS KO mice (Leo et al., 2021).

Several studies have examined the role of sGC in  $\gamma$ -globin expression *in vitro*. Specifically, the treatment of K562 cells with the sGC-stimulator Bay41-2272 has been shown to increase  $\gamma$ -globin expression (Ferreira et al., 2020), whereas the inhibition of sGC or PKG results in decreased  $\gamma$ -globin expression (Ikuta et al., 2001).

The first *in vivo* study investigating the role of sGC in RBCs was performed in 2016 by Ikuta et al. (Ikuta et al., 2016). In this study, transgenic mice that overexpress rat sGC in erythroid and myeloid cells were generated. The increase in sGC expression led to an increase in erythropoietic activity induced by increasing lineage-specific transcription factors like GATA-1, KLF-1, and c-Myb, which leads to an increase in RBC count, total hemoglobin, and hematocrit. Furthermore, it has been shown that the deletion of PKG, the downstream enzyme of sGC, in the whole body leads to intravascular hemolysis and anemia (Foller et al., 2008). A following study revealed an iron deficiency in the global PKG KO mice (Angermeier et al., 2016).

Accumulating evidence suggests that the Arg1/eNOS/sGC pathway plays a role in erythroid differentiation. However, the *in vivo* role of Arg1 and sGC in erythroid cells is still unknown.



## 2 Aim of the study

RBCs are known for their role as gas transporters. Recently, it has been shown that eNOS expressed in RBCs regulates BP and circulating NO metabolites independently from eNOS expressed in ECs. RBCs also express Arg1, the upstream enzyme of eNOS, and sGC, its downstream enzyme, but their *in vivo* function remains unknown.

This study hypothesizes that the Arg1/eNOS/sGC pathway plays a role in the regulation of RBC physiology and function *in vivo*.

The aim of this study was to analyze the role of Arg1 and sGC in RBCs *in vivo*. To address this hypothesis, three transgenic mouse lines were generated: EC Arg1 KO mice, RBC Arg1 KO mice, and RBC sGC KO mice.

Therefore, this study focuses on three main goals:

1. The role of EC Arg1 in eNOS-signaling.  
The EC Arg1 KO mice and WT littermates will be analyzed for systemic hemodynamics, vascular function, and NO metabolites.
2. The role of RBC Arg1 in eNOS-signaling in RBCs and erythroid cells.  
The RBC Arg1 KO mice and WT littermates will be analyzed for NO metabolites, systemic hemodynamics, and potential effects on erythroid differentiation.
3. The role of sGC in the physiology of RBCs and erythroid cells.  
The RBC sGC KO mice and littermates will be analyzed for effects on erythroid differentiation in the bone marrow and spleen and NO metabolites and compared to global sGC KO mice.

## Aim of the study

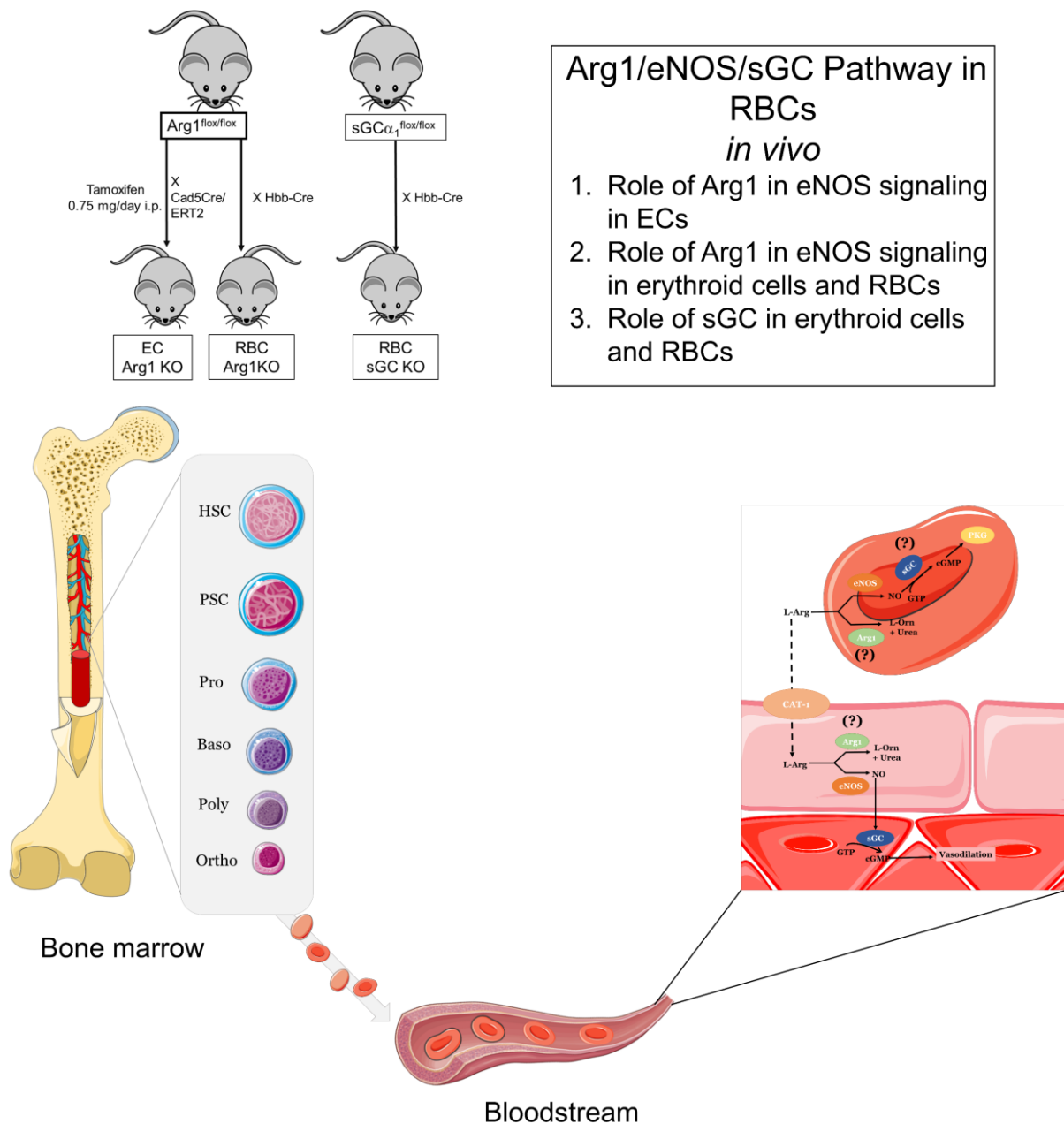


**Figure 4 - Graphical abstract.** This study hypothesizes that the Arg1/eNOS/sGC pathway plays a role in the regulation of RBC physiology *in vivo*. The aim of this study is to analyze Arg1/eNOS/sGC signaling in RBCs by the generation of EC and RBC-specific KO-models. (1) The role of Arg1 in eNOS signaling in ECs. Mice are characterized for vascular function, hemodynamics, and NO metabolites. (2) The role of Arg1 in eNOS signaling in erythroid cells and RBCs. RBC Arg1 KO mice are characterized for NO metabolites, vascular function, and erythropoiesis. (3) The role of sGC in erythroid cells and RBCs. Mice are characterized for NO metabolites and hematological phenotypes.

### 3 Materials and Methods

#### 3.1 Material

**Table 1 Chemicals**

Chemical	Manufacturer	Headquarter
<b><sup>13</sup>C- labeled L-arginine</b>	Merck	Darmstadt, Germany
<b>Triphenyl tetrazolium chloride (TTC)</b>	Merck	Darmstadt, Germany
<b>7-AAD</b>	BD Biosciences	Franklin Lakes, New Jersey, USA
<b>Acetonitrile</b>	Merck	Darmstadt, Germany
<b>Acetylcholine</b>	Merck	Darmstadt, Germany
<b><math>\alpha</math>-isonitrosopiophenone</b>	Merck	Darmstadt, Germany
<b>Ammonium Chloride</b>	Merck	Darmstadt, Germany
<b>Ammonium persulfate</b>	Merck	Darmstadt, Germany
<b>Anti-APC-Microbeads</b>	Milteny Biotec	Bergisch Gladbach, Germany
<b>Anti-CD31-Microbeads</b>	Milteny Biotec	Bergisch Gladbach, Germany
<b>Anti-CD45-Microbeads</b>	Milteny Biotec	Bergisch Gladbach, Germany
<b>Anti-Ter119-Mircobeads</b>	Milteny Biotec	Bergisch Gladbach, Germany
<b><math>\beta</math>-mercaptoethanol</b>	Merck	Darmstadt, Germany
<b>Bovine Serum Albumin (BSA)</b>	Merck	Darmstadt, Germany
<b>Carl Roth Gel-Solution</b>	Carl Roth	Karlsruhe, Germany
<b>Collagenase I</b>	Worthington Biochemical Corporation	Troisdorf, Germany
<b>Detection Agent</b>	ThermoFisher	Waltham, USA
<b>DNase I</b>	Merck	Darmstadt, Germany
<b>EDTA</b>	Merck	Darmstadt, Germany
<b>Fast Advanced MasterMix</b>	Thermo Fisher Scientific	Schwerte, Germany
<b>FcR-Blocker reagent, mouse</b>	Milteny Biotec	Bergisch Gladbach, Germany
<b>Ferricyanide</b>	Merck	Darmstadt, Germany
<b>Formic acid</b>	Merck	Darmstadt, Germany
<b>Grims Soluttion</b>	Merck	Darmstadt, Germany
<b>Hanks balanced buffer</b>	Merck	Darmstadt, Germany
<b>Iodine</b>	Merck	Darmstadt, Germany
<b>Isoflurane</b>	Piramal	Munich, Germany
<b>L-arginine</b>	Merck	Darmstadt, Germany
<b>L-Citrulline</b>	Merck	Darmstadt, Germany
<b>L-Ornithine</b>	Merck	Darmstadt, Germany

## Materials and Methods

<b>Manganese Chloride (MnCl<sub>2</sub>)</b>	Merck	Darmstadt, Germany
<b>May-Grunwald-Solution</b>	Merck	Darmstadt, Germany
<b>Methanol</b>	Merck	Darmstadt, Germany
<b>MethoCult</b>	Stemcell	Vancouver, Canada
<b>N-ethylmaleimide (NEM)</b>	Merck	Darmstadt, Germany
<b>Nonidet™ P 40</b>	Merck	Darmstadt, Germany
<b>PBS</b>	Merck	Darmstadt, Germany
<b>Peanut oil</b>	Merck	Darmstadt, Germany
<b>Phenylephrine</b>	Merck	Darmstadt, Germany
<b>Phosphoric acid</b>	Merck	Darmstadt, Germany
<b>Potassium ferricyanide</b>	Merck	Darmstadt, Germany
<b>Potassium hexacyanoferrate (III)</b>	Merck	Darmstadt, Germany
<b>Primer for DNA-recombination</b>	Eurofine	Ebersberg, Germany
<b>Protease inhibitor cocktail</b>	Roche	Basel, Switzerland
<b>Proteinase K</b>	Qiagen	Hilden, Germany
<b>SDS</b>	Merck	Darmstadt, Germany
<b>Skim milk powder</b>	Merck	Darmstadt, Germany
<b>Sodium hydrogen carbonate</b>	Merck	Darmstadt, Germany
<b>Sodium nitrite</b>	Merck	Darmstadt, Germany
<b>SsoAdvacend PreAmp Super</b>	BioRad	Hercules, US
<b>Sulfanilamide</b>	Merck	Darmstadt, Germany
<b>Sulfuric acid</b>	Carl Roth	Karlsruhe, Germany
<b>Tamoxifen</b>	Merck	Darmstadt, Germany
<b>TEMED</b>	Carl Roth	Karlsruhe, Germany
<b>Thiazol orange</b>	Merck	Darmstadt, Germany
<b>Tris base</b>	Merck	Darmstadt, Germany
<b>Tween 20</b>	Merck	Darmstadt, Germany
<b>RNAlater</b>	Merck	Darmstadt, Germany
<b>Urea</b>	Merck	Darmstadt, Germany
<b>Arginase 1 Recombinant Polyclonal Antibody (24HCLC) (711765)</b>	Thermo Fisher Scientific	Schwerte, Germany
<b>12 nm Colloidal Gold AffiniPure Goat Anti-Rabbit IgG (111-205-144)</b>	Jackson ImmunoResearch	Ely, United Kingdom

**Table 2 Commercial Kits**

<b>Kit</b>	<b>Manufacturer</b>	<b>Headquarter</b>
<b>Allprep DNA/RNA kit</b>	Qiagen	Hilden, Germany
<b>Lowry Assay</b>	BioRad	Hercules, US
<b>RNAeasy kit</b>	Qiagen	Hilden, Germany
<b>QuantiTect reverse transcription kit</b>	Qiagen	Hilden, Germany
<b>RNase-Free DNase Set</b>	Qiagen	Hilden, Germany

## Materials and Methods

<b>SuperSignal™ West Pico Plus chemiluminescent substrate</b>	Thermo Fisher Scientific	Waltham, USA
<b>SuperSignal™ West Femto Maximum chemiluminescent substrate</b>	Thermo Fisher Scientific	Waltham, USA
<b>Transferrin ELISA</b>	Abcam	Cambridge, UK
<b>Ferritin ELISA</b>	Abcam	Cambridge, UK
<b>EPO ELISA</b>	Abcam	Cambridge, UK
<b>Hemoglobin ELISA</b>	Abcam	Cambridge, UK
<b>Arginase1 ELISA</b>	Abcam	Cambridge, UK

**Table 3 Antibodies used for flow cytometry**

Antibody	Catalog	Manufacturer	Headquarter
<b>Anti-CD73-APC</b>	130-111-332	Milteny Biotec	Bergisch Gladbach, Germany
<b>Anti-Ter119-PE</b>	130-049-901	Milteny Biotec	Bergisch Gladbach, Germany
<b>Anti-CD45-FITC</b>	130-110-796	Milteny Biotec	Bergisch Gladbach, Germany
<b>Anti-CD45 APC-Cy7</b>	561037	BD Biosciences	Franklin Lakes, New Jersey, USA
<b>Anti-CD-44- PE Vio bright</b>		Milteny Biotec	Bergisch Gladbach, Germany

**Table 4 Antibodies used for western blot**

Protein	Antibody	Dilution	Code
<b>Arginase 1</b>	Mouse anti-Arg1	1:100 in 5% BSA	610708
<b>eNOS</b>	Mouse anti-eNOS	1:100 in 5% BSA	624086
<b>β-actin</b>	Mouse Anti-beta-actin	1:1000 in 5% BSA	A1978
<b>α-tubulin</b>	Mouse anti-alpha-tubulin	1:5000 in 5% BSA	T6199
<b>Goat anti-mouse Ig</b>	Goat anti-mouse Ig	1:5000 in 5% BSA	554002

**Table 5 Composition of solutions**

Solution	Composition
<b>Blocking buffer for WB</b>	Skim milk powder 5%, T-TBS 1x
<b>Hanks'balanced salt solution</b>	0.185 g CaCl <sub>2</sub> *2H <sub>2</sub> O, 0.09767 MgSO <sub>4</sub> , 0.4g KCl 0.06g KH <sub>2</sub> PO <sub>4</sub> , 8.0g NaCl, 0.04788g Na <sub>2</sub> HPO <sub>4</sub> , 1g D-glucose, 0.35g NaHCO <sub>3</sub> in 1L H <sub>2</sub> O
<b>Hanks'balanced salt solution w/o Ca<sup>2+</sup>&amp;Mg<sup>2+</sup></b>	0.185 g 0.4 g KCl 0.06 g KH <sub>2</sub> PO <sub>4</sub> , 8.0 g NaCl, 0.04788 g Na <sub>2</sub> HPO <sub>4</sub> , 1 g D-glucose, 0.35 g NaHCO <sub>3</sub> in 1L H <sub>2</sub> O
<b>NEM/EDTA/PBS solution</b>	0.5 mL EDTA 500 mM, 10mL NEM 100 mM, PBS to 100 mL
<b>PBS</b>	8.54 mM Na <sub>2</sub> HPO <sub>4</sub> and 1.46 mM KH <sub>2</sub> PO <sub>4</sub> , 2.7 mM KCl and 137mM NaCl
<b>Potassium ferricyanide</b>	1.646 g in 100 mL PBS
<b>RBC lysis-Buffer (Ammonium chloride-buffer) 10x</b>	8.02 g Ammonium chloride, 1g potassium bicarbonate, 37.2 g disodium EDTA in 100 mL H <sub>2</sub> O

## Materials and Methods

<b>Separation-buffer</b>	0.5% BSA (w/v), 2 mM EDTA in PBS
<b>Stripping buffer</b>	10 mL SDS 10%, 3.33 mL Tris pH 8.8, 390 µL 2-mecaptoethanol in 50 in 50 mL H <sub>2</sub> O
<b>Sulfanilamide</b>	0.5 g in 10 mL 1 M HCl
<b>Tamoxifen injection solution</b>	60 mg of tamoxifen solved in EtOH at 60°C and diluted 1:60 with peanut oil
<b>TBS 20X</b>	200 mM Tris base, 2M NaCl in dd H <sub>2</sub> O
<b>Transfer buffer 10x</b>	250 mM Tris base, 1.92 mM glycine
<b>Transfer buffer 1x</b>	10% transfer buffer 10X, 20% methanol in dd H <sub>2</sub> O
<b>Tris-buffer</b>	50mM Tris base
<b>T-TBS</b>	TBS 20x, tween20 0,1% dd H <sub>2</sub> O
<b>Running buffer</b>	250 mM Tris-base, 1,92 mM glycine, 35 mM SDS in dd H <sub>2</sub> O

**Figure 5 Table of instruments**

<b>Instrument</b>	<b>Manufacturer</b>	<b>Headquarter</b>
<b>Vet ABC™ Hematology Analyzer</b>	Sciil animal care company – division of Henry Schein Animal Health	Gurnee, USA
<b>GentleMACS Dissociator</b>	Milteny Biotec	Bergisch Gladbach, Germany
<b>StepOnePlus Real-Time PCR System</b>	AB Applied Biosystems	Waltham, USA
<b>Nanodrop One</b>	Thermo Fisher Scientific	Waltham, USA
<b>ChemiDOC™ Imaging System</b>	Bio-Rad Laboratories GmbH	München, Germany
<b>BD FACSLyric™</b>	BD Biosciences	Franklin Lakes, New Jersey, USA
<b>iBright™ CL1500 Imaging System</b>	Thermo Fisher Scientific	Waltham, USA
<b>FLUOstar Optima</b>	BMG LABTECH	Ortenberg, Germany
<b>6550 QTOF-MS</b>	Agilent Technologies	Waldbronn, Germany
<b>Agilent 1290 Infinity HPLC</b>	Agilent Technologies	Waldbronn, Germany
<b>nCLD 88</b>	ECO PHYSICS AG	Duernten, Switzerland
<b>JEOL 6400 scanning electron microscope</b>	JOEL	Tokyo, Japan

**Table 6 Table of softwares**

Software	Manufacturer	Headquarter
<b>Prism 9.1.1</b>	GraphPad	San Diego, CA, USA
<b>LabChart</b>	ADInstruments	Sidney, Australia
<b>Vevo2100</b>	Visual Sonics Inc.	Toronto, Canada
<b>PowerChrome</b>	eDAQ	Colorado Springy, USA
<b>FlowJo</b>	BD Biosciences	Franklin Lakes, New Jersey, USA
<b>StepOne Software</b>	AB Applied Biosystems	Waltham, USA
<b>Image Lab Software</b>	Bio-Rad Laboratories GmbH	München, Germany
<b>Brachial Analyzer 5</b>	Medical Imaging Applications	Coralville, USA

## 3.2 Animals

All experiments in this study were approved by the LANUV (Landesamt für Natur, Umwelt und Verbraucherschutz Nordrhein-Westfalen) and by the Regional Stockholm North Ethical Committee on Animal Experiments, according to the rules of the European Convention for the protection of vertebrate animals used for experimental and other scientific purposes. Animal care was provided following institutional guidelines. Experimental groups were randomly built by choosing mice of the same age and genotype (*i.e.*, RBC Arg1 KO mice or WT littermates).

### 3.2.1 Generation of EC Arg1 KO mice

Arg1<sup>flox/flox</sup> mice were purchased from Jackson Laboratory (Jax stock:008817) (El Kasmi et al., 2008; Sorensen et al., 2009). EC Arg1 KO mice were generated by crossing Arg1<sup>flox/flox</sup> mice with EC-specific tamoxifen-inducible Cdh5-Cre/ERT2<sup>pos</sup> mice to obtain Arg1<sup>flox/flox</sup>Cdh5-Cre/ERT2<sup>pos</sup> and Arg1<sup>flox/flox</sup>Cdh5-Cre/ERT2<sup>neg</sup> mice (Sorensen et al., 2009). To induce EC-specific activation of the Cre-recombinase, 8 weeks old EC Arg1 KO mice and WT control mice were treated for 5 consecutive days with tamoxifen (33 mg/kg/day, *i.p.*), and a waiting time of 21 days was allowed.

### 3.2.2 Generation of RBC Arg1 KO mice

RBC-specific Arg1 KO mice were generated by crossing homozygous Arg1<sup>flox/flox</sup> mice with RBC-specific Hbb-Cre<sup>pos</sup> mice (Peterson et al., 2004) to obtain Arg1<sup>flox/flox</sup> Hbb-Cre<sup>pos</sup> and Arg1<sup>flox/flox</sup> Hbb-Cre<sup>neg</sup> mice. The mice used in the experiments were 3-6 months old.

### 3.2.3 Generation of RBC sGC KO mice

RBC-specific sGC KO mice were generated by crossing sGC $\alpha_1$ <sup>flox/flox</sup> mice (Mergia et al., 2006) with RBC-specific Hbb-Cre<sup>pos</sup> mice to obtain sGC<sup>flox/flox</sup> Hbb-Cre<sup>pos</sup> and sGC<sup>flox/flox</sup> Hbb-Cre<sup>neg</sup> mice, respectively. Mice between the age of 3-12 months were used. The global sGC KO mice were kindly provided by Dr. Evanthia Mergia from Rhein-Ruhr University and are already fully

## Materials and Methods

characterized (Mergia et al., 2006). In the following, the global sGC $_{\alpha 1}$  KO will be called global sGC KO mice.

To ensure that the effects found in the RBC-specific mouse lines were not due to the expression of Cre-recombinase, Hbb-Cre mice<sup>pos/neg</sup> mice were analyzed.

### 3.3 Collection of mouse tissues, blood, and cells

#### 3.3.1 Tissue collection

Mice were anesthetized with isoflurane and killed by exsanguination, and organs were explanted after perfusion with phosphate-buffered saline (PBS) and frozen in liquid nitrogen for later use.

#### 3.3.2 Blood collection and isolation of RBCs

Blood was collected by heart puncture and transferred to blood collection tubes containing EDTA as an anticoagulant (final concentration of 5 mM EDTA). Blood was centrifuged at 800xg for 10 min at 4°C. The blood divides into three layers. The upper layer contained plasma, which was collected and frozen in liquid nitrogen. The second layer was the buffy coat. It mostly contains WBCs and platelets and is discarded, including the upper layer of RBCs. RBCs were cleaned to avoid potential contamination with WBCs and platelets.

For the collection of platelet-rich plasma, blood was centrifuged at 150 x g for 10 minutes at room temperature. Plasma containing platelets was collected.

#### 3.3.3 Purification of RBC suspension

RBCs were cleaned in two steps from WBCs and platelets. WBCs were removed using a WBC filter. RBCs were resuspended to the starting volume after removal of the buffy coat and plasma in the separation buffer. WBC filters were connected to a 10 mL syringe, wetted with separation buffer, and mounted to a 50 mL falcon. The RBC suspension was added to a syringe and filtered under gravity. The filter was washed three times with separation buffer. For the collection of WBCs, the filter was turned around, the WBCs were flushed out with separation buffer, and the remaining RBCs were lysed in RBC lysis buffer for 7 minutes on ice. The WBCs were frozen in liquid nitrogen.

The RBCs pellet was resuspended in separation buffer, and anti-CD73-APC antibody was added to the RBC suspension and incubated for 15 minutes in the fridge. Afterward, anti-APC microbeads were added and incubated for 15 minutes in the fridge. The RBC suspension was transferred to a whole blood column, and the CD73<sup>-</sup> fraction (flow-through) was collected by washing three times with separation buffer.



## Materials and Methods

### 3.3.4 Bone marrow cells collection

Bone marrow cells were collected from the tibia and femur by opening both ends of the bones with scissors and placing them in a 0.5 mL tube with a hole in the bottom. The tube was placed in a 2 mL tube and centrifuged for 30 s at  $10,000 \times g$  at  $4^{\circ}\text{C}$ . RNeasy Lysis Buffer was added to the 2 mL tube if the samples were needed for RNA/DNA analysis.

### 3.3.5 Isolation of ECs from the heart and the lung

ECs ( $\text{CD31}^+ \text{CD45}^-$ ) were isolated from the heart and lung homogenates of EC Arg1 KO mice using magnetic anti-CD45 and anti-CD31 microbeads in two separate steps following the manufacturer's protocols (Milteny Biotec, Bergisch Gladbach, Germany), as previously described (Cortese-Krott et al., 2022).

Hearts were explanted, retrogradely perfused with Hanks' balanced buffer containing collagenase (450 U/mL) and DNase (60 U/mL) for 30 minutes at  $37^{\circ}\text{C}$ , minced with scissors, and incubated for an additional 15 minutes at  $37^{\circ}\text{C}$  in the perfusion solution. The cell suspension was filtered once through a  $100 \mu\text{m}$  strainer and afterward through a  $40 \mu\text{m}$  cell strainer.

From the same mouse, the lungs were explanted, homogenized in a C-tube using GentleMACS (Milteny Biotec), and incubated in collagenase enzymatic solution for 45 minutes at  $37^{\circ}\text{C}$ . The cell suspension from the lung was filtered through a  $70 \mu\text{m}$  cell strainer to obtain a single-cell suspension.

RBCs from both lung and heart cell suspensions were lysed with ammonium chloride solution at room temperature for 5 minutes.

ECs were extracted by two independent steps of magnetic separation, consisting of negative selection using anti-CD45 microbeads and positive selection using anti-CD31 microbeads. The cell suspension was labeled with anti-CD45 microbeads and incubated for 15 minutes in the fridge. The labeled cell suspension was added onto an LS-column, and the  $\text{CD45}^-$  fraction was collected in a 15 mL falcon containing separation buffer. The  $\text{CD45}^-$ -cell fraction was centrifuged and resuspended in separation buffer. For CD31 positive selection, the cell suspension was labeled with anti-CD31 microbeads and incubated for 15 minutes in the fridge. The cell suspension was washed and separated on an LS column. The flow-through was discarded, and the fraction held back during magnetic separation was collected, which is the  $\text{CD31}^+$  fraction. The purity and yield of the cells were determined by flow cytometry analysis using specific antibodies. The purity of the cells was 95%  $\text{CD31}^+$  cells of the total cells. After extraction,  $\text{CD31}^+$  cells were preserved in RNeasy Lysis Buffer and kept at  $-80^{\circ}\text{C}$  until later use.

## Materials and Methods

### 3.3.6 Isolation of erythroid cells (Ter119<sup>+</sup>) from bone marrow cells

Erythroid cells (Ter119<sup>+</sup> CD45<sup>-</sup>) were isolated from the bone marrow using magnetic anti-CD45 and anti-Ter119 microbeads in two separate steps following the manufacturer's protocols (Milteny Biotec, Bergisch Gladbach, Germany) as previously described (Leo et al., 2021). Bone marrow cells were centrifuged in a tube filled with separation buffer containing DNase (10 U/mL). RBCs were lysed with RBC-lysis buffer for 7 minutes on ice, and the cell suspension was filtered through a 40 µm cell strainer to obtain a single-cell suspension. To avoid unwanted binding of microbeads, cells were treated with FcR-blocker in the fridge for 10 minutes and then incubated with anti-CD45 microbeads for negative selection for 15 minutes in the fridge. The cell suspension was washed and resuspended in separation buffer, loaded on an LS-column, and the negative fraction (flow-through) was collected as the CD45<sup>-</sup> fraction. CD45<sup>-</sup> cells were loaded a second time onto an LS column to remove the remaining CD45<sup>+</sup> cells. For the positive selection of Ter119<sup>+</sup>-cells, the CD45<sup>-</sup>-fraction was treated with FcR-blocker for 10 minutes in the fridge and incubated with anti-Ter119 microbeads for 15 minutes in the fridge. The labeled cells were washed and resuspended in separation buffer. The cell suspension was added to a new LS column, and the Ter119<sup>+</sup> fraction was collected by removing the column from the magnet and flushing out Ter119<sup>+</sup> cells with the separation buffer. The purity and yield of the cells were determined by flow cytometry. After extraction, Ter119<sup>+</sup> cells were preserved in RNAlater and kept at -80°C until later use.

## 3.4 Molecular characterization of transgenic mice

### 3.4.1 Analysis of DNA recombination

Recombination of the DNA locus by Cre-recombinase was determined by real-time polymerase chain reaction (qPCR) in the targeted tissue/cells. Primers and probes recognizing the floxed allele and the allele targeting the deletion were designed by Transnetyx ( $\Delta$ -allele was tested by amplification of a DNA region spanning the loxP sequences by real time PCR by using specific primers as indicated in **Table 7**. The amplification was normalized by amplifying the TFRC-gene locus as a reporter. Therefore, 20 ng genomic DNA was mixed with MasterMix containing 10 µL TaqMan Gene Fast Advanced Master Mix and 1 µL Primer Assay (containing 1:5.5 primer and 1:20 reporter (**Fehler! Ungültiger Eigenverweis auf Textmarke.**)). The run consisted of 10 minutes activation/denaturation at 95°C, followed by 40 cycles of 15 seconds denaturation at 95°C degree and 1 minute annealing/DNA synthesis at 60°C. The presence of the  $\Delta$ -allele was calculated as relative copy number as following:

$$(1) \text{RCN} = 2^{-(\text{Target CT1} - \text{Housekeeper CT})}$$

The same method was applied to quantify the  $\Delta$ -allele in aorta samples of EC Arg1 KO mice, however these analyses were carried out by Transnetyx.

## Materials and Methods

**Table 7).** DNA from the bone marrow was extracted using the Allprep DNA/RNA kit. RNA later was removed from bone marrow cells after centrifugation 5000 x g for 10 minutes. Cells were lysed by adding RLT plus buffer containing 2-mercaptoethanol and homogenized with a Tissue Ruptor. The lysate was transferred to a Qiashredder and centrifuged for 3 minutes at 10,000 x g. Lysate was collected from the collection tube, transferred to the AllPrep spin column, and centrifuged for 30 seconds at 8,000 x g. The spin column containing the DNA was stored at room temperature. Ethanol 70% was added to the flow-through, and the solution was added to the RNeasy mini spin column and centrifuged for 15 s at 8,000 x g, and the flow-through was discarded. RWI buffer was added to the column and centrifuged, the flow-through was discarded, and the column was washed twice with RPE buffer. The RNA was eluted by adding water and centrifuging for 1 minute at maximum speed. An AllPrep column was used to elute DNA. AW1-buffer was added to the column and centrifuged at 8,000 x g for 15 seconds. To wash the column, AW2-buffer was added and centrifuged for 2 minutes at maximum speed. To elute the DNA from the column, EB-buffer was added to the column, incubated at room temperature for 1 minute, and centrifuged for 1 minute at 8,000 x g. The concentrations of RNA and DNA were determined with a NanoDrop spectrophotometer by analyzing A260/A280 nm absorption. The presence/absence of the  $\Delta$ -allele was tested by amplification of a DNA region spanning the loxP sequences by real time PCR by using specific primers as indicated in **Table 7**. The amplification was normalized by amplifying the TFRC-gene locus as a reporter. Therefore, 20 ng genomic DNA was mixed with MasterMix containing 10  $\mu$ L TaqMan Gene Fast Advanced Master Mix and 1  $\mu$ L Primer Assay (containing 1:5.5 primer and 1:20 reporter (**Fehler! Ungültiger Eigenverweis auf Textmarke.**)). The run consisted of 10 minutes activation/denaturation at 95°C, followed by 40 cycles of 15 seconds denaturation at 95°C degree and 1 minute annealing/DNA synthesis at 60°C. The presence of the  $\Delta$ -allele was calculated as relative copy number as following:

$$(2) \text{RCN} = 2^{-(\text{Target CT1} - \text{Housekeeper CT})}$$

The same method was applied to quantify the  $\Delta$ -allele in aorta samples of EC Arg1 KO mice, however these analyses were carried out by Transnetyx.

**Table 7 Primers for DNA recombination.** *Specific probes designed for each gene of cell-specific Arg1 KO mice and RBC-specific sGC KO mice (Transnetyx, Cordova, TN).*

Gene	Forward Primer	Reverse Primer
	Arg1 -KO	
$\Delta$ -allele	CGCAGGCTGCTAATAAAATTTAGGT	AGAGTATCCATGTACAAGAGAGGAACA
LoxP	GCTATACGAAGTTATTAGGTGATATCAGAT CC	GGGCTTTCAGCTTAAAGTGTTTAG
	sGC-KO	

## Materials and Methods

$\Delta$ -allele	CATAAGTTTGAAAGAGATCAAGGAGGC	GCACTTTACTTACTGAGCCATCTTGC
LoxP	GGTAGAGGAATCAGAAGTTCAAAGCCGTTT TGATTACA	AGCATACATTATACGAAGTTATCCTACAGG CTC

### 3.4.2 Analysis of mRNA expression in targeted and non-targeted tissues by real-time RT-PCR

Gene expression was analyzed by RT-qPCR and carried out as described previously (Leo et al., 2021). The cells were lysed by adding RLT buffer containing 2-mercaptoethanol. Tissue and organs were lysed in RLT buffer containing 2-mercaptoethanol and homogenized using a Tissue Ruptor, followed by treatment with 10  $\mu$ L proteinase K for 10 minutes at 55°C (Qiagen). The RNeasy Mini Kit combined with DNase I digestion was used to extract total RNA. Isolation of RNA was carried out as described above, but with an extra step of on-column incubation of DNase for 15 minutes at room temperature after washing with AW1-buffer. The concentration of total RNA was assessed using a NanoDrop spectrophotometer. Reverse transcription was carried out with the QuantiTect reverse transcription kit. The remaining DNA was removed by incubating the sample with gDNA wipe-out buffer for 2 minutes at 42°C. cDNA was generated from RNA by adding MasterMix containing RT, RT-primers, and RT-buffer. The sample was incubated for 15 minutes at 42°C, followed by incubation at 95°C for 3 minutes.

### 3.4.3 Reaction for the enrichment of low abundant yield

Because of the low yield of RNA in Ter119<sup>+</sup> cells and ECs, pre-amplification was carried out with SsoAdvacend PreAmp Supermix. A primer mix was prepared from the required primer by adding 5  $\mu$ L of each primer and filling it with RNase-free water to a total volume of 500  $\mu$ L.

12.5  $\mu$ L of cDNA was mixed with 12.5  $\mu$ L of primer-mix and 25  $\mu$ L of PreAmp Supermix. Pre-amplification was carried out by incubation at 95°C for 3 minutes followed by 10 cycles of 15 s at 95°C and 4 minutes at 58°C.

### 3.4.4 qPCR carried out with TaqMan-assay

- (3) To measure mRNA expression, cDNA was mixed with MasterMix containing 10  $\mu$ L TaqMan Gene Fast Advanced Master Mix and 1  $\mu$ L TaqMan Gene Expression Assay

$$(\Delta\Delta CT = \text{Sample } \Delta Ct - \text{Average Control Group } \Delta Ct)$$

$$(4) R = 2^{-\Delta\Delta Ct}$$

**Table 8).** The qPCR run was built out of 2 minutes at 50°C and 2 minutes at 95°C, followed by 40 cycles consistent with 3 seconds at 95°C and 30 seconds at 60°C and was performed using the Applied Biosystems StepOnePlus Real-time PCR System. Data were analyzed using the

## Materials and Methods

$\Delta\Delta CT$  method, as described previously (Livak et al., 2001). The mRNA expression of the gene of interest was normalized to that of Rplp0. The calculation was as following:

$$(5) \text{Average Control Group } \Delta Ct = \text{Gene of Interest } Ct_{\text{Control}} - \text{Housekeeping Gene } Ct_{\text{Control}}$$

$$(6) \Delta\Delta CT = \text{Sample } \Delta Ct - \text{Average Control Group } \Delta Ct$$

$$(7) R = 2^{-\Delta\Delta Ct}$$

**Table 8 Primer used for mRNA expression**

Gene	Assay ID	Manufacturer	Headquarter
<b>Rplp0</b>	Mm00725448_s1	ThermoFisher	Waltham, USA
<b>Gucy1a3</b>	Mm00517661_m1	ThermoFisher	Waltham, USA
<b>Nos3</b>	Mm01134920_m1	ThermoFisher	Waltham, USA
<b>Arg1</b>	Mm01190441_g1	ThermoFisher	Waltham, USA

### 3.4.5 Analysis of targeted protein levels via Western blot and ELISA

Western blot analysis and detection were carried out as described previously (Erkens et al., 2015). Targeted and non-targeted tissues from WT and KO mice were lysed in RIPA buffer containing protease inhibitor cocktail (Roche) and homogenized on ice, followed by sonication and centrifugation at  $10,000 \times g$  for 10 minutes. Lysates were loaded onto a 10% SDS Bis-Tris gel and transferred to a nitrocellulose membrane. The membranes were blocked for 1 hour with 5% milk (BioRad) in T-TBS. The membranes were incubated overnight at 4°C with antibodies (**Table 4**). After washing for 1 hour in T-TBS, the membrane was incubated with HRP-conjugated antibodies for 1 hour at room temperature and the bands were detected using super signaling solution and quantified using Image Lab Software.

### 3.4.6 Determination of Arg1 protein levels in the aorta

Quantitative measurement of Arg1 protein levels in the aorta were measured using a commercially available enzyme-linked immunosorbent assay (ELISA) kit (Abcam, ab269541). Aorta was lysed in cell lysis buffer and the standard curve was prepared from Arg1 standard by serial dilution (500 pg/mL – 7.81 pg/mL). The sample and standard (50  $\mu$ L) were added to the well, and 50  $\mu$ L antibody-mix was added and incubated for 1 hour at room temperature. The wells were washed three times with washing solution. TMB solution (100  $\mu$ L) was added and incubated for 10 minutes at room temperature in the dark. The reaction was stopped by adding 100  $\mu$ L of stop-solution, and absorption was measured at 450 nm.

## Materials and Methods

### 3.4.7 Determination of *Agr1* expression by immunotransmission electronic microscopy

The immunotransmission electronic microscopy (immunoTEM) was performed a previously described (Johnstone et al., 2012). RBCs were isolated by cardiac puncture and fixed in 4% PFA containing 0.05% glutaraldehyde. RBCs were spun down, embedded in LR White, and sectioned into 70 nm sections. RBC were stained overnight with 1:10 rabbit-Arg1 antibody. Goat anti-rabbit 12 nm gold beads (1:50) were used to resolve protein localization on the RBCs and imaged using an electron microscope.

### 3.4.8 Urea assay for determination of arginase activity in targeted tissues.

Lysates of tissues and cells were incubated with 10 mM  $MnCl_2$  (final concentration 6 mM) for 10 minutes at 60°C for activation of arginase. Afterward, the sample was incubated with 500 mM L-arginine (final concentration 142.86 mM) at 37°C, as shown in **Table 9**. The reaction was stopped by adding an acid mix ( $H_2SO_4$ ,  $H_3PO_4$ , and  $H_2O$  1:3:7) and  $\alpha$ -isonitrosopropiophenone was added and incubated for 1 hour at 100°C for a colorimetric reaction with the produced urea. The urea concentration was determined at 540 nm, and the activity was calculated as nmol/urea/mg protein/h.

**Table 9 Parameters for arginase assay**

Tissue	Protein amount [ $\mu$ g]	Incubation at 37°C
<b>Aorta</b>	75	1 hour
<b>RBCs</b>	250	3 hours
<b>WBCs</b>	70	3 hours
<b>Platelets</b>	100	3 hours
<b>Plasma</b>	800	2 hours

## 3.5 Characterization of systemic hemodynamics and vascular function

### 3.5.1 Blood pressure measurements by Millar catheterization

Systemic hemodynamics were measured by invasive catheterization using a 1.4F Millar pressure-conductance catheter (SPR-839, Millar Instrument, Houston, TX, USA). The catheter was placed in the right carotid artery, and cardiac performance was measured in the left ventricle of the heart as outlined previously (Erkens et al., 2015). The measurement was recorded with a Millar box, and LabChart 7 (AD Instruments, Oxford, UK) was used for analysis.

### 3.5.2 Measurement of vascular function in vivo

Vascular function was assessed by flow-mediated dilation (FMD) using a Vevo 2100 with a 30-70 MHz linear array Microscan transducer (VisualSonics), as previously described (Erkens et

## Materials and Methods

al., 2018). Changes in vessel diameter of the iliac artery in response to shear stress were measured. Mice were anesthetized with isoflurane (2-3%) with a breathing rate of 100 breaths/minute. To measure FMD a vascular occluder was placed around the lower limb of a leg to induce occlusion of the iliac artery for 5 minutes followed by 5 minutes reperfusion. Pictures of the vessel were taken every 20-30 second during occlusion and reperfusion. The diameter of the iliac artery at different time points was analyzed using Brachial Analyzer 5 software.

### *3.5.3 Measurement of endothelial function ex vivo*

Functional studies for both conductance vessels (aorta) and small resistance vessels (third branch mesenteric arteries) were carried out as described before (Moretti et al., 2019; McCann Haworth et al., 2021). The vessels were immediately excised and cleaned, and vessel rings were mounted onto a myograph chamber (model 620 M; Danish Myo Technology, Denmark). The vessels were then equilibrated for 45 minutes in physiological saline solution and bubbled with carbogen gas. The different types of vessel rings underwent a standard normalization process, and a loading force was applied to replicate the pressure found in the physiological vessel wall. Vessels were pre-constricted with increasing concentrations of phenylephrine (Phe, 0.1 nM to 10  $\mu$ M) to reach 80% of maximal high potassium physiological solution-induced contraction. After reaching a stable contraction plateau, the vessels were exposed to increasing concentrations of acetylcholine (ACh, 1 nM to 100  $\mu$ M) for testing endothelium-dependent relaxation. Endothelium-independent relaxation was tested using cumulative concentrations of sodium nitroprusside (SNP, 1 nM to 100  $\mu$ M).

### *3.5.4 Induction of acute myocardial infarction (AMI) and measurement of infarct size and left ventricular function*

Myocardial ischemia was carried out as described before with some modifications (Erkens et al., 2018). For myocardial ischemia, mice were intubated and anesthetized (2% isoflurane), and the left anterior descending coronary artery was occluded for 45 minutes. Following this, 24 hours period of reperfusion was performed. For the evaluation of areas at risk (AAR) and non-ischemic areas, computer-assisted planimetry was used. The infarct size was determined by staining with 2,3,5-triphenyl tetrazolium chloride (TTC), as described (Erkens et al., 2018). Left ventricular (LV) function was analyzed by echocardiography in anesthetized mice (2.5% isoflurane) before and after AMI.

### **3.6 Hematological analysis**

#### *3.6.1 Blood count and reticulocyte count*

Blood was transferred to blood collecting tubes containing EDTA as an anticoagulant, and blood counts were performed using a Coulter counter. Reticulocyte count was performed by flow cytometry as described previously (Nobes et al., 1990). Blood was diluted 1:1000 in PBS and stained for 30 minutes with thiazole orange in the dark at room temperature. A non-stained control was used for each sample. The percentage of reticulocytes in the total circulating blood cells was measured by flow cytometry.

#### *3.6.2 Measurement of transferrin levels in plasma*

Transferrin levels in plasma were measured using a commercially available ELISA. The standard curve was prepared from transferrin standard by serial dilution (100 ng/mL – 3.125 ng/ml) and plasma samples were diluted 1:100,000. 100 µL of standard or sample were added into the well of the ELISA. The solution was incubated for 30 minutes at room temperature. The solution was discarded, and the wells were washed four times. Then, 100 µL of enzyme-antibody was added and incubated for 30 minutes in the dark. Wells were washed and TMB-solution was added and incubated in the dark for 10 minutes at room temperature. The stop solution (100 µL) was added, and the absorption was measured at 450 nm.

#### *3.6.3 Measurement of ferritin levels in plasma*

Ferritin levels in plasma were measured using a commercially available ELISA. A standard curve of ferritin was prepared by serial dilution (400 ng/mL – 12.5 ng/mL) and plasma samples were diluted 1:10. 100 µL of the sample and standard were incubated for 60 minutes in the well. The wells were washed four times and 100 µL of enzyme-antibody solution was incubated in the well for 10 minutes in the dark. The wells were washed again four times and incubated with 100 µL of TMB-solution for 10 minutes at room temperature in the dark. The reaction was stopped by adding 100 µL of stop solution, and absorption was measured at 450 nm.

#### *3.6.4 Measurement of EPO levels in plasma*

EPO levels in the plasma were measured using a mouse EPO-ELISA kit. A standard curve was prepared (160 pg/mL – 1.34 pg/mL) and plasma samples were diluted 1:2. 100 µL of samples or standard was added into the well and incubated for 2.5 hours at room temperature with gentle shaking. Wells were washed four times with washing solution, and 100 µL of biotinylated antibody was added to each well and incubated for 1 hour. Wells were washed again four times and 100 µL of streptavidin-HRP-solution was added and incubated for 45 minutes. The wells were washed four more times and TMB-solution was added and incubated



## Materials and Methods

for 30 minutes in the dark at room temperature. The stop solution (50  $\mu$ L) was added, and the absorption was measured at 450 nm.

### *3.6.5 Measurement of free hemoglobin in plasma*

Free hemoglobin was measured using a commercially available ELISA. A standard curve was prepared in the range of 400 ng/ml – 12.5 ng/mL and plasma was diluted 1:4000. The standard and sample (100  $\mu$ L) were incubated in the well for 60 minutes. The solution was discarded, and the wells were washed four times. The enzyme-antibody solution (100  $\mu$ L) was incubated for 30 minutes in the dark, and the wells were washed four times. The TMB-solution (100  $\mu$ L) was added and incubated for 10 minutes in the dark. The stop-solution was added, and the absorption was measured at 450 nm.

### *3.6.6 Quantitative analysis of erythroid differentiation in bone marrow and spleen*

Erythroid differentiation was analyzed by flow cytometry, as described previously (Liu et al., 2013). Bone marrow cells were collected in a tube containing separation buffer with DNase (10 units/mL) and passed through a 40  $\mu$ m cell strainer. The spleen was minced with scissors and passed through a 70  $\mu$ m cell strainer. The cell suspensions were incubated with FcR-blocker for 10 minutes in the fridge. Afterward, anti-CD45 microbeads were added and incubated for 15 minutes in the fridge. The cell suspension was added to an LS-column and the CD45 negative fraction was collected. CD45<sup>-</sup> cells were stained with Anti-CD45, anti-CD44, and anti-Ter119 antibodies for 20 minutes and washed. Additionally, 7-AAD for live/dead staining was used by incubation for 10 minutes in the fridge. Dead cells and CD45<sup>+</sup> cells were gated out. The proerythroblast population was gated as CD44<sup>hi</sup>/Ter119<sup>low</sup>. Basophilic, polychromatic, and orthochromatic erythroblasts, as well as reticulocytes and RBCs, are gated by size (FSC) and CD44 expression.

### *3.6.7 Pappenheim-staining of bone marrow cells*

Bone marrow cells were centrifuged in a tube containing 5  $\mu$ L citrate buffer as an anticoagulant. A bone marrow smear was done, and microscope slides were stained for Pappenheim staining. Briefly, microscope slides were incubated first in May-Grunwald-solution for 10 minutes and briefly washed in dd-H<sub>2</sub>O for two minutes followed by a second staining in diluted Grims-solution (1:10) for 20 minutes. Quantification of erythropoiesis and granulopoiesis was performed under a microscope at 100x magnification by counting 400 cells and calculating the percentage of each cell type.

### *3.6.8 Semisolid colony forming assay for bone marrow and spleen cells*

For bone marrow cells, the tibia and femur were opened, and the cells were centrifuged in 300  $\mu$ L PBS. A single-cell suspension was obtained by passing cells through a 40  $\mu$ m strainer. The

## Materials and Methods

spleen was minced with scissors and pressed through a 40  $\mu\text{m}$  strainer. The single-cell suspension was centrifuged at 300 g for 10 minutes and the supernatant was removed. The spleen suspension was resuspended in 3 mL of PBS, and big partials were allowed to settle. The supernatant was then transferred to a new Falcon tube. The cell number was identified by the Neubauer cell count.  $6.25 \times 10^4$  bone marrow and  $5 \times 10^5$  spleen cells were mixed with 2.5 mL MethoCult (GF-M-3434) and 1 mL of cell-solution was dispensed into 35-mm dishes. Semisolid cultures were maintained for 10 days in a humidified  $\text{CO}_2$  incubator at  $37^\circ\text{C}$ . Colonies were counted under a microscope at 4x/10x magnification.

### 3.7 Measurement of metabolites in tissue, cells, and plasma

#### 3.7.1 *Measurement of NO metabolites in blood and organs*

Nitrite, nitrosyl heme (NO-heme), and nitrosated (S-nitroso and N-nitroso) product (RXNO) levels were measured in tissues, cells, and plasma using gas phase chemiluminescence, as described previously (Bryan et al., 2004). Blood was collected by heart puncture and transferred to a 2 mL tube containing 0.1 mL NEM/EDTA solution (100 mM). Whole blood was centrifuged at  $3000 \times g$  for 2 minutes at  $4^\circ\text{C}$ . Plasma and RBC were separated and frozen in liquid nitrogen. Organs were perfused with NEM/EDTA solution and weighed after collection. All samples were stored at  $-80^\circ\text{C}$ . All samples from each organ were measured on the same day. The organs and tissues were homogenized in NEM/PBS/EDTA. All organs and tissues, except the aorta, were diluted 1:12.5, aorta 1:40. RBCs were lysed with a solution of NEM 10mM/EDTA 2.5 mM/MilliQ water 1:3. Plasma was injected without any dilution. NO-heme levels were quantified by denitrosation in potassium hexacyanoferrate (III) in PBS. Nitrite and RXNOs were determined by reductive cleavage with an iodide/triiodide solution. Released NO from these reactions was detected by chemiluminescent reaction with ozone. Solutions of each metabolite were injected into different reaction chambers. Measurement of nitrite and RXNOs was performed in a  $60^\circ\text{C}$  chamber, and NO-heme levels were determined in a  $37^\circ\text{C}$  chamber. To detect nitroso species, sulfanilamide was added at a ratio of 1:10 and incubated for 15 minutes at room temperature.

For the quantification of nitrate levels, the samples were deproteinized with ice-cold methanol (1:1 v/v) and cleared by centrifugation. Nitrate levels were measured by high-performance liquid chromatography using a dedicated nitrite/nitrate analyzer.

#### 3.7.2 *Measurement of L-arginine, L-ornithine, and L-citrulline concentrations in plasma by LC-MS*

The concentrations of amino acids were detected by LC-MS as described before (Heuser et al., 2022). Plasma was diluted 1:10 with MeOH containing 0.1% formic acid and centrifuged for 10 minutes at  $16,000 \times g$  for protein precipitation. The supernatant was spiked with the

## Materials and Methods

internal standard 2  $\mu\text{M}$   $^{13}\text{C}$ -labeled L-arginine for quantification. The samples were loaded on an Agilent 1290 Infinity HPLC system to a 6550 qTOF-MS (Agilent Technologies, Waldbronn, Germany).

### **3.8 Statistical analysis**

Unless otherwise specified, all results are presented as mean  $\pm$  standard deviation (SD). Statistical analysis was carried out with GraphPad 9 for Windows (Version 9.3.1(471)). Unpaired Student's t-test with Welch's correction was used to determine statistical significance between two independent groups. For multiple comparisons, the Holm-Šídák method was used. Differences were considered statistically significant at  $p < 0.05$ .

## 4 Results

### 4.1 The role of EC Arg1 in the regulation of vascular function *in vivo*

The role of Arg1 in ECs is controversial and not completely understood. The aim of this study was to characterize EC-specific Arg1 KO mice and investigate the role of Arg1 in ECs in the regulation of systemic hemodynamics, vascular function, and L-arginine and NO bioavailability.

#### 4.1.1 Generation of EC Arg1 KO mice

To generate EC Arg1 KO mice, Arg1<sup>flox/flox</sup> mice were crossed with tamoxifen-inducible EC-specific Cdh5-Cre/ERT2<sup>pos</sup> mice to obtain Arg1<sup>flox/flox</sup>Cdh5-Cre/ERT2<sup>pos</sup> mice and Arg1<sup>flox/flox</sup>Cdh5-Cre/ERT2<sup>neg</sup> mice as WT littermates. Mice at the age of 8-9 weeks were treated for 5 constitutive days with tamoxifen to induce Cre-recombinase activity in Arg1<sup>flox/flox</sup>Cdh5-Cre/ERT2<sup>pos</sup> mice. Tamoxifen treatment leads to Cre-induced DNA recombination by removing exons 7 and 8, resulting in the generation of EC Arg1 KO mice. Recombination of the DNA locus in the aorta was confirmed by real-time PCR (**Figure 6 C**).

## Results

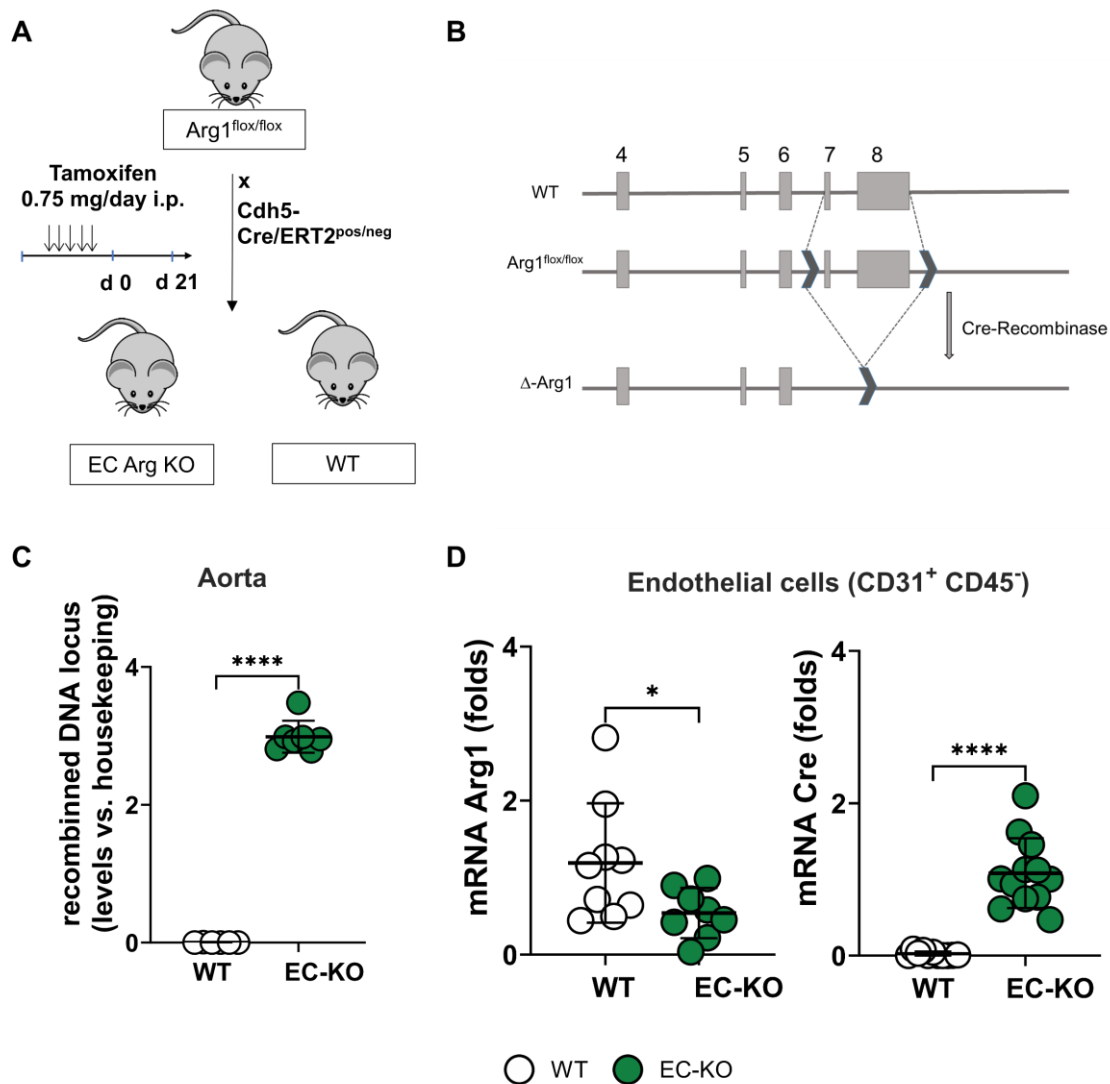


**Figure 6 - Genetic characterization of EC Arg1 KO mice.** (A) Schematic representation of the crossing strategy of EC Arg1 KO mice. *Arg1<sup>flox/flox</sup>* mice were crossed with EC-specific tamoxifen-inducible Cre mice (*Cdh5-Cre/ERT2<sup>pos</sup>*) and treated with tamoxifen for 5 days after 21 days mice were used for experiments. (B) Scheme describing the gene-targeting strategy. (C) Analysis of tissue-specific recombination of the DNA locus in the aorta using real-time PCR. DNA recombination was only found in EC Arg1 KO mice but not in littermate controls. (D) Real-time reverse PCR analysis of *Arg1* expression in ECs isolated from the heart and lung showed a significant decrease in mRNA expression in EC Arg1 KO mice. Expression of Cre-recombinase was only found in the EC Arg1 KO mice but not in the WT control group.

Furthermore, ECs (CD31<sup>+</sup>CD45<sup>-</sup>) isolated from heart and lung tissues of EC Arg1 KO mice showed a significantly reduced expression of *Arg1* but showed the expression of Cre-recombinase. WT littermates expressed *Arg1* but not Cre-recombinase (**Figure 6 D**). To investigate whether the lack of *Arg1* in ECs affects hematological parameters, a blood count was performed, as shown in **Table 10**. The analysis did not show any significant differences between EC Arg1 KO mice and WT littermates.

## Results

**Table 10 Results of blood count of EC Arg1 KO mice and WT littermate controls** The table summarizes the blood count parameters measured in EC Arg1 KO mice and WT controls. Abbreviations: RBC, red blood cells; HCT, hematocrit; HGB, hemoglobin; RDW, RBC distribution width; MCHC, mean corpuscular hemoglobin concentration; MCH, mean corpuscular hemoglobin; MCV, mean corpuscular volume; WBC, white blood cells; Lymph, lymphocytes; Mo, monocytes; Gra, granulocytes; PLT, platelet count; MPV, mean platelet volume. All data are expressed as the mean  $\pm$  SD. Welch's t-test.

	WT	EC Arg1 KO	p
n	7	8	
<b>Red blood cell count</b>			
RBC ( $10^6/\mu\text{l}$ )	8.0 $\pm$ 0.9	8.3 $\pm$ 0.9	0.524
HCT (%)	40.1 $\pm$ 6.4	41.8 $\pm$ 6.8	0.669
HGB (g/dl)	12.4 $\pm$ 2.1	12.8 $\pm$ 2.1	0.769
<b>Red blood cell indexes</b>			
RDW (%)	16.2 $\pm$ 1.0	15.8 $\pm$ 1.2	0.548
MCHC (g/dl)	30.9 $\pm$ 0.8	30.6 $\pm$ 1.1	0.599
MCH (pg)	15.5 $\pm$ 1.2	15.2 $\pm$ 1.3	0.764
MCV ( $\mu\text{m}^3$ )	50 $\pm$ 3.0	50.0 $\pm$ 3.5	1.000
<b>White blood cell count</b>			
WBC ( $10^3/\mu\text{l}$ )	5.4 $\pm$ 1.3	5.2 $\pm$ 1.9	0.861
Lymph ( $10^3/\mu\text{l}$ )	3.5 $\pm$ 0.6	3.1 $\pm$ 0.8	0.391
Lymph (%)	68.4 $\pm$ 9.8	65.1 $\pm$ 12.1	0.614
Mo ( $10^3/\mu\text{l}$ )	0.3 $\pm$ 0.2	0.3 $\pm$ 0.1	0.926
Mo (%)	5.5 $\pm$ 1.3	6.9 $\pm$ 2.1	0.187
Gra ( $10^3/\mu\text{l}$ )	1.6 $\pm$ 0.7	1.7 $\pm$ 1.0	0.773
Gra (%)	26.2 $\pm$ 8.6	28.0 $\pm$ 10.7	0.744
<b>Platelet count</b>			
PLT ( $10^3/\mu\text{l}$ )	1357.7 $\pm$ 806.0	1528.8 $\pm$ 768.4	0.774
MPV ( $\mu\text{m}^3$ )	5.4 $\pm$ 0.4	5.4 $\pm$ 0.4	0.747

### 4.1.2 Reduced mRNA expression of Arg1 but increased arginase activity in the aorta

RT-qPCR and western blotting were carried out to analyze whether the cell-specific deletion of Arg1 in ECs leads to reduced expression or activity of Arg1 in the aorta. Analysis of mRNA expression in the aorta of EC Arg1 KO mice showed a significant decrease in the expression of Arg1 compared to the WT control (**Figure 7 A**). On the other hand, no changes in protein levels were found in the aorta detected by Western blot analysis and ELISA (**Figure 7 B+C**). Moreover, a significant increase in Arg1 activity was found in the aorta (**Figure 7 D**), indicating that the lack of Arg1 in ECs leads to a compensatory increase in Arg1 expression in other compartments.

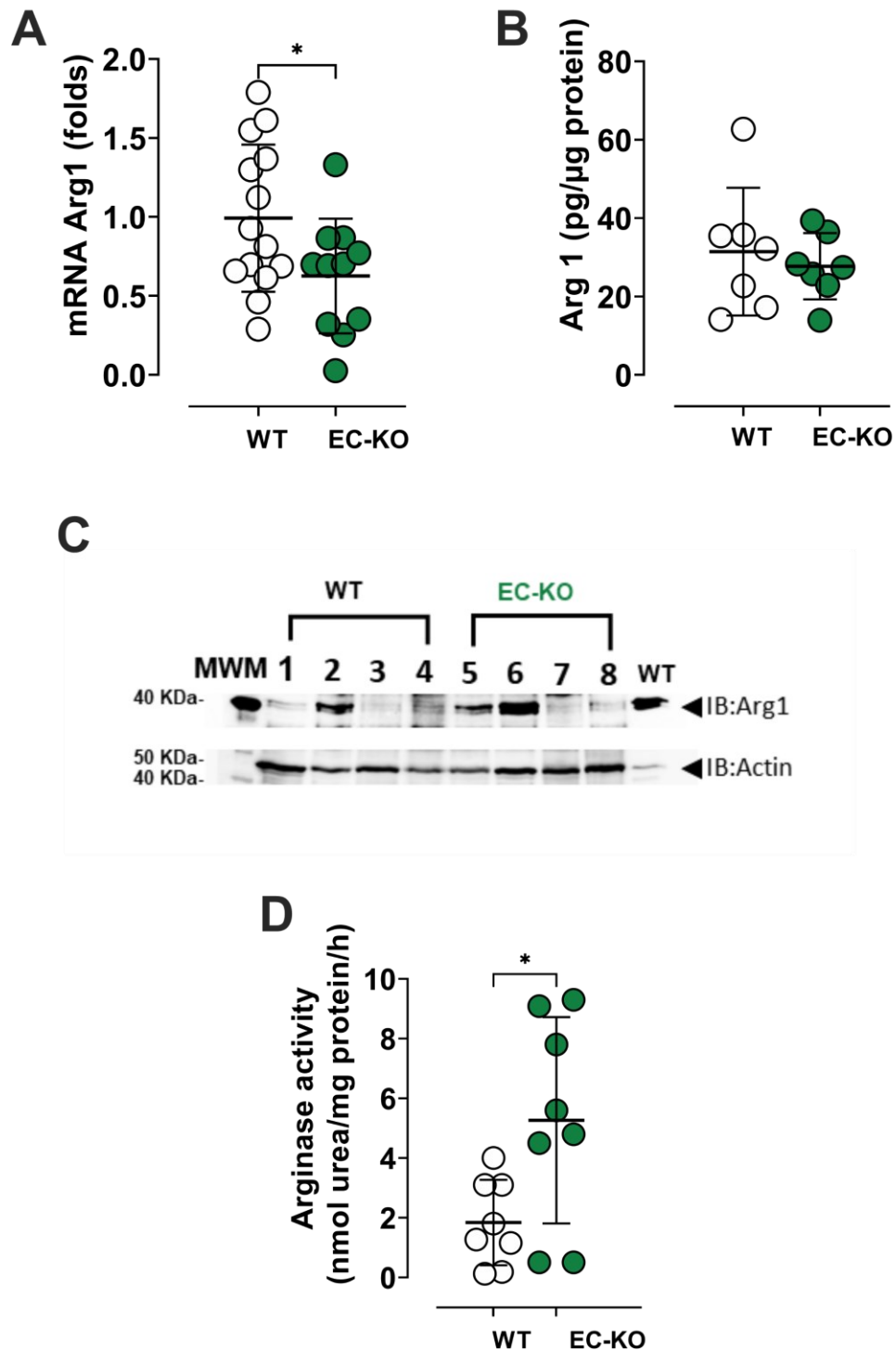


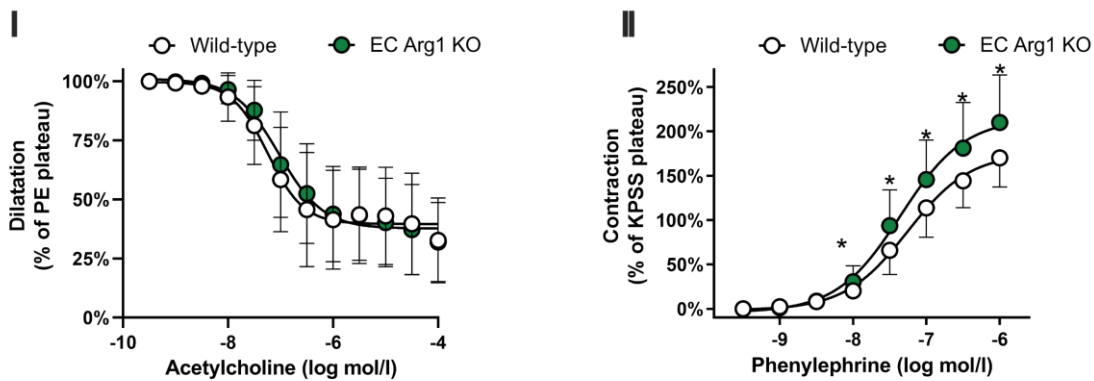
**Figure 7 - Decreased Arg1 expression in aorta but preserved protein levels** A) mRNA expression of Arg1 in lysate of aorta showed a significant decrease in EC Arg1 KO mice as compared to the WT littermate controls (Welch's t-test; \* $p < 0.05$ ). B) The total arginase protein concentration in the aorta was analyzed by ELISA and did not show any differences (Welch's t-test; ns). C) Protein levels of Arg1 in the lysate of the aorta were determined by Western Blot and did not show any differences between EC Arg1 KO mice and WT littermates. D) Overall arginase activity in the aorta was significantly increased in EC Arg1 KO mice as compared to the WT controls (Welch's t-test, \* $p < 0.05$ ).

## Results

### 4.1.3 Endothelial function is preserved in EC Arg1 KO mice.

Arg1 and eNOS are expressed in ECs and use L-arginine as a substrate. Previously, it was speculated that Arg1 may steal L-arginine from eNOS and indirectly regulate eNOS activity. To analyze whether the lack of EC Arg1 KO mice has an impact on vascular function, endothelium-dependent vasorelaxation in response to Ach was analyzed *ex vivo*. It was expected that the lack of Arg 1 in the ECs would improve eNOS-dependent vasorelaxation in both conduit arteries and mesentery arteries. Interestingly, isolated vessels from EC Arg1 KO mice showed fully preserved eNOS-dependent vasorelaxation towards ACh in both conduit arteries and resistance vessels (**Figure 8 A-I+B-I**). Moreover, mesenteric arteries did not show any changes in response to the vasoconstrictor PE (**Figure 8 B-II**).

#### A Aorta



#### B Mesentery Artery

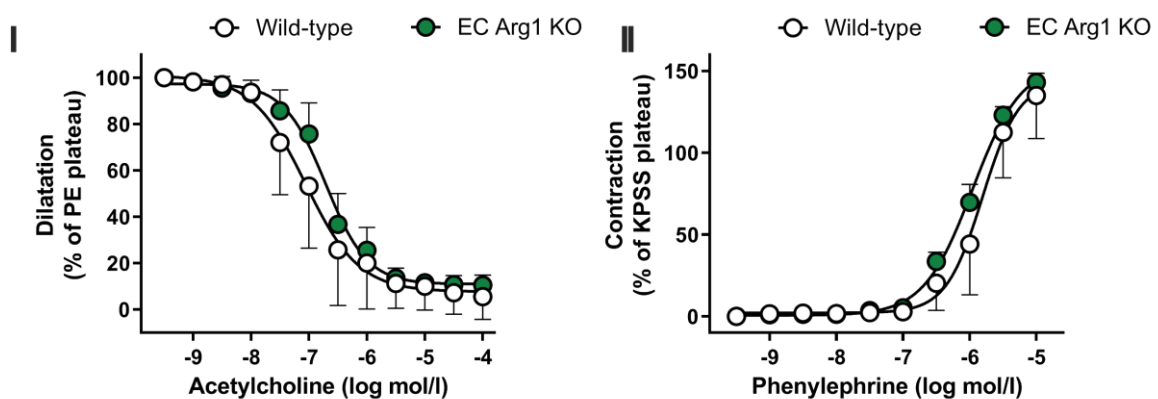


**Figure 8 - Preserved vascular response to ACh in resistance and conductance arteries of EC Arg1 KO mice.** A) Aortic rings: (I) endothelial-dependent vasorelaxation curve to acetylcholine (ACh) in pre-constricted aortic rings (n=8). (II) Vasocontractile response curve to phenylephrine in aortic rings (n=8), unpaired t-test, \*p<0.05. B) 3<sup>rd</sup> order mesentery artery: (I) Endothelial-dependent vasorelaxation (II) Vasocontractile response curve to phenylephrine



## Results

This finding is consistent with the preserved systemic hemodynamics and cardiac performance observed in EC Arg1 KO mice (**Table 11**). In contrast, an increased contractility response to PE was found in aortic rings isolated from EC Arg1 mice compared to littermate controls (**Figure 8 A-II**). These results indicate that Arg1 expressed in ECs plays a minor role in the regulation of vascular function and systemic hemodynamics by affecting the contractility response to PE.

**Table 11 Parameters of systemic hemodynamics and cardiac function in EC Arg1 KO mice and WT littermate controls.** Data are reported as mean  $\pm$  SD. n= number of analyzed mice. Differences between WT and EC Arg1 KO were calculated using Welch's t-test.

Parameter	WT		EC Arg1 KO		p
	Mean $\pm$ SD	n	Mean $\pm$ SD	n	
Heart rate (bpm)	467 $\pm$ 64	9	456 $\pm$ 50	8	0.3907
Systolic blood pressure (mmHg)	96 $\pm$ 3	9	94 $\pm$ 5	8	0.2491
Diastolic blood pressure (mmHg)	64 $\pm$ 6	9	61 $\pm$ 7	8	0.3735
Mean arterial pressure (mmHg)	75 $\pm$ 5	9	72 $\pm$ 6	8	0.3175
dP/dt <sub>max</sub> (mmHg/s)	7331 $\pm$ 1945	9	7491 $\pm$ 1096	8	0.8432
dP/dt <sub>min</sub> (mmHg/s)	-7803 $\pm$ 1897	9	-7135 $\pm$ 910	8	0.6856

#### 4.1.4 Downregulation of eNOS expression but preserved systemic NO metabolites and L-arginine bioavailability.

Next, the effect of the lack of Arg1 in ECs on eNOS expression in the aorta, as well as systemic NO metabolites and global L-arginine bioavailability was investigated. It was assumed that the lack of EC Arg1 has an impact on the global L-arginine bioavailability or increases the levels of NO metabolites (Bhatta et al., 2017). It was surprising to see a decrease in eNOS mRNA levels in the aorta, as well as a decrease in eNOS protein levels in the aorta of EC arg1 KO mice compared to the littermate controls (**Figure 9**).

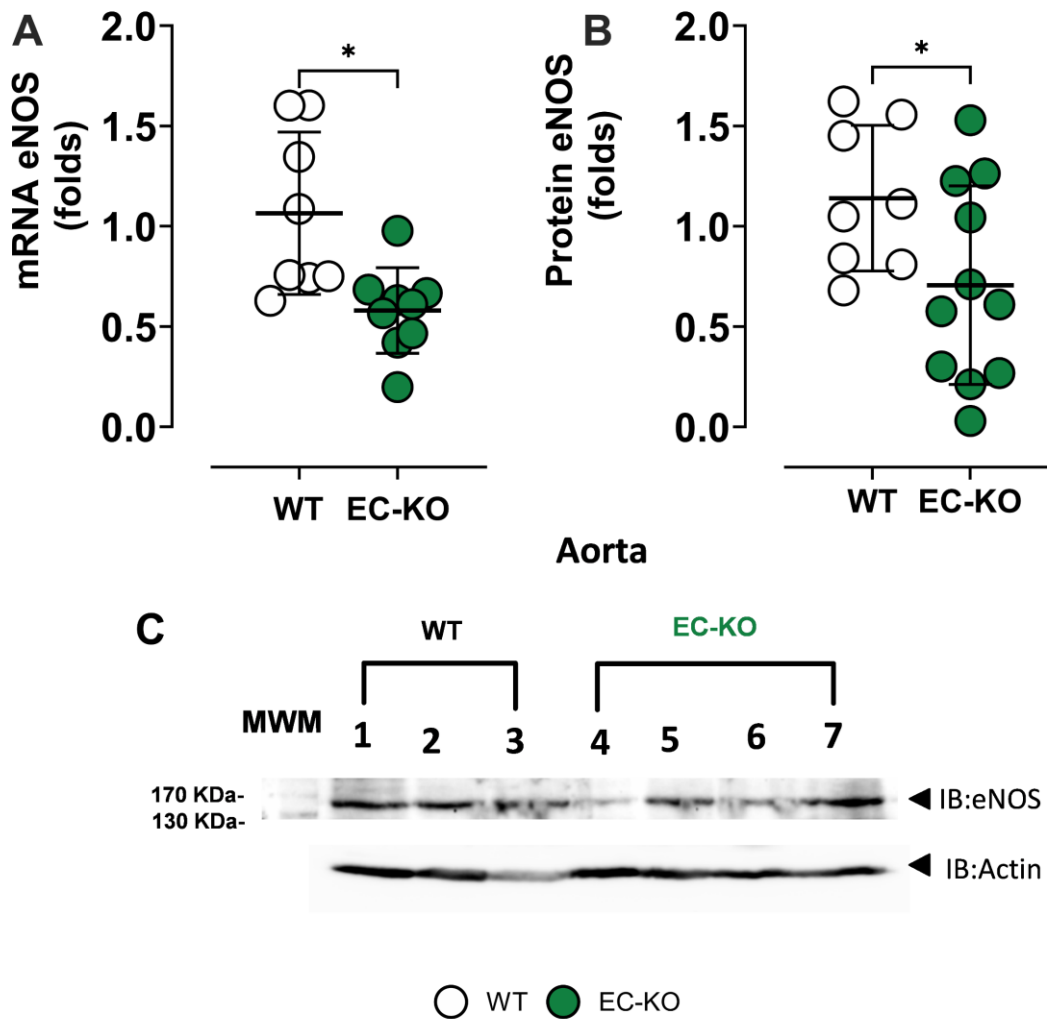


**Figure 9 - Downregulation of eNOS in the endothelium.** A) The mRNA expression of eNOS in the aorta quantified by RT-qPCR showed a significant decrease in EC Arg1 KO mice (Welch's t-test;  $* < 0.05$ ). B+C) Relative eNOS protein expression quantified by Western blot and normalized to actin showed a significant decrease in EC Arg1 KO mice.

In contrast, no changes in nitrite levels were found in the plasma and aorta, as well as in all other organs (**Figure 10, Table 12**). Interestingly, decreased heme-NO levels in the lung and increased levels in the liver of EC Arg1 KO mice were detected (**Table 12**).

## Results

**Table 12 Distribution of NO metabolites in blood and organs of EC Arg1 KO mice and corresponding WT littermate controls. Welch's t-test between the groups. \* $p < 0.05$  \*\* $p < 0.01$  \*\*\* $p < 0.001$ ; †one value was excluded as outlier according to the Tukey test, §Two values were not determined/available, or one was excluded as an outlier according to the Tukey test.**

Metabolite		WT	EC Arg1 KO	p
n		8	8	
<b>Heart</b>				
Nitrite	$\mu M$	0.72 $\pm$ 0.26	0.89 $\pm$ 0.27	0.2433
RXNO	nM	11.07 $\pm$ 4.39 <sup>†</sup>	14.86 $\pm$ 9.38	0.3302
heme-NO	nM	7.73 $\pm$ 1.95	8.34 $\pm$ 3.74	0.6902
Total NO species	$\mu M$	0.74 $\pm$ 0.26	0.91 $\pm$ 0.27	0.2256
<b>Lung</b>				
Nitrite	$\mu M$	2.42 $\pm$ 0.24	2.48 $\pm$ 0.48 <sup>§</sup>	0.8019
RXNO	nM	104.32 $\pm$ 54.12	74.42 $\pm$ 16.23	0.1717
heme-NO	nM	15.32 $\pm$ 4.60 <sup>†</sup>	8.28 $\pm$ 3.00	0.0060**
Total NO species	$\mu M$	2.54 $\pm$ 0.26	2.21 $\pm$ 0.11 <sup>†</sup>	0.4450
<b>Liver</b>				
Nitrite	$\mu M$	2.71 $\pm$ 1.14	3.10 $\pm$ 1.39 <sup>†</sup>	0.5672
RXNO	$\mu M$	0.49 $\pm$ 0.30	0.56 $\pm$ 0.26	0.6241
heme-NO	nM	46.96 $\pm$ 22.05	110.02 $\pm$ 68.64	0.0370*
Total NO species	$\mu M$	3.25 $\pm$ 1.46	3.74 $\pm$ 1.71 <sup>†</sup>	0.5616
<b>Aorta</b>				
Nitrite	$\mu M$	12.60 $\pm$ 5.88	20.39 $\pm$ 17.86	0.2729
RXNO	nM	152.63 $\pm$ 102.77	109.20 $\pm$ 55.29	0.3516
heme-NO	nM	22.81 $\pm$ 8.89 <sup>†</sup>	28.28 $\pm$ 12.98 <sup>†</sup>	0.3778
Total NO species	$\mu M$	1.28 $\pm$ 0.59	2.05 $\pm$ 1.79	0.2756
<b>Plasma</b>				
Nitrate	$\mu M$	13.38 $\pm$ 4.64	12.70 $\pm$ 5.20	0.7797
Nitrite	nM	196.76 $\pm$ 50.70 <sup>†</sup>	239.55 $\pm$ 56.05	0.1447
RXNO	nM	6.74 $\pm$ 4.52 <sup>†</sup>	3.85 $\pm$ 0.71	0.1435
Total NO species	nM	203.49 $\pm$ 53.84 <sup>†</sup>	242.91 $\pm$ 55.72	0.1877
<b>Erythrocytes</b>				
Nitrite	nM	405.63 $\pm$ 90.31	442.26 $\pm$ 56.62	0.3506
RXNO	nM	29.08 $\pm$ 7.54	40.75 $\pm$ 15.19	0.0793
heme-NO	nM	1.27 $\pm$ 0.54	1.97 $\pm$ 0.88	0.0794
Total NO species	nM	435.98 $\pm$ 93.14	484.99 $\pm$ 59.78	0.2344

## Results

Moreover, the L-arginine bioavailability was analyzed by measuring the levels of L-arginine, L-ornithine, and L-citrulline in the plasma and using the ratio [L-arginine/(L-ornithine+L-citrulline)]. Plasma levels of all three amino acids and L-arginine bioavailability were unchanged in the EC Arg1 KO mice compared to the control group (**Figure 10**). These findings indicate that EC Arg1 plays a minor role in controlling the specific levels of L-arginine in plasma and global L-arginine bioavailability under homeostatic conditions, and indicates that other compartments may play a predominant role.

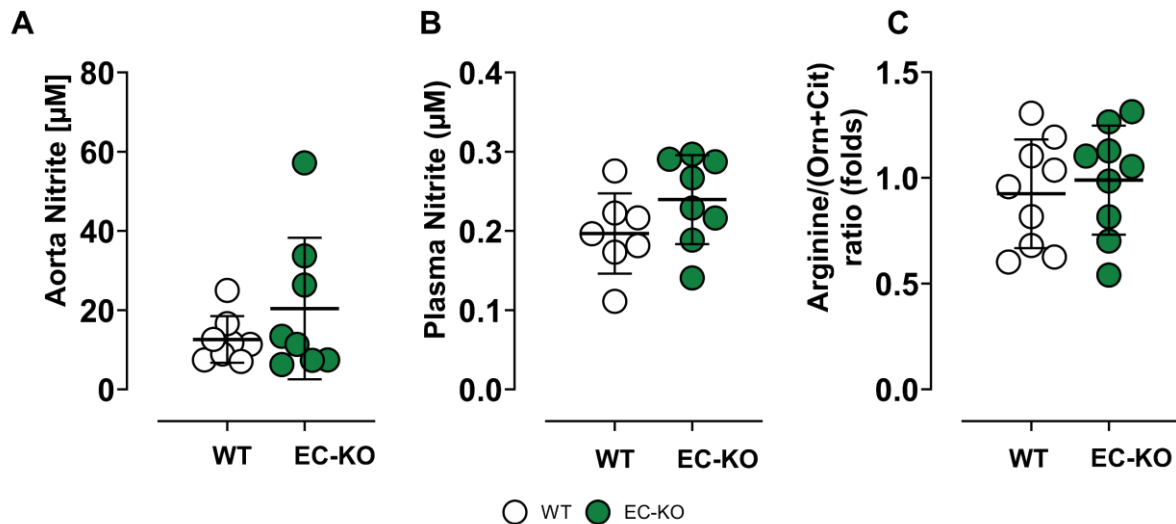


**Figure 10 - Preserved NO metabolites and L-arginine bioavailability.** A) Nitrite levels measured in the aorta did not show any changes between WT and EC Arg1 KO mice; B) No changes were found in circulating nitrite levels measured in plasma. C) The lack of Arg1 in ECs did not affect the global L-arginine bioavailability.

### 4.1.5 Summary of results in EC Arg1 KO mice

Systemic hemodynamics and vascular function were unchanged in the EC Arg1 KO mice compared to the WT control, although the mice showed a decrease in eNOS expression in the aorta. Moreover, NO metabolites and global L-arginine bioavailability were preserved. These data point to a co-regulation of Arg1 and eNOS expression in ECs.

## 4.2 The role of Arg1 in RBC erythroid cells *in vivo*

The second aim of this study was to characterize Arg1 KO mice in RBCs and examine the role of red cell Arg1 in the regulation of erythroid differentiation, systemic hemodynamics, vascular function, and NO bioavailability.

### 4.2.1 Generation of RBC-specific KO mice

RBC-specific Arg1 KO mice were generated by crossing Arg1<sup>flox/flox</sup> mice with erythroid-specific Hbb-Cre<sup>pos</sup> mice to obtain Arg1<sup>flox/flox</sup>Hbb<sup>pos</sup> and Arg1<sup>flox/flox</sup>Hbb<sup>neg</sup> mice. Recombination of the DNA locus in erythroid cells was confirmed by qPCR of bone marrow cells. DNA recombination was observed in RBC Arg1 KO mice, but not in WT control mice (**Figure 11 C**). Additionally, the expression of Arg1 in erythroid cells (Ter119<sup>+</sup>CD45<sup>-</sup> cells) isolated from the bone marrow showed reduced mRNA expression of Arg1 compared to the WT control (**Figure 11 D**).

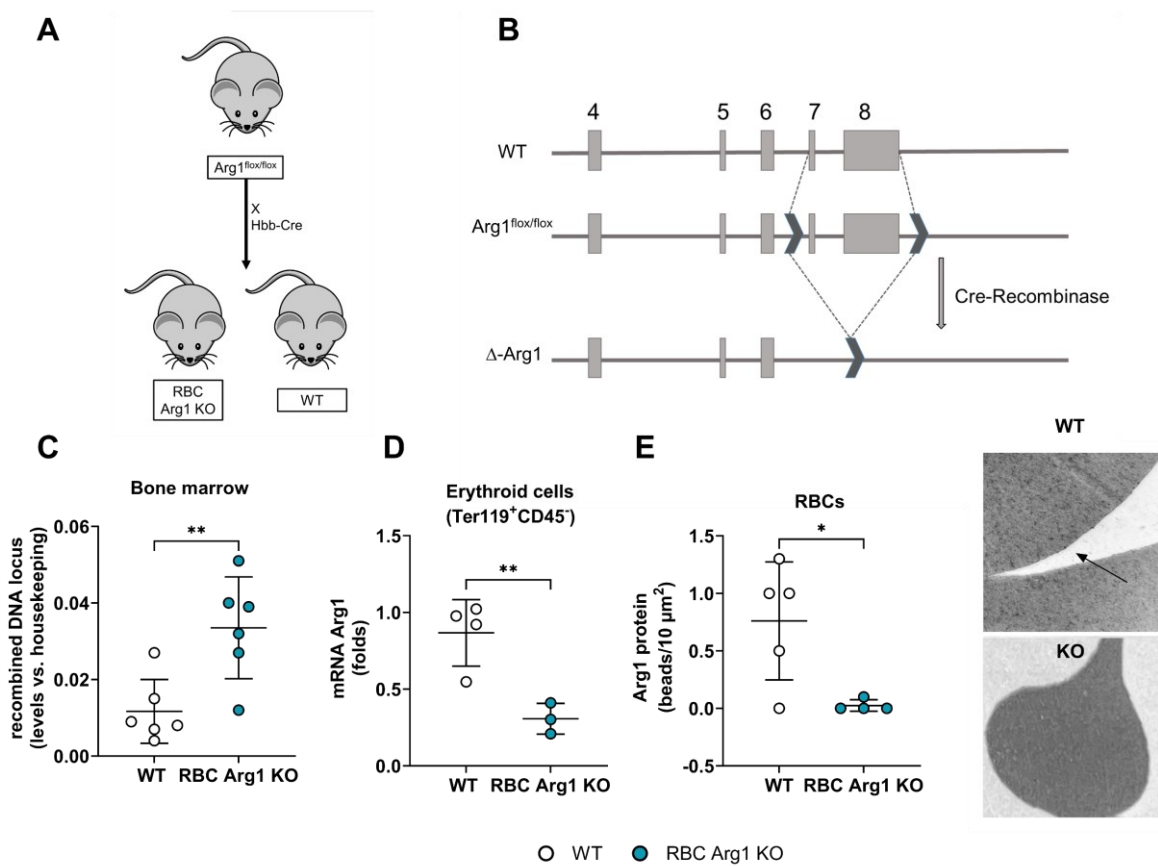


**Figure 11 - Genetic characterization of RBC Arg1 KO mice.** A) Schematic representation of the crossing strategy of RBC Arg1 KO mice. Arg1<sup>flox/flox</sup> mice were crossed with RBC-specific Hbb-Cre mice. B) Schematic description of the DNA locus. C) Analysis of cell-specific DNA recombination in bone marrow analyzed by qPCR. DNA recombination was found only in the bone marrow of RBC Arg1 KO mice and not in that of WT mice. D) mRNA expression of Arg1 in Ter119<sup>+</sup>-cells extracted from the bone marrow, is found in the WT, but not in RBC Arg1 KO mice. E) Quantification of immunotransmission electronic microscopy of RBCs from Arg1 KO mice and WT mice. Showing a very low expression of Arg1 in the WT mice and no expression of Arg1 in RBC Arg1 KO mice.

## Results

### 4.2.2 Arginase activity in other blood compartments is higher than in RBCs

Next, arginase activity in RBC was analyzed. To obtain clean RBCs, platelets and WBC were removed by washing, and WBC depletion was carried out using WBC filters (**Figure 12 A**). The arginase activity in RBC-ghosts was decreased, as measured by urea assay and determination of L-ornithine formation by qTOF (**Figure 12 B+C**). In addition, arginase activity was measured in other blood compartments to analyze whether compensatory changes occurred. The arginase activity in platelets, WBC, and plasma was preserved in RBC Arg1 KO mice compared to WT controls (**Figure 12 D+E**).

Interestingly, WBC (WT  $0.2387 \pm 0.130$  nmol urea/ $\mu$ g/h) and platelets (WT  $0.045 \pm 0.039$  nmol urea/ $\mu$ g/h) showed higher arginase activity than in RBC-ghosts (WT  $0.0062 \pm 0.002$  nmol urea/ $\mu$ g/h). This indicates that RBCs have the lowest Arg1 activity in the blood.

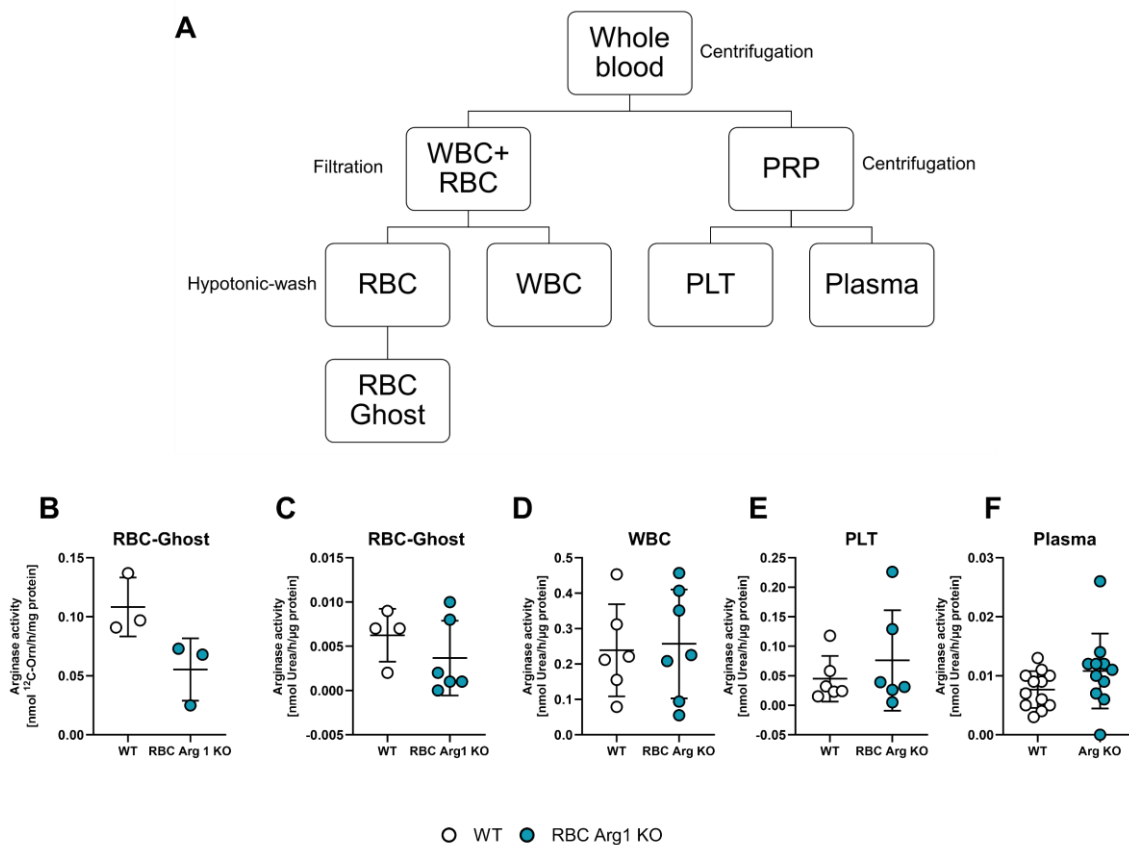


**Figure 12 - Arginase activity in different blood compartments.** A) Workflow of RBC-cleaning; B) Arginase activity in RBC-ghosts shows a decrease in arginase activity in the RBC Arg1 KO mice determined by LC-MS. C) Arginase activity in RBC ghosts determined by urea assay. D) Arginase activity in WBC did not show changes between RBC Arg1 KO mice and WT littermates. E) Arginase activity in platelets (PLT) is higher than that in RBC-ghosts. F) Arginase activity in the plasma is preserved in RBC Arg1 KO mice compared to the control.

## Results

### 4.2.3 Hematological analysis showed no changes in blood count and EPO levels.

To investigate whether the lack of Arg1 in the RBCs has any impact on hematological parameters of RBC Arg1 KO mice, a blood count was carried out. The blood count did not show any changes in RBC, WBC, and platelet counts, as well as the reticulocyte count, between the RBC Arg1 KO mice and the WT control (**Table 13**). Furthermore, RBC Arg1 KO mice showed preserved EPO levels in the plasma (**Table 13**). Interestingly, the plasma ferritin levels were significantly reduced in the RBC Arg1 KO mice compared to their WT littermates, indicating iron deficiency without affecting the RBC count.

**Table 13 Results of blood count of RBC Arg1 KO mice.** The table summarizes the blood count parameters measured in RBC Arg1 KO mice and WT controls. Abbreviations: RBC, red blood cells; HCT, hematocrit; HGB, hemoglobin; RDW, RBC distribution width; MCHC, mean corpuscular hemoglobin concentration; MCH, mean corpuscular hemoglobin; MCV, mean corpuscular volume; WBC, white blood cells; Lymph, lymphocytes; Mo, monocytes; Neu, Neutrophils; PLT, platelet count; MPV, mean platelet volume; EPO, erythropoietin. All data are expressed as the mean  $\pm$  SD. Welch's t-test.

	WT	RBC Arg1 KO	p
n	8	9	
<b>Red blood cell count</b>			
RBC ( $10^{12}/L$ )	9,3 $\pm$ 0.8	8.9 $\pm$ 0.8	0.386
HCT (%)	39.2 $\pm$ 3.0	37.5 $\pm$ 3.5	0.283
HGB (g/dl)	12.8 $\pm$ 0.8	12.7 $\pm$ 1.6	0.919
Reticulocytes (%)	4.63 $\pm$ 0.3	5.01 $\pm$ 0.9	0.543
<b>Red blood cell indices</b>			
RDW (%)	19.8 $\pm$ 1.0	19.6 $\pm$ 0.7	0.453
MCHC (g/dl)	33.4 $\pm$ 0.8 +	33.9 $\pm$ 1.3	0.282
MCH (pg)	14.1 $\pm$ 0.5 +	14.0 $\pm$ 0.8	0.660
MCV (fl)	42.3 $\pm$ 0.7	42.0 $\pm$ 0.8	0.383
<b>White blood cell count</b>			
WBC ( $10^9/L$ )	2.9 $\pm$ 1.3	3.4 $\pm$ 1.3	0.414
Lymph ( $10^9/L$ )	1.6 $\pm$ 0.4 +	2.1 $\pm$ 0.8	0.102
Lymph (%)	67.3 $\pm$ 21.3	64.3 $\pm$ 23.3	0.769
Mo ( $10^9/L$ )	0.2 $\pm$ 0.1	0.2 $\pm$ 0.1	0.504
Mo (%)	4.7 $\pm$ 1.7	5.8 $\pm$ 2.8	0.346
Neu ( $10^9/L$ )	0.9 $\pm$ 0.8	29.9 $\pm$ 20.7	0.673
Neu (%)	27.3 $\pm$ 19.4	1.1 $\pm$ 0.9	0.777
<b>Platelet count</b>			
PLT ( $10^9/L$ )	499.7 $\pm$ 66.1	455.6 $\pm$ 65.3	0.151
MPV (fl)	6.0 $\pm$ 0.4	6.2 $\pm$ 0.2	0.204

## Results

Plasma			
<b>EPO (pg/mL)</b>	39.7 ± 13.5	43.2 ± 4.50	0.548
<b>Ferritin (mg/mL)</b>	814 ± 326	449 ± 285	0.037*
<b>Transferrin</b>	4.27 ± 0.9	3.34 ± 0.56	0.055
<b>Spleen/body weight ratio</b>	3.100 ± 0.458	3.252 ± 0.444	0.594

### 4.2.4 No changes in erythropoietic activity in bone marrow and spleen

To study the role of Arg1 in erythroid cells in erythropoiesis, erythroid differentiation was analyzed in the bone marrow and spleen by flow cytometry. The quantitative analysis of erythroid differentiation of proerythroblasts, basophilic, polychromatic, and orthochromatic erythroblasts was performed by size (FSC) and the expression of the surface maker CD44 and the erythroid-specific surface marker Ter119. As shown in **Table 14**, the ratio of proerythroblasts, basophilic, polychromic, and orthochromatic erythroblasts was preserved in the RBC Arg1 KO mice as compared to the WT group. Furthermore, the erythroid cell populations were unchanged in the spleen, and the spleen size was preserved. This indicates that erythroid-cell Arg1 is not involved in the differentiation of RBCs.

**Table 14 Quantification of terminal erythroid differentiation in bone marrow and spleen of RBC Arg1 KO mice.** The population at each distinct stage of maturation was normalized based on the total nucleated cells. All data are expressed as the mean ± SD. Welch's t-test

	WT	RBC Arg 1 KO	p	WT	RBC Arg 1 KO	p
	Bone marrow			Spleen		
<b>n</b>	5	5		5	5	
<b>Proerythroblast (%)</b>	5.98 ±1.15	4.04 ±1.70	0.013	4.54 ± 1.33	6.09 ±1.86	0.061
<b>Basophilic erythroblast (%)</b>	14.52 ±3.80	14.73 ±5.00	0.919	12.35 ± 2.94	10.58 ±2.14	0.168
<b>Polychromic erythroblast (%)</b>	27.60 ±9.54	27.85 ±9.46	0.958	31.51 ± 3.64	31.20 ±2.21	0.830
<b>Orthochromatic erythroblast (%)</b>	51.90 ±6.62	53.38 ± 4.41	0.584	51.60 ± 5.89	52.12 ±4.33	0.832
<b>Nucleated erythroblasts (%)</b>	43.60 ±12.28	43.64 ±11.41	0.995	2.88 ±1.61	4.98±1.76	0.021



## Results

### 4.2.5 Preserved vascular function and systemic hemodynamics in RBC Arg1 KO mice

To investigate whether the lack of Arg1 in RBCs affects vascular function, eNOS-dependent vasorelaxation in the aorta of RBC Arg1 KO mice and WT littermates was measured *ex vivo*. RBC Arg1 KO mice showed reduced contractility to KPSS, but no significant changes in endothelium-dependent relaxation to ACh, as well as no changes in the contractile response to PE (Figure 13 D-G).

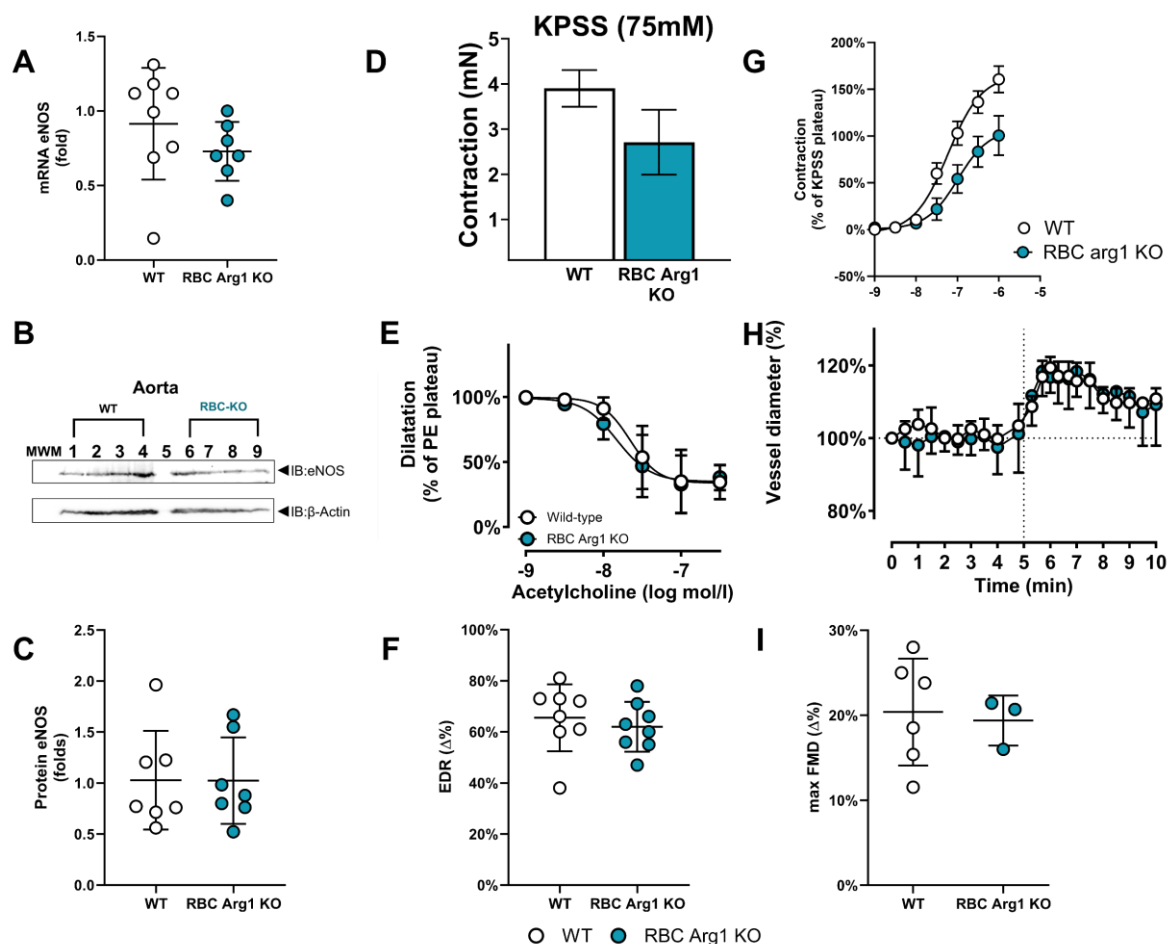


**Figure 13 - Vascular function is preserved in Arg1 KO mice.** A) Preserved expression of Arg1 in the aorta was measured using qPCR. B+C) Unchanged protein levels of eNOS in the aorta determined by Western Blot. D-G) Vascular function was investigated *in vivo* by myography. RBC Arg1 KO mice showed reduced contractility towards KPSS, but no changes in endothelium-dependent relaxation to ACh or contractility to PE. H + I) Vascular function was analyzed *in vivo* using FMD. No changes were found between RBC Arg1 KO mice and their WT littermates.

Additionally, FMD was analyzed *in vivo* in RBC Arg1 KO mice and WT controls. The lack of Arg1 in RBC did not lead to any changes in vessel diameter between RBC Arg1 KO mice and their WT control, before and after cuff release for 5 min, and in maximal FMD response (Figure 13 H+I). This is also reflected in unchanged systemic hemodynamic parameters (Table 15) and underlined by preserved expression of eNOS in the aorta (Figure 13 A-C).

## Results

**Table 15 Parameters of systemic hemodynamics in RBC Arg1 KO mice and WT littermate control.** Data are reported as mean  $\pm$  SD. n= number of analyzed mice. Differences between WT and EC Arg1 KO were calculated using Welch's t-test.

Parameter	WT		RBC Arg1 KO		p
	Mean $\pm$ SD	n	Mean $\pm$ SD	n	
<b>Heart rate (bpm)</b>	503 $\pm$ 64	20	472 $\pm$ 64	19	0.6025
<b>Systolic blood pressure (mmHg)</b>	91 $\pm$ 11	20	96 $\pm$ 11	19	0.1291
<b>Diastolic blood pressure (mmHg)</b>	64 $\pm$ 11	20	64 $\pm$ 7	19	0.9056
<b>Mean arterial pressure (mmHg)</b>	72 $\pm$ 11	20	75 $\pm$ 8	19	0.1397

### 4.2.6 Lack of Arg1 in RBC is not affecting infarct size or LV- dysfunction after AMI

To analyze whether Arg1 expressed in RBCs plays a role in the outcome of AMI *in vivo*, RBC Arg1 KO mice and WT control mice underwent ischemia/reperfusion (I/R) injury, with 45 min of open-chest coronary occlusion followed by 24 hours of reperfusion. LV function was determined *in vivo* by echocardiography measurements performed before and after induction of AMI (Figure 14, Table 16). RBC Arg1 KO mice did not show any changes in LV function before and after AMI compared to WT controls.

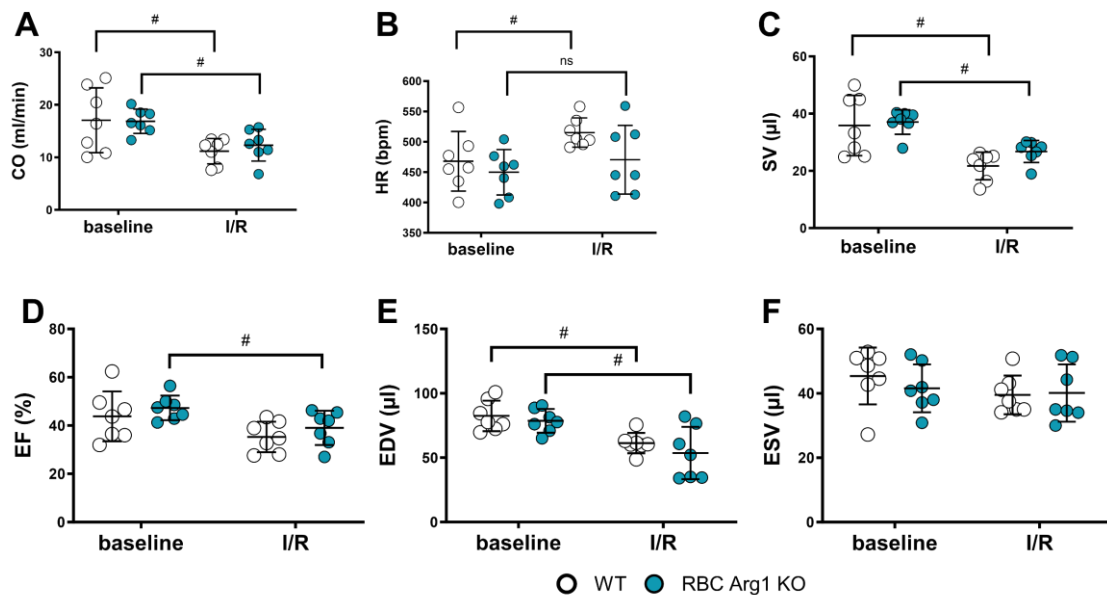


**Figure 14 - LV dysfunction after acute myocardial infarction is not affected by the lack of Arg1 in RBCs.** Evaluation of left ventricular (LV) function before and 24h after acute myocardial infarcts (AMI) Abbreviations: CO, cardiac output; HR, heart rate; SV, stroke volume; EF, ejection fraction; EDV, end-diastolic volume; ESV, end-systolic volume

## Results

Furthermore, the area of risk and infarct size did not differ between the two groups (**Figure 15**). The data demonstrate that Arg1 expressed in RBC does not modulate the infarct size of LV function after AMI *in vivo* in mice.

**Table 16** Echocardiographic parameters were assessed in RBC Arg1 KO mice by high-resolution ultrasound before and after AMI. Data are reported as mean  $\pm$  SD; n = number of mice. Differences between KO/WT pre-/post-AMI were calculated using an unpaired t-test (\*p<0.05). HR, heart rate; CO, cardiac output; SV, stroke volume; EF, ejection fraction; FS, fractional shortening; ESV, end-systolic volume; EDV, end-diastolic volume.

Parameter	Baseline			Post-AMI		
	WT Arg1 <sup>flox/flox</sup>	RBC Arg KO Arg1 <sup>flox/flox</sup> HbbCre <sup>pos</sup>	p	WT Arg1 <sup>flox/flox</sup>	RBC Arg KO Arg1 <sup>flox/flox</sup> HbbCre <sup>pos</sup>	p
	7	7		7	7	
HR (bpm)	468 $\pm$ 49	450 $\pm$ 37	0.4586	515 $\pm$ 24	470 $\pm$ 56	0.4542
CO (mL/min)	17 $\pm$ 6	17 $\pm$ 2	0.9397	11 $\pm$ 2	12 $\pm$ 3	0.0891
SV ( $\mu$ L)	36 $\pm$ 11	37 $\pm$ 4	0.7880	22 $\pm$ 5	27 $\pm$ 4	0.0519
EF (%)	44 $\pm$ 10	47 $\pm$ 5	0.4483	35 $\pm$ 6	39 $\pm$ 7	0.3201
FS (%)	10 $\pm$ 2	14 $\pm$ 3	0.0361*	10 $\pm$ 3	9 $\pm$ 3	0.4100
ESV ( $\mu$ L)	45 $\pm$ 9	42 $\pm$ 7	0.3998	40 $\pm$ 6	40 $\pm$ 9	0.3766
EDV ( $\mu$ L)	82 $\pm$ 12	79 $\pm$ 9	0.5189	61 $\pm$ 8	54 $\pm$ 20	0.8839

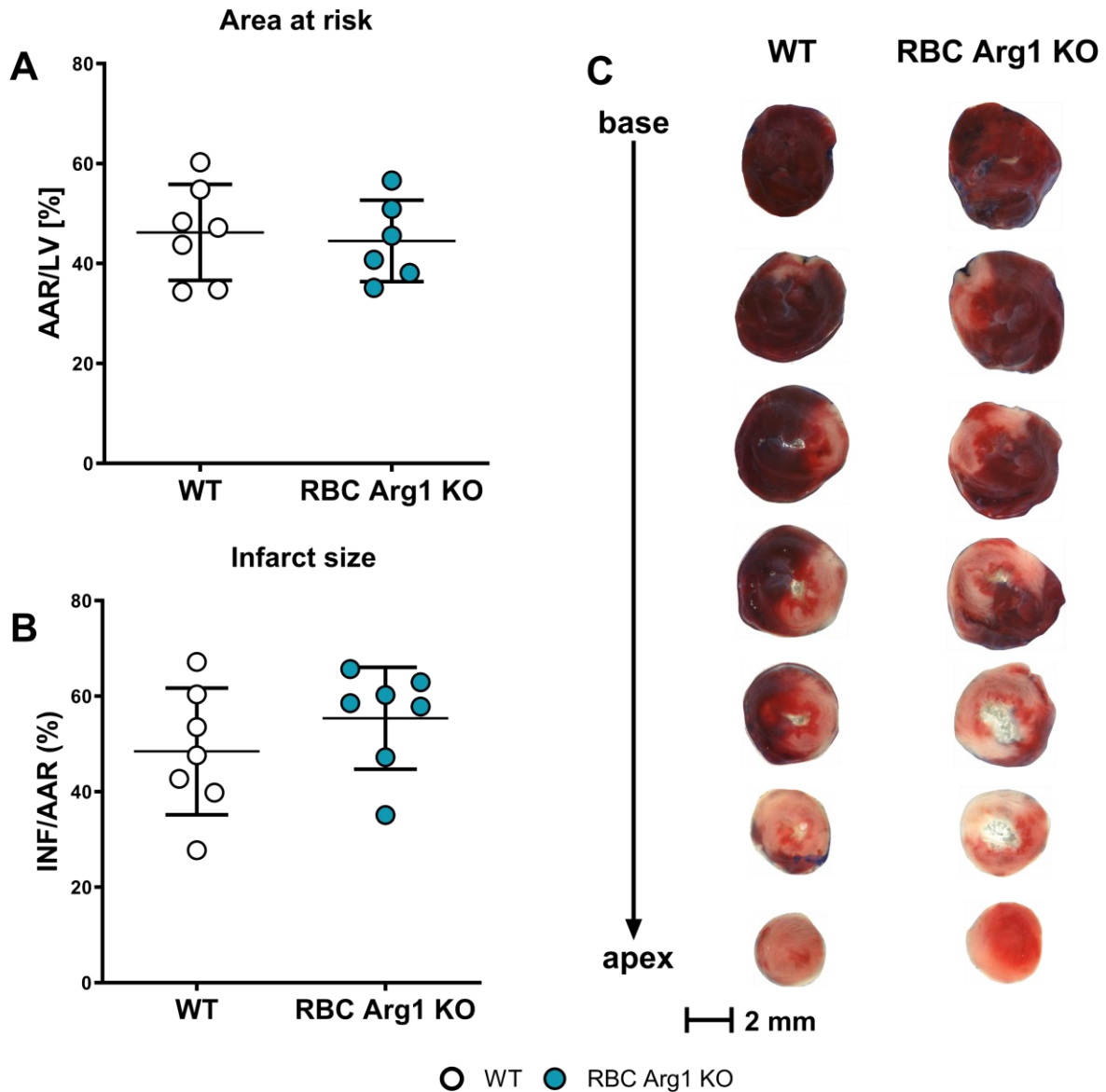


**Figure 15 - Area of risk and infarct size of RBC Arg1 KO mice** The percentage of A) area at risk (AAR) and B) infarct size/area at risk (INF/AAR) was calculated after I/R in RBC Arg1 KO mice and WT littermate controls. C) Representative TTC staining showing no differences in myocardial damage after AMI.

#### 4.2.7 Preserved global L-arginine bioavailability and increased nitrate levels in plasma but reduced nitrite levels in RBCs

To analyze whether the lack of Arg1 in the RBC affects circulating L-arginine metabolites, the plasma levels of L-arginine, L-ornithine, and L-citrulline were measured using LC-MS. RBC Arg1 KO mice showed a significant decrease in L-ornithine levels, but no changes in plasma levels of L-citrulline and L-arginine (**Figure 16 A**). In addition, the L-arginine/L-ornithine ratio and global L-arginine bioavailability were preserved (**Figure 16 B**).

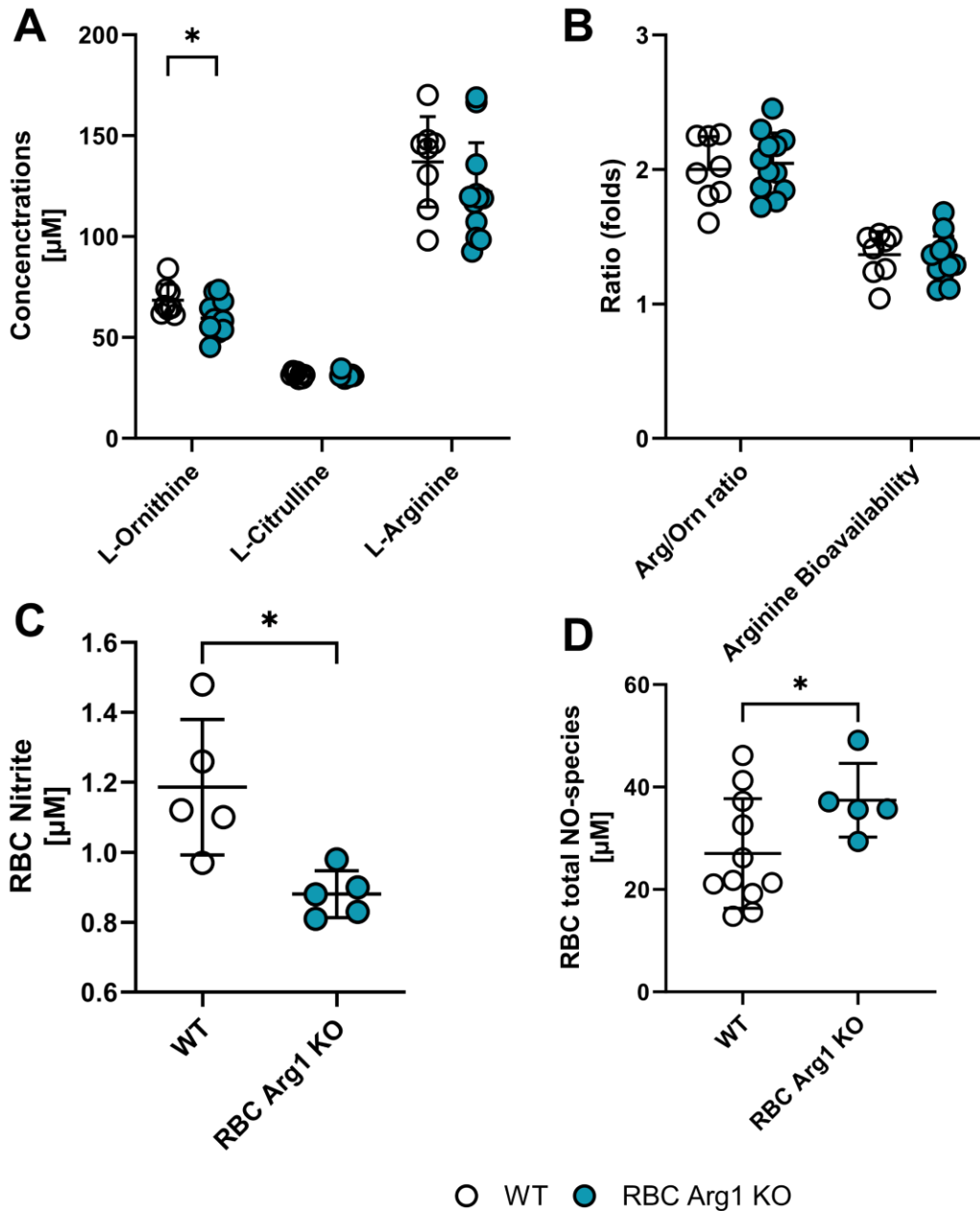


**Figure 16 - L-arginine-metabolites in plasma and NO metabolites in RBCs of RBC Arg1 KO mice.** A) Levels of L-arginine and L-citrulline in the plasma of RBC Arg1 KO mice did not show any changes compared to the control group. However, they showed a significant decrease in L-ornithine levels. B) The Arg/Orn Ratio and L-arginine bioavailability are preserved in RBC Arg1 KO mice. C) RBC nitrite levels were reduced in RBC Arg1 KO mice, but D) total NO species in RBCs were increased.

On the other hand, a significant increase in total NO species was found in plasma and RBCs in RBC Arg1 KO mice compared to the control. In contrast, RBC Arg1 KO mice showed a significant decrease in RBC nitrite levels (**Figure 16 C+D**). Tissue NO metabolites remained unchanged, except for RXNO levels in the aorta (**Table 17**). These findings suggest that Arg1 plays a minor role in the regulation of global L-arginine bioavailability.

## Results

**Table 17 Distribution of NO metabolites in blood and organs of RBC Arg1 KO mice and corresponding WT littermate controls.**

Welch's *t*-test between the groups. \**p*<0.05 \*\**p*<0.01 \*\*\**p*<0.001; §*n*=5; §*n*=9; #=*n*=6; †*n*=10

Metabolite		WT Arg1 <sup>flox/flox</sup>	RBC Arg1 KO Arg1 <sup>flox/flox</sup> HbbCre <sup>pos</sup>	p
<i>n</i>		11	5	
<b>Heart</b>				
Nitrite	μM	1.55 ± 0.77	1.06 ± 0.10	0.0651
Nitrate	μM	44.64 ± 20.42	54.51 ± 24.63	0.4610
RXNO	nM	92.06 ± 35.70 <sup>†</sup>	67.13 ± 23.46	0.1324
heme-NO	nM	75.79 ± 37.87	64.32 ± 20.66	0.4619
Total NO species	μM	46.34 ± 20.36	55.71 ± 24.72	0.4846
<b>Lung</b>				
Nitrite	μM	0.93 ± 0.38	1.68 ± 1.22	0.2416
Nitrate	μM	39.97 ± 21.54	68.67 ± 33.80	0.1358
RXNO	nM	125.18 ± 57.69	144.5 ± 86.03	0.6642
heme-NO	nM	112.74 ± 32.18	105.27 ± 87.30	0.8611
Total NO species	μM	41.13 ± 21.85	70.60 ± 35.01	0.1382
<b>Liver</b>				
Nitrite	μM	0.50 ± 0.14 <sup>§</sup>	0.46 ± 0.19	0.7371
Nitrate	μM	25.60 ± 10.71	39.88 ± 27.59	0.3181
RXNO	nM	2248.66 ± 889.73 <sup>†</sup>	2266.08 ± 1365.16	0.9802
heme-NO	nM	162.12 ± 86.66 <sup>§</sup>	364.05 ± 194.44	0.0821
Total NO species	μM	28.12 ± 10.74	42.98 ± 29.00	0.3221
<b>Aorta</b>				
Nitrite	μM	129.33 ± 47.82 <sup>#</sup>	116.40 ± 30.39	0.6006
Nitrate	μM	4360.85 ± 1639.74 <sup>§</sup>	4346.08 ± 1874.54	0.9897
RXNO	nM	1803.14 ± 571.09 <sup>†</sup>	3358.88 ± 971.58	0.0189*
Total NO-species	μM	4500.50 ± 1669.79	4465.90 ± 1885.30	0.9763
<b>Plasma</b>				
Nitrite	μM	0.79 ± 0.39	0.68 ± 0.36	0.5819
Nitrate	μM	15.74 ± 5.23	24.27 ± 4.22	0.0063**
RXNO	nM	18.59 ± 6.65	81.78 ± 37.88	0.0196*
Total NO species	μM	16.54 ± 5.52	25.02 ± 4.49	0.0092**
<b>Erythrocytes</b>				
Nitrite	μM	1.19 ± 0.19 <sup>§</sup>	0.88 ± 0.07	0.0210*
Nitrate	μM	26.18 ± 10.20	36.37 ± 7.24	0.0436*
RXNO	nM	244.00 ± 125.28	104.85 ± 41.37	0.0054**
heme-NO	nM	53.75 ± 23.46	58.62 ± 15.37	0.6307
Total NO species	μM	27.02 ± 10.69	37.41 ± 7.21	0.0426*

## Results

### 4.2.8 Summary of results on RBC Arg1 KO mice

RBC Arg1 KO mice showed preserved erythroid differentiation and blood count compared to the WT control. Furthermore, no changes in systemic hemodynamics or vascular function were observed, and no changes in the outcome of AMI *in vivo*. The lack of Arg1 in RBCs leads to decreased L-ornithine levels and a significant increase in nitrate levels in the plasma, but a decrease in nitrite levels in RBCs. This finding suggests that Arg1 expressed in RBCs plays a minor role in erythroid differentiation and the regulation of vascular tone.

### 4.3 The role of red cell sGC in hematopoiesis *in vivo*

RBCs carry a functional sGC (Cortese-Krott et al., 2018), but the *in vivo* function of sGC in erythroid cells and RBCs remains unknown. To investigate the role of sGC in RBCs, RBC-specific sGC KO mice were generated and characterized. In this study, the role of sGC in erythropoiesis and the lifespan of RBCs was investigated and compared to the hematological phenotype of global  $\alpha 1$  sGC KO mice.

#### 4.3.1 Generation of RBC-specific sGC KO mice

RBCs carry only the  $\alpha 1\beta 1$ -subunit of sGC. To generate RBC-specific sGC KO mice, sGC  $\alpha 1^{\text{flox/flox}}$  mice were crossed with Hbb-Cre positive mice to obtain sGC  $\alpha 1^{\text{flox/flox}}$  Hbb-Cre<sup>pos</sup> mice and their littermate controls, sGC  $\alpha 1^{\text{flox/flox}}$  Hbb-Cre<sup>neg</sup> mice. **Figure 17 B** is a schematic representation of the gene targeting construct, showing that exon 4 is targeted by the LoxP sequence and removed after the expression of Cre recombinase (Mergia et al., 2006). DNA recombination in erythroid cells (Ter119<sup>+</sup>CD45<sup>-</sup>cells) was analyzed by qPCR, showing that the recombined DNA locus was found only in RBC sGC KO mice but not in the control group (**Figure 17 C**).



## Results

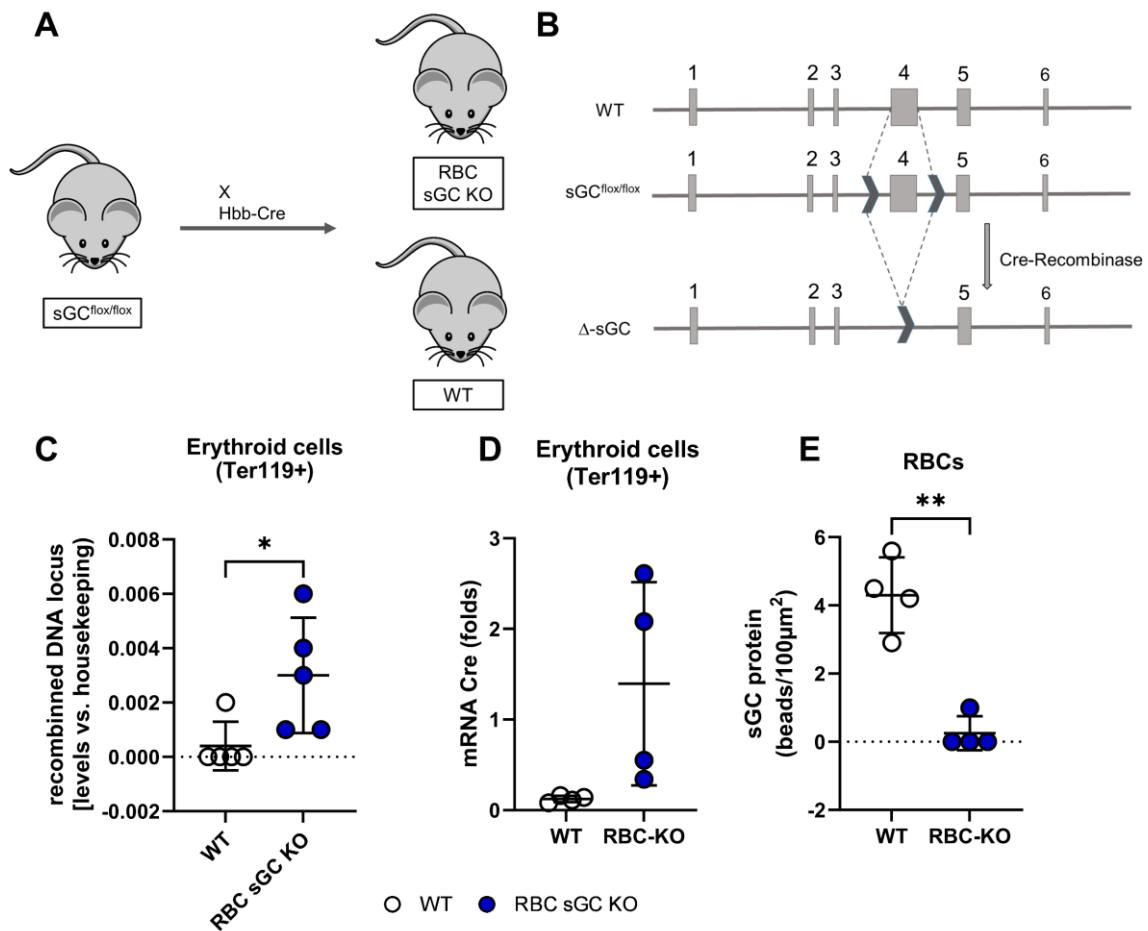


**Figure 17 - Genetic characterization of RBC sGC KO mice.** A)  $sGC\alpha^{flox/flox}$  mice were crossed with *Hbb-Cre* positive mice to generate erythroid-specific sGC KO mice. B) Scheme of DNA locus. C) Testing for DNA recombination of the DNA locus of RBC sGC KO mice by qPCR. Welch's test \*  $p > 0.05$  D) mRNA expression of Cre-recombinase in erythroid cells of RBC sGC KO mice but not WT mice. E) Quantification of immunotransmission electronic microscopy of RBCs from RBC sGC KO mice and WT mice. Showing expression of sGC in RBC sGC KO mice.

### 4.3.2 The bone marrow of RBC sGC KO mice showed reduced erythropoiesis.

To investigate if the lack of sGC affects erythropoiesis, the bone marrow of RBC sGC KO mice and WT control mice was analyzed. Bone marrow morphology was analyzed using Pappenheim-staining (**Table 18**). Bone marrow cells of old RBC sGC KO mice showed a significant decrease by 37.08% in erythropoietic activity (WT:  $23.57 \pm 2.07$  vs. RBC sGC KO  $14.83 \pm 5.34$ ) and an increase in granulopoiesis by 13.51% compared to the control group.

**Table 18 Results of Pappenheim-staining of RBC sGC KO and global sGC KO mice.**

	WT	RBC sGC KO	p	WT	Global sGC KO	p

## Results

n	7	6		7	7	
<b>Erythropoiesis</b>	23.57 ± 2.07	14.83 ± 5.34	0.008**	29.1 ± 12.3	32.0 ± 10.6	0.649
<b>Granulopoiesis</b>	63.14 ± 5.21	71.67 ± 6.41	0.027*	55.0 ± 10.4	46.3 ± 11.7	0.168

Quantitative analysis of erythroid differentiation was performed by identifying different development stadiums by the expression of the surface markers CD44 and Ter119 and the size of the cell (FSC) via flow cytometry. RBC sGC KO mice showed a significant decrease in the population of proerythroblasts (WT 5.984 ±1.15; RBC sGC KO 4.039 ±1.70), but no changes in further differentiation of erythroid progenitor cells (**Figure 18, A Table 20**). This indicates disrupted erythropoiesis in the early state of RBC sGC KO mice.

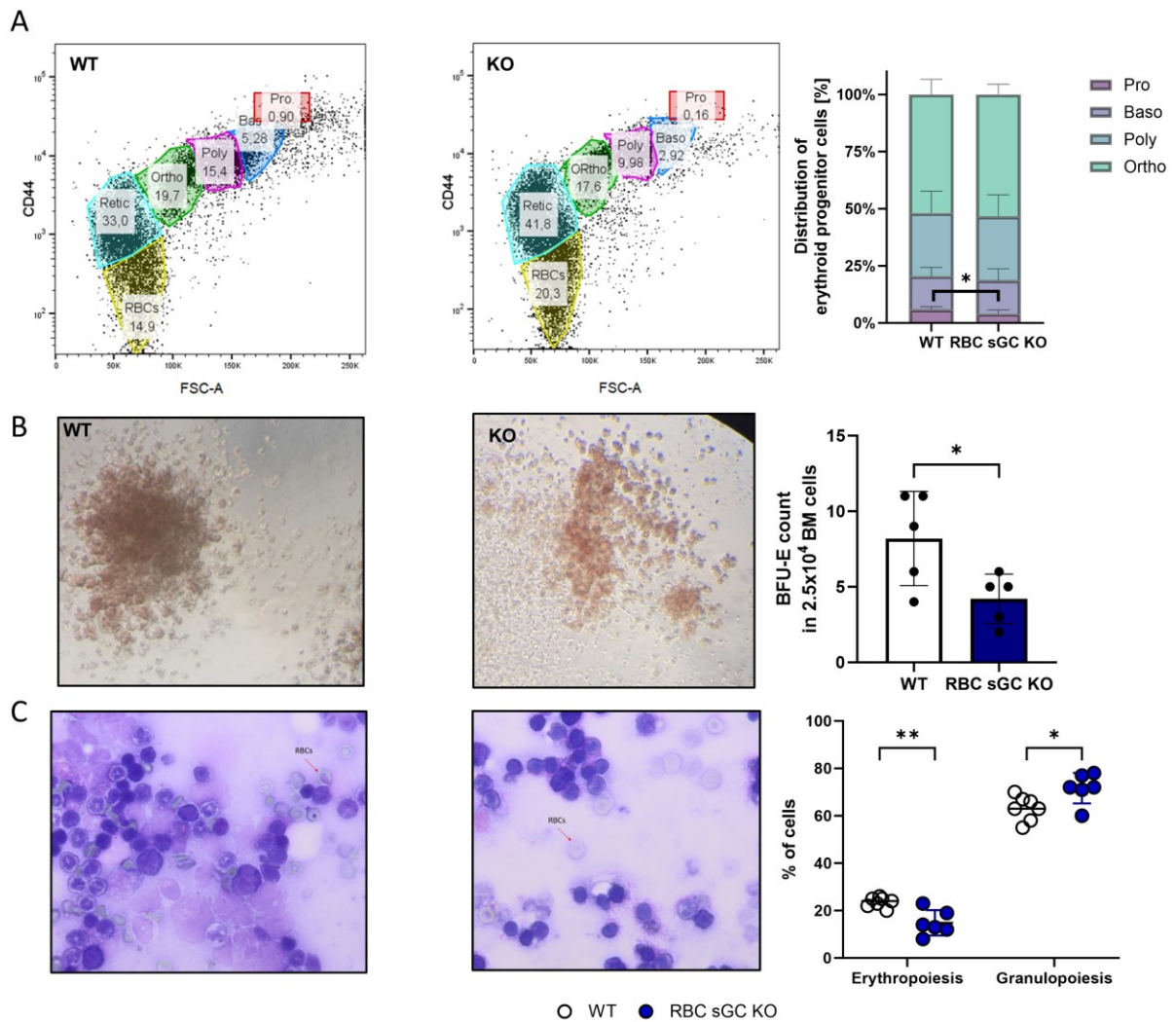


**Figure 18 - Steady-state-erythropoiesis in RBC sGC KO mice.** A) Example dot plot of flow cytometry analysis of erythroid differentiation in the bone marrow. RBC sGC KO mice showed a significant reduction in proerythroblasts. B) BFU-E colonies show changes in size and density, as well as a reduction in the number of BFU-E colonies in RBC sGC KO mice. C) Analysis of the bone marrow by Pappenheim-staining showed a reduction in erythropoiesis of RBC sGC KO mice. Welch's test, \* $p < 0.05$  \*\* $p < 0.01$

## Results

Furthermore, the proliferation of erythroid progenitor cells was analyzed by CFU-assay. Interestingly, RBC sGC KO mice showed smaller and less dense BFU-E colonies in the bone marrow (**Figure 18 B**), but also a significantly reduced number of BFU-Es (**Figure 18 B, Table 20**). However, no changes in the colonies of WBC proliferation were found. These findings suggest that a lack of sGC leads to disrupted erythropoiesis in the early stages.

**Table 19 CFU-Assay in bone marrow of RBC sGC KO and global sGC KO mice and their controls.** Welch's t-test between the groups. \* $p < 0.05$  \*\* $p < 0.01$  \*\*\* $p < 0.001$

	<b>WT</b>	<b>RBC sGC KO</b>	<b>p</b>	<b>WT</b>	<b>Global sGC KO</b>	<b>p</b>
<b>n</b>	5	5		2	5	
<b>CFU-GM</b>	33.4 ± 7.80	36.2 ± 5.76	0.538	45.3 ± 4.86	63.3 ± 9.67	0.013*
<b>BFU-E</b>	8.2 ± 3.14	4.2 ± 1.63	0.043*	7.8 ± 2.02	6.3 ± 1.84	0.343

The same analysis was performed on global sGC KO mice. Interestingly, they did not show changes in erythropoiesis or granulopoiesis analyzed by Pappenheim-staining, as well as preserved terminal erythroid differentiation (**Table 20**). The CFU assay of global sGC-KO mice showed a significant increase in CFU-GMs, but the number of BFU-Es was preserved (**Table 19**).

**Table 20 Quantification of terminal erythroid differentiation in bone marrow of RBC sGC KO mice and global sGC KO mice and their littermate controls.** The population at each distinct stage of maturation was normalized based on the total nucleated cells. All data are expressed as the mean ± SD. Welch's t-test \* $p < 0.05$

	<b>WT</b>	<b>RBC sGC KO</b>	<b>p</b>	<b>WT</b>	<b>Global sGC KO</b>	<b>p</b>
<b>n</b>	9	9		5	5	
<b>Proerythroblast (%)</b>	5.98 ± 1.15	4.04 ± 1.70	0.013*	6.3878 ± 2.15	4.64 ± 1.27	0.166
<b>Basophilic erythroblast (%)</b>	14.52 ± 3.80	14.73 ± 5.00	0.919	14.32 ± 3.11	14.47 ± 0.96	0.951
<b>Polychromic erythroblast (%)</b>	27.63 ± 9.54	27.85 ± 9.46	0.958	28.16 ± 2.35	26.97 ± 2.15	0.427
<b>Orthochromatic erythroblast (%)</b>	51.90 ± 6.62	53.38 ± 4.41	0.584	51.08 ± 1.561	53.92 ± 2.94	0.105
<b>Nucleated erythroblasts (%)</b>	43.60 ± 12.28	43.64 ± 11.41	0.995	51.98 ± 7.460	52.95 ± 11.58	0.880

## Results

### 4.3.3 The lack of sGC in RBCs causes splenomegaly and stress erythropoiesis in the spleen

The spleen is not only responsible for the removal of disrupted RBCs. In pathological conditions that lead to defective erythropoiesis in the bone marrow, the spleen contributes to RBC production in so-called stress erythropoiesis. The RBC sGC KO mice showed a significant increase in spleen/body weight ratio by 26.52% from  $2.55 \text{ mg/g} \pm 0.32$  to  $3.02 \text{ mg/g} \pm 0.43$ , compared to their WT littermate control (**Figure 19 A**). The quantitative analysis of erythroid differentiation in the spleen of RBC sGC KO mice showed no changes in the differentiation itself, but the percentage of nucleated erythroblasts increased by 74.57% compared to the control group (**Figure 19 C**).

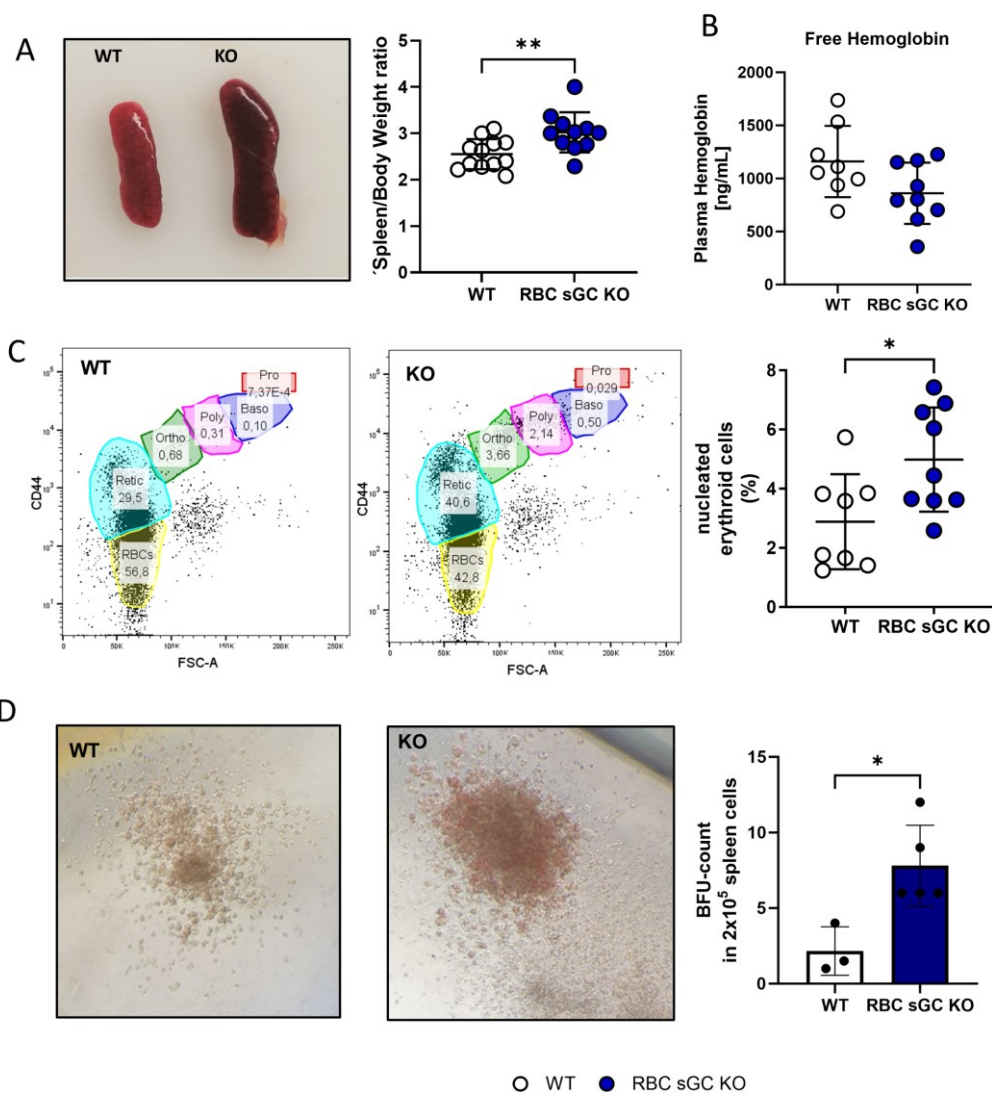


**Figure 19 - Characterization of Spleen of RBC sGC KO mice.** A) Comparison of spleen sizes from WT and RBC sGC KO mice and spleen/body weight ratio. RBC sGC KO mice showed a significant increase in the spleen/body weight ratio. B) Free hemoglobin in the plasma is measured as an indicator of intravascular hemolysis. No changes between WT and RBC sGC mice were found; C) Example of dot plot from spleen for

## Results

analysis of erythroid differentiation. RBC sGC KO mice do not show changes in the different populations but an overall increase in nucleated cells; D) CFU-Assays from spleen cells show changes in size and density of the BFU-E colonies as well as a significant increase in the count of BFU-Es in the bone marrow of RBC sGC KO mice.

Moreover, an increase in BFU-E colonies was observed in the CFU assay (**Figure 19, Table 21**). These findings show that the spleen of RBC sGC KO mice compensates for reduced erythropoiesis in the bone marrow. Additionally, free hemoglobin in the plasma was measured as a parameter for intravascular hemolysis, and no difference was observed between RBC sGC KO mice and the control group.

**Table 21 CFU-Assay in the spleen of RBC-sGC KO and global sGC KO mice.** Welch's t-test between the groups. \* $p < 0.05$  \*\* $p < 0.01$  \*\*\* $p < 0.001$

	<b>WT</b>	<b>RBC sGC KO</b>	<b>p</b>	<b>WT</b>	<b>Global sGC KO</b>	<b>p</b>
<b>n</b>	3	5		2	5	
<b>CFU-GM</b>	8.33 ± 3.51	9.60 ± 3.36	0.641	6.00 ± 0.71	20.20 ± 5.03	0.002*
<b>BFU-E</b>	2.17 ± 1.61	7.80 ± 2.68	0.010*	4.37 ± 1.59	8.25 ± 3.15	0.096
<b>n</b>	12	11		10	10	
<b>Spleen/BW ratio</b>	2.55 ± 0.32	3.02 ± 0.43	0.009**	2.92 ± 0.68	3.188 ± 0.50	0.340

### 4.3.4 Preserved spleen size and no stress-erythropoiesis in global sGC KO mice

In addition, the spleen of global sGC KO mice was analyzed for hematological properties. The spleen/body weight ratio of the global sGC KO mice was preserved as well as the BFU-E colonies. Interestingly, an increase in CFU-GM colonies was observed in the spleen of global sGC KO mice. This indicates that the lack of sGC in all tissues leads to a proinflammatory state in the body.

**Table 22 Quantification of terminal erythroid differentiation in the spleen of RBC sGC KO mice and global sGC KO mice.** The population at each distinct stage of maturation was normalized based on the total nucleated cells. All data are expressed as the mean ± SD. Welch's t-test

	<b>WT</b>	<b>RBC sGC KO</b>	<b>p</b>	<b>WT</b>	<b>Global sGC KO</b>	<b>p</b>
<b>n</b>	9	9		5	5	
Proerythroblast (%)	4.55 ± 1.33	6.09 ± 1.86	0.061	5.97 ± 1.03	4.25 ± 1.98	0.135
Basophilic erythroblast (%)	12.35 ± 2.94	10.58 ± 2.14	0.168	12.45 ± 2.22	11.07 ± 2.70	0.403
Polychromic erythroblast (%)	31.51 ± 3.64	31.20 ± 2.21	0.830	23.49 ± 4.60	23.83 ± 4.37	0.376

## Results

Orthochromatic erythroblast (%)	51.60 ± 5.89	52.12 ± 4.33	0.832	55.09 ± 5.61	60.85 ± 7.44	0.206
Nucleated erythroblasts (%)	2.88 ± 1.61	4.98 ± 1.76	0.021*	15.34 ± 12.22	17.25 ± 13.41	0.404

### 4.3.5 Preserved blood count in RBC sGC KO mice

To analyze whether disrupted erythropoiesis causes changes in the number of RBC or in the hematocrit, a blood count was conducted (**Table 23**). RBC sGC KO mice did not show any changes in the number of RBCs. Furthermore, they showed preserved RBC indices and reticulocyte counts. In addition, the number of WBC was preserved, but an increase in monocytes was observed. This indicates that stress erythropoiesis fully compensates for disrupted erythropoiesis in the bone marrow.

**Table 23 Results of blood count of RBC sGC KO mice and WT littermate control.** The table summarizes the blood count parameters measured in RBC sGC KO mice and WT controls. Abbreviations: RBC, red blood cells; HCT, hematocrit; HGB, hemoglobin; RDW, RBC distribution width; MCHC, mean corpuscular hemoglobin concentration; MCH, mean corpuscular hemoglobin; MCV, mean corpuscular volume; WBC, white blood cells; Lymph, lymphocytes; Mo, monocytes; Neu, Neutrophils; PLT, platelet count; MPV, mean platelet volume. All data are expressed as the mean ± SD. Welch's t-test. <sup>§</sup>n=10; <sup>§</sup>n=11; # n=8, <sup>†</sup>n=7

	WT	RBC sGC KO	p
n	12	11	
<b>Red blood cell count</b>			
<b>RBC (10<sup>12</sup>/L)</b>	9.20 ± 0.45	9.22 ± 0.30	0.906
<b>HCT (%)</b>	39.68 ± 1.69	40.12 ± 1.23	0.479
<b>HGB (g/dl)</b>	13.22 ± 0.74	13.30 ± 0.61	0.772
<b>Retic (%)</b>	5.80 ± 1.15 <sup>§</sup>	6.52 ± 1.00 <sup>§</sup>	0.202
<b>Red blood cell indices</b>			
<b>RDW (%)</b>	19.11 ± 0.42	18.69 ± 0.57	0.062
<b>MCHC (g/dl)</b>	33.30 ± 0.92	33.15 ± 1.21	0.736
<b>MCH (pg)</b>	14.37 ± 0.44	14.42 ± 0.51	0.789
<b>MCV (fl)</b>	43.17 ± 0.58	43.45 ± 0.52	0.223
<b>White blood cell count</b>			
<b>WBC (10<sup>9</sup>/L)</b>	3.43 ± 1.02	2.98 ± 0.93	0.276
<b>Lymph (10<sup>9</sup>/L)</b>	3.07 ± 1.03	2.37 ± 0.68	0.067
<b>Lymph (%)</b>	88.88 ± 6.99	82.05 ± 14.49	0.178
<b>Mo (10<sup>9</sup>/L)</b>	0.08 ± 0.05	0.13 ± 0.08	0.107
<b>Mo (%)</b>	2.42 ± 1.13	4.14 ± 1.76	0.013*

## Results

<b>Neu (10<sup>9</sup>/L)</b>	0.28 ± 0.21	0.48 ± 0.53	0.269
<b>Neu (%)</b>	8.71 ± 6.52	13.82 ± 13.21	0.265
<b>Platelet count</b>			
<b>PLT (10<sup>9</sup>/L)</b>	452.17 ± 62.35	424.18 ± 56.28	0.271
<b>MPV (fl)</b>	5.94 ± 0.20	5.85 ± 0.13	0.186
<b>Iron status</b>			
<b>Transferrin (mg/mL)</b>	2.6 ± 0.5 <sup>#</sup>	2.3 ± 0.6 <sup>†</sup>	0.285
<b>Ferritin (mg/mL)</b>	795.9 ± 386.4 <sup>§</sup>	901.1 ± 112.4 <sup>§</sup>	0.403
<b>Epo (pg/mL)</b>	59.77 ± 34.49 <sup>#</sup>	40.30 ± 4.894 <sup>†</sup>	0.156

### 4.3.6 Global KO of sGC leads to changes in WBC count

To analyze whether the lack of sGC in all tissues leads to changes in the blood count. The blood count of the global sGC KO mice showed a preserved number of RBCs. However, a significant increase in MCV was observed. The reticulocyte count was also preserved. Interestingly, global sGC KO mice showed changes in WBC count. The number of WBC was preserved; however, the lack of the  $\alpha 1$  subunit of sGC in all tissues caused a decrease in the percentage of leukocytes. Additionally, the number of monocytes and neutrophils increases. On the other hand, even if sGC ( $\alpha 1\beta 1$ -subunits) was highly expressed in platelets, the platelet count was unchanged, but a decrease in the mean platelet volume was found (**Table 24**). The increased number of CFU-GMs in the bone marrow and spleen, as well as changes in the WBC count, could be an indication of a proinflammatory state that may confound the phenotype.

**Table 24 Results of blood count of global sGC KO mice and WT littermate control.** The table summarizes the blood count parameters measured in RBC sGC KO mice and WT controls. Abbreviations: RBC, red blood cells; HCT, hematocrit; HGB, hemoglobin; RDW, RBC distribution width; MCHC, mean corpuscular hemoglobin concentration; MCH, mean corpuscular hemoglobin; MCV, mean corpuscular volume; WBC, white blood cells; Lymph, lymphocytes; Mo, monocytes; Neu, Neutrophils; PLT, platelet count; MPV, mean platelet volume. All data are expressed as the mean ± SD. Welch's t-test.

	<b>WT</b>	<b>Global sGC KO</b>	<b>p</b>
<b>n</b>	5	9	
<b>Red blood cell count</b>			
<b>RBC (10<sup>12</sup>/L)</b>	9.30 ± 0.56	8.78 ± 0.51	0.127
<b>HCT (%)</b>	39.19 ± 2.43	37.87 ± 2.13	0.341
<b>HGB (g/dl)</b>	13.00 ± 0.95	12.43 ± 0.94	0.312
<b>Retic (%)</b>	5.38 ± 0.09	5.89 ± 1.38	0.451
<b>Red blood cell indices</b>			
<b>RDW (%)</b>	20.68 ± 0.80	20.30 ± 0.44	0.370

## Results

<b>MCHC (g/dl)</b>	33.16 ± 0.76	32.81 ± 1.00	0.481
<b>MCH (pg)</b>	13.96 ± 0.34	14.17 ± 0.55	0.406
<b>MCV (fl)</b>	42.00 ± 0.71	43.11 ± 0.60	0.020
<b>White blood cell count</b>			
<b>WBC (10<sup>9</sup>/L)</b>	3.05 ± 0.94	4.06 ± 1.36	0.131
<b>Lymph (10<sup>9</sup>/L)</b>	2.75 ± 0.82	3.22 ± 1.16	0.401
<b>Lymph (%)</b>	90.40 ± 2.03	79.19 ± 8.69	0.005**
<b>Mo (10<sup>9</sup>/L)</b>	0.06 ± 0.02	0.14 ± 0.09	0.024*
<b>Mo (%)</b>	2.20 ± 1.01	3.87 ± 2.41	0.097
<b>Neu (10<sup>9</sup>/L)</b>	0.24 ± 0.14	0.69 ± 0.34	0.005**
<b>Neu (%)</b>	7.40 ± 2.51	16.94 ± 7.52	0.005**
<b>Platelet count</b>			
<b>PLT (10<sup>9</sup>/L)</b>	522.00 ± 129	546 ± 133	0.752
<b>MPV (fl)</b>	6.10 ± 0.16	5.88 ± 0.16	0.036*

### 4.3.7 Preserved iron status in RBC sGC KO mice

To investigate whether defective erythropoiesis may be linked to changes in iron status or EPO production, transferrin, ferritin, and EPO levels were measured in plasma (**Table 23**). RBC sGC KO mice did not show any changes compared to the WT control, indicating that changes in erythropoiesis are not due to iron deficiency or reduced EPO levels.

### 4.3.8 Preserved circulating NO metabolites in RBC sGC KO mice

Since sGC is a receptor of NO, the lack of sGC in RBCs could cause changes in NO metabolite levels in blood and tissues. NO metabolites were measured in plasma, RBCs, and multiple organs (**Table 25**). Interestingly, no changes in the circulating NO metabolites in plasma and RBCs were found in RBC sGC KO mice, but a decrease in nitrite levels in the liver and increased levels of nitrite in the lung and aorta were observed. Furthermore, an increase in RXNO levels was found in the heart of RBC sGC KO mice.



## Results

**Table 25 Distribution of NO metabolites in blood and organs of RBC sGC KO mice and corresponding WT littermate controls. Welch's t-test between the groups. \* $p < 0.05$  \*\* $p < 0.01$  \*\*\* $p < 0.001$ ; † $n = 7$ ; § $n = 6$**

		WT	RBC sGC KO	
Metabolite		8	8	p
n				
<b>Heart</b>				
Nitrite	$\mu M$	1.47 $\pm$ 0.70	1.09 $\pm$ 0.34 <sup>†</sup>	0.201
RXNO	nM	52.7 $\pm$ 19.9	102 $\pm$ 43.20	0.016*
heme-NO	nM	27.7 $\pm$ 18.6	22.6 $\pm$ 10.20	0.516
<b>Lung</b>				
Nitrite	$\mu M$	0.74 $\pm$ 0.29 <sup>§</sup>	2.27 $\pm$ 1.64	0.034*
RXNO	nM	80.7 $\pm$ 41.6	90.7 $\pm$ 48.5	0.665
heme-NO	nM	10.5 $\pm$ 3.79	10.2 $\pm$ 6.19	0.900
<b>Liver</b>				
Nitrite	$\mu M$	0.79 $\pm$ 0.31	0.45 $\pm$ 0.23 <sup>†</sup>	0.034*
RXNO	nM	435 $\pm$ 153	449 $\pm$ 136	0.852
heme-NO	nM	164 $\pm$ 57	164 $\pm$ 46.4	0.983
<b>Aorta</b>				
Nitrite	$\mu M$	2.65 $\pm$ 1.34 <sup>§</sup>	6.52 $\pm$ 3.64 <sup>§</sup>	0.048*
RXNO	nM	226 $\pm$ 119	277 $\pm$ 109	0.388
heme-NO	nM	32.4 $\pm$ 9.71	35.6 $\pm$ 14.8	0.624
<b>Kidney</b>				
Nitrite	$\mu M$	1.88 $\pm$ 0.39	1.98 $\pm$ 0.63	0.715
RXNO	nM	292 $\pm$ 143 <sup>†</sup>	159 $\pm$ 59.1 <sup>†</sup>	0.053
heme-NO	nM	62.4 $\pm$ 51.8	55.4 $\pm$ 30.8	0.748
<b>Spleen</b>				
Nitrite	$\mu M$	2.13 $\pm$ 1.28	1.85 $\pm$ 0.45	0.599
RXNO	nM	40.3 $\pm$ 13.5	29.0 $\pm$ 17.1	0.177
heme-NO	nM	3.26 $\pm$ 1.51	2.41 $\pm$ 1.54	0.284
<b>Plasma</b>				
Nitrite	$\mu M$	0.78 $\pm$ 0.31	0.723 $\pm$ 0.25	0.698
RXNO	nM	25.4 $\pm$ 3.26 <sup>†</sup>	17.4 $\pm$ 10.6	0.073
<b>Erythrocytes</b>				
Nitrite	$\mu M$	0.390 $\pm$ 0.135 <sup>†</sup>	0.335 $\pm$ 0.128 <sup>†</sup>	0.419
RXNO	nM	316 $\pm$ 186	347 $\pm$ 69.1	0.670
heme-NO	nM	2.91 $\pm$ 1.05	3.08 $\pm$ 1.53	0.806

## Results

### 4.3.9 *Summary of results on RBC sGC KO mice*

To analyze the role of sGC expressed in RBCs, RBC-specific sGC KO mice were generated. The lack of sGC in RBCs did causes disrupted erythropoiesis, as shown by a decrease in BFU-Es and a decrease in proerythroblasts in the bone marrow. In contrast, the spleen of RBC sGC KO mice showed an increase in spleen size, nucleated erythroid cells, and BFU-E count. Thus, disrupted erythropoiesis in the bone marrow could be fully compensated by the spleen, so that RBC sGC KO mice did not show changes in RBC count and hematocrit.

Global sGC KO mice, on the other hand, showed a decrease in RBCs as well as changes in the WBC count. In contrast to RBC sGC KO mice, erythropoietic activity was preserved in the bone marrow, but an increase in CFU-GM colonies was found. Moreover, spleen size was preserved in global sGC KO mice, and no increase in BFU-E colonies was found. However, the spleen showed a significant increase in CFU-GMs.

These data suggest that sGC expressed in erythroid cells plays a role in erythroid differentiation in the bone marrow but not in the spleen. This phenotype was not found in the global sGC mice, which may be due to a proinflammatory state confounding the phenotype.

#### 4.4 Analysis of hematological phenotype of Hbb-Cre<sup>pos</sup> mice

To verify that changes found in the hematological phenotype of RBC Arg1 KO mice or RBC sGC KO mice were not due to the expression of Cre-recombinase in erythroid cells, Hbb-Cre<sup>pos</sup> and Hbb-Cre<sup>neg</sup> mice were analyzed.

##### 4.4.1 Preserved blood count of Hbb-Cre<sup>pos</sup> mice

To investigate whether the expression of Cre-recombinase affects erythroid differentiation or RBCs, a blood count was carried out, and no differences in RBC, WBC, or platelet counts were found between Hbb-Cre<sup>pos</sup> mice and their control group (**Table 26**). In addition, the reticulocyte count and RBC indices were unchanged.

**Table 26 Results of blood count of Hbb-Cre<sup>pos</sup> mice and WT littermate control.** The table summarizes the blood count parameters measured in RBC sGC KO mice and WT controls. Abbreviations: RBC, red blood cells; HCT, hematocrit; HGB, hemoglobin; RDW, RBC distribution width; MCHC, mean corpuscular hemoglobin concentration; MCH, mean corpuscular hemoglobin; MCV, mean corpuscular volume; WBC, white blood cells; Lymph, lymphocytes; Mo, monocytes; Neu, Neutrophils; PLT, platelet count; MPV, mean platelet volume. All data are expressed as the mean  $\pm$  SD. Welch's t-test.

	Hbb-Cre <sup>neg</sup>	Hbb-Cre <sup>pos</sup>	p
n	10	10	
<b>Red blood cell count</b>			
RBC (10 <sup>12</sup> /L)	8.96 $\pm$ 0.66	8.85 $\pm$ 0.71	0.725
HCT (%)	37.94 $\pm$ 2.44	37.43 $\pm$ 1.18	0.869
HGB (g/dl)	12.53 $\pm$ 1.47	12.92 $\pm$ 2.83	0.985
Reticulocytes (%)	5.19 $\pm$ 1.48	4.15 $\pm$ 0.61	0.263
<b>Red blood cell indices</b>			
RDW (%)	20.08 $\pm$ 0.81	20.07 $\pm$ 0.68	0.910
MCHC (g/dl)	33.98 $\pm$ 1.73	32.74 $\pm$ 1.10	0.075
MCH (pg)	13.95 $\pm$ 1.01	14.03 $\pm$ 0.45	0.823
MCV (fl)	42.30 $\pm$ 1.16	42.90 $\pm$ 1.45	0.321
<b>White blood cell count</b>			
WBC (10 <sup>9</sup> /L)	4.41 $\pm$ 0.70	4.17 $\pm$ 1.72	0.693
Lymph (10 <sup>9</sup> /L)	3.22 $\pm$ 1.00	3.22 $\pm$ 1.18	0.997
Lymph (%)	71.86 $\pm$ 23.41	81.06 $\pm$ 19.32	0.351
Mo (10 <sup>9</sup> /L)	0.18 $\pm$ 0.12	0.19 $\pm$ 0.17	0.845
Mo (%)	3.78 $\pm$ 2.36	3.91 $\pm$ 2.59	0.910
Neu (10 <sup>9</sup> /L)	1.01 $\pm$ 0.95	0.76 $\pm$ 0.98	0.568
Neu (%)	22.38 $\pm$ 20.40	14.86 $\pm$ 16.97	0.382
<b>Platelet count</b>			

## Results

<b>PLT (10<sup>9</sup>/L)</b>	495.88 ± 127.78	548.10 ± 125.84	0.399
<b>MPV (fl)</b>	6.04 ± 0.26	5.85 ± 0.18	0.109

### 4.4.2 No changes in erythropoietic activity in *Hbb-Cre<sup>pos</sup>* mice

To analyze steady-state erythropoiesis, erythroid differentiation in the bone marrow was analyzed using flow cytometry. Preserved erythroid differentiation and no changes in the different erythroid populations were observed (**Table 27**). In line with this finding, the CFU-assay did not show changes in BFU-E colonies (**Table 28**).

**Table 27 Quantification of terminal erythroid differentiation in the bone marrow of *Hbb-Cre<sup>pos</sup>* mice and WT control.** The population at each distinct stage of maturation was normalized based on the total nucleated cells. All data are expressed as the mean ± SD. Welch's t-test

	<b>WT</b>	<b>RBC sGC KO</b>	<b>p</b>
	Bone marrow		
<b>n</b>	4	4	
<b>Proerythroblast (%)</b>	5.05 ± 1.62	5.79 ± 1.94	0.585
<b>Basophilic erythroblast (%)</b>	15.57 ± 2.50	14.13 ± 1.31	0.357
<b>Polychromic erythroblast (%)</b>	27.06 ± 2.10	30.05 ± 2.77	0.140
<b>Orthochromatic erythroblast (%)</b>	52.31 ± 2.11	50.03 ± 2.15	0.182
<b>Nucleated erythroblasts (%)</b>	44.80 ± 9.15	39.30 ± 2.46	0.320

**Table 28 CFU-Assay in the bone marrow of *Hbb-Cre<sup>pos</sup>* mice and WT littermate control.** Welch's t-test between the groups. \**p*<0.05 \*\**p*<0.01 \*\*\**p*<0.001

	<b><i>Hbb-Cre<sup>neg</sup></i></b>	<b><i>Hbb-Cre<sup>pos</sup></i></b>	<b><i>p</i></b>
	Bone marrow		
<b><i>n</i></b>	7	4	
<b><i>CFU-GM</i></b>	49.40 ± 10.80	46.20 ± 8.94	0.627
<b><i>BFU-E</i></b>	8.32 ± 3.94	9.31 ± 4.67	0.734

In addition, analysis of the bone marrow by Pappenheim staining did not show any changes in erythropoiesis and granulopoiesis between *Hbb-Cre<sup>pos</sup>* mice and the control group (**Figure 20**).

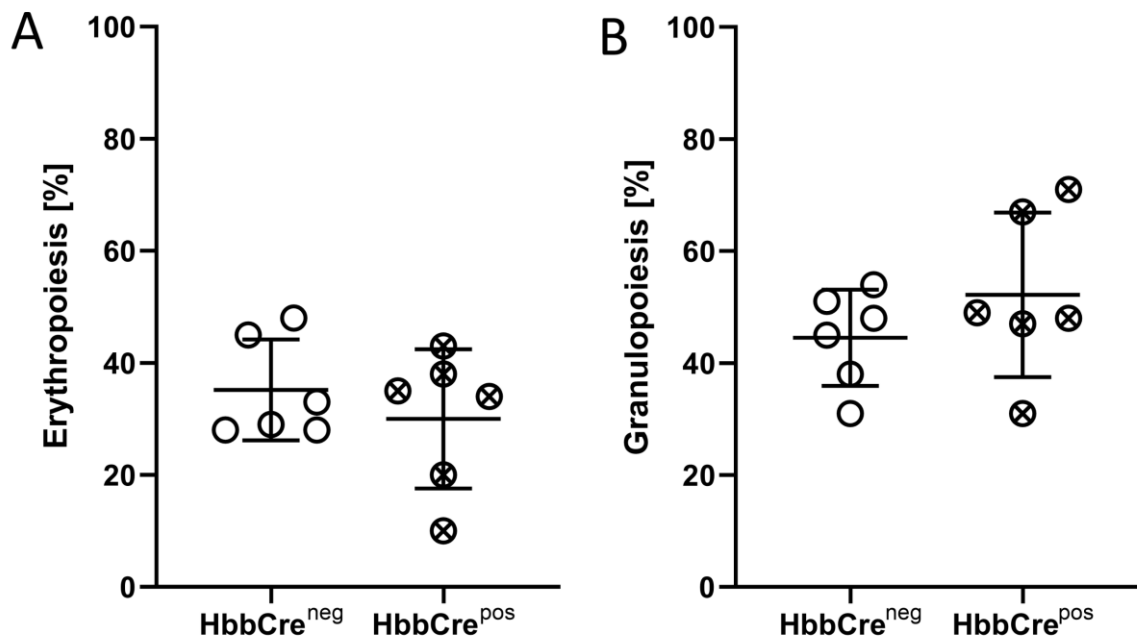


**Figure 20 - Pappenheim-staining of bone marrow cells of Hbb-Cre mice.** (A) Percentage of erythropoietic cells in the bone marrow. The percentage of erythropoietic cells did not change in Hbb-Cre<sup>pos</sup> mice. (B) Granulopoiesis was unchanged in the Hbb-Cre<sup>pos</sup> mice.

#### 4.4.3 Hbb-Cre<sup>pos</sup> mice do not show stress-erythropoiesis

In addition, the erythropoietic status of the spleen was investigated and a preserved spleen/body weight ratio was observed. Low erythropoietic activity was indicated by low numbers of colonies and no changes in erythroid differentiation (**Table 29** and **Table 30**).

**Table 29 CFU-Assay in the spleen of Hbb-Cre<sup>pos</sup> mice and WT.** Welch's t-test between the groups. \* $p < 0.05$   
\*\* $p < 0.01$  \*\*\* $p < 0.001$

	Hbb-Cre <sup>neg</sup>	Hbb-Cre <sup>pos</sup>	p
	<b>Spleen</b>		
<b>n</b>	7	5	
<b>CFU-GM</b>	11.4 ± 8.59	17.3 ± 13.3	0.436
<b>BFU-E</b>	4.21 ± 3.12	5.05 ± 3.31	0.670
<b>Spleen/BW ratio</b>	3.63 ± 0.35	3.76 ± 0.95	0.764

## Results

**Table 30 Quantification of terminal erythroid differentiation in the spleen of *Hbb-Cre<sup>pos</sup>* mice and WT control** The population at each distinct stage of maturation was normalized based on the total nucleated cells. All data are expressed as the mean  $\pm$  SD. Welch's t-test

	<i>Hbb-Cre<sup>neg</sup></i>	<i>Hbb-Cre<sup>pos</sup></i>	p
	<b>Spleen</b>		
<b>n</b>	4	4	
<b>Proerythroblast (%)</b>	5.86 $\pm$ 2.75	7.17 $\pm$ 1.11	0.425
<b>Basophilic erythroblast (%)</b>	15.12 $\pm$ 4.12	11.09 $\pm$ 1.25	0.144
<b>Polychromic erythroblast (%)</b>	23.32 $\pm$ 2.22	22.41 $\pm$ 1.51	0.527
<b>Orthochromatic erythroblast (%)</b>	55.69 $\pm$ 6.50	59.32 $\pm$ 1.47	0.348
<b>Nucleated erythroblasts (%)</b>	9.67 $\pm$ 5.47	6.32 $\pm$ 2.97	0.335

#### 4.4.4 Summary of results on *Hbb-Cre<sup>pos/neg</sup>* mice

*Hbb-Cre<sup>pos</sup>* mice did not show any changes in blood count or erythroid differentiation in the bone marrow. In addition, the spleen did not show any changes in size and erythroid differentiation after the expression of Cre-recombinase in erythroid cells. These data suggest that the expression of Cre-recombinase in erythroid cells does not affect erythroid differentiation.

## 5 Discussion

	EC Arg1 KO	RBC Arg1 KO	RBC sGC KO
Systemic hemodynamics	=	=	N/A
Vascular function	=	=	N/A
Blood count	=	=	=
Erythropoiesis in bone marrow	N/A	=	↓
Erythropoiesis in Spleen	N/A	=	↑

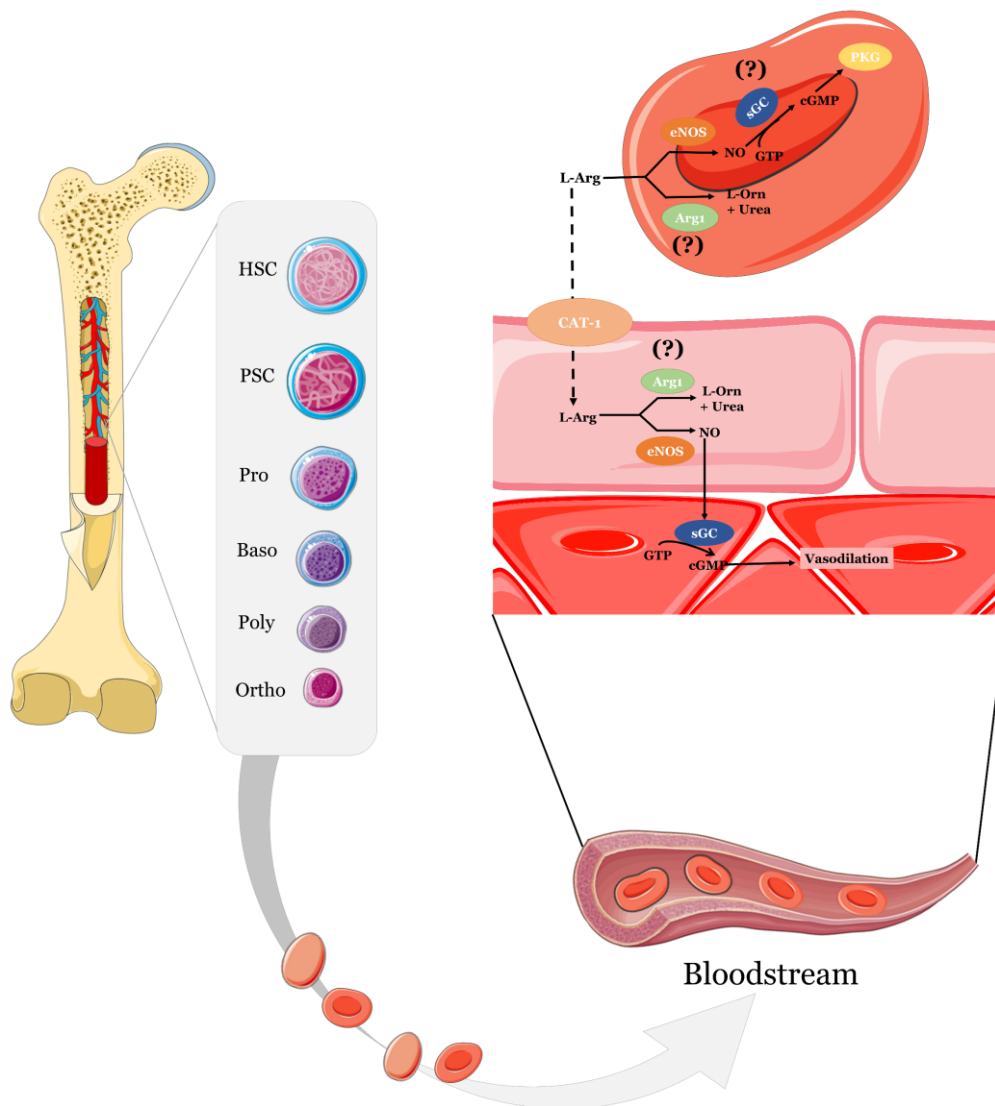


**Figure 21 Arg1/eNOS/sGC pathway in RBCs in vivo.** 1) The lack of Arg1 in ECs leads to downregulation of eNOS in the vessel wall and preserved vascular function. 2) The lack of red cell Arg1 increase circulating nitrate levels in plasma but does not improve vascular function or contribute to cardioprotection after I/R. 3) the lack of sGC in erythroid cells leads to disrupted erythropoiesis in the bone marrow, which is fully rescued by stress erythropoiesis in the spleen shown by preserved hematocrit and hemoglobin levels in the blood

## Discussion

The aim of this study was to analyze the role of the Arg1/eNOS/sGC pathway in RBCs *in vivo*. This study had three goals: to analyze (1) the role of Arg1 in EC eNOS-signaling in ECs under homeostatic conditions, (2) the role of Arg1 in eNOS-signaling in erythroid cells and RBCs, and (3) the role of sGC in erythroid cells and RBCs.

To this aim three cell-specific mice model were generated, EC Arg1 KO mice, RBC Arg1 KO mice and RBC GC KO mice.

The main findings were:

1. Lack of Arg1 in ECs leads to downregulation of eNOS in the vessel wall and preserved vascular function.
2. The lack of red cell Arg1 increases circulating nitrate levels in plasma but does not improve vascular function or contribute to cardioprotection after I/R.
3. Lack of sGC in erythroid cells leads to disrupted erythropoiesis in the bone marrow, which is fully rescued by stress erythropoiesis in the spleen.



## 5.1 Lack of Arg1 in ECs leads to downregulation of eNOS but preserved vascular function

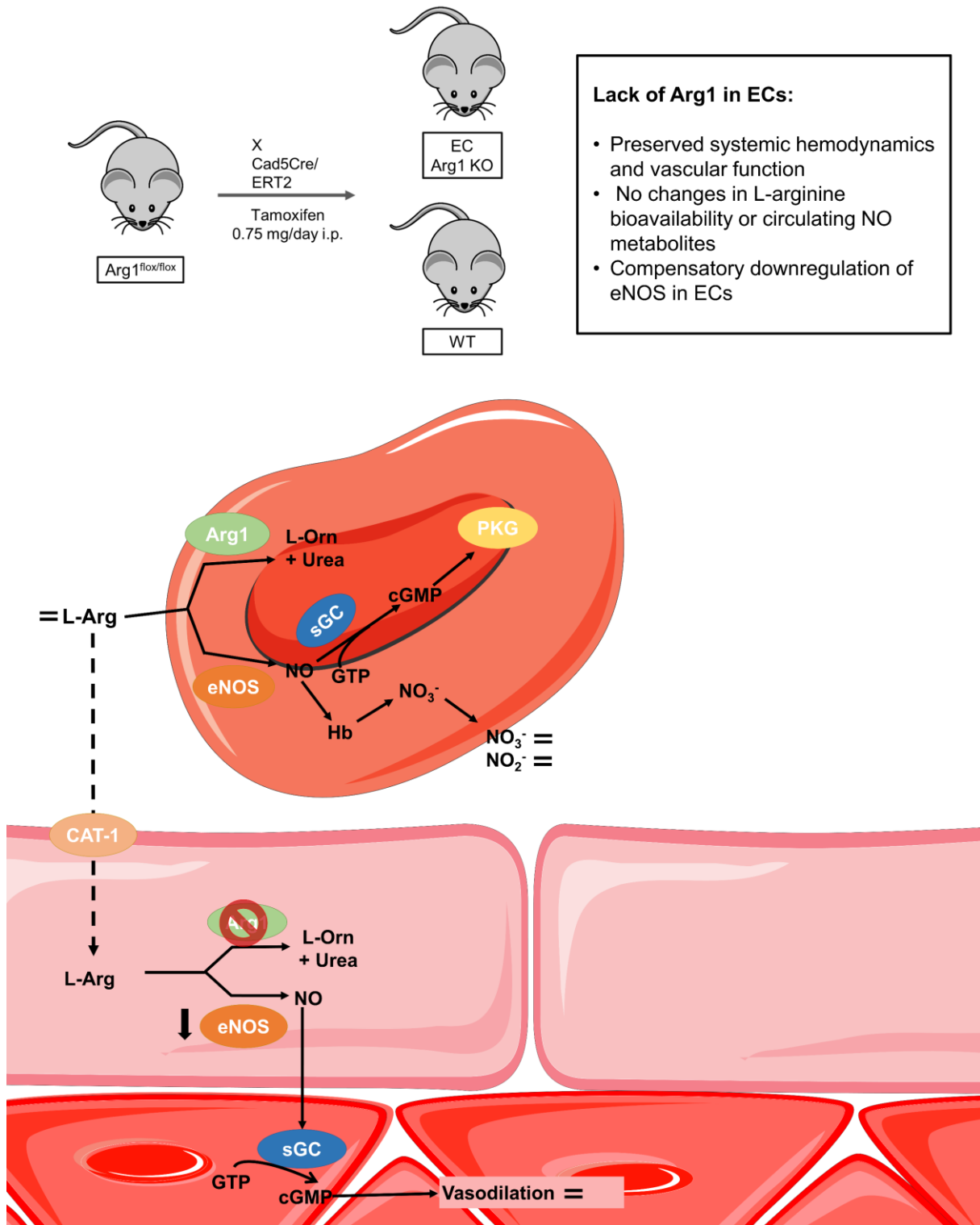


**Figure 22** Lack of Arg1 in ECs leads to downregulation of eNOS in the vessel wall but preserved vascular function. The lack of Arg1 in ECs did not improve the L-arginine bioavailability or the circulating NO metabolites. In the endothelium a reduced expression of eNOS was found, which did not lead to change in vascular function or hemodynamics.

## Discussion

In the first part of this study, EC-specific Arg1 mice were successfully generated by crossing Arg1<sup>flox/flox</sup> mice (El Kasmi et al., 2008) with mice express the tamoxifen-inducible Cre-recombination under the control of the promoter of the Cdh5 gene (Sorensen et al., 2009). The use of an inducible KO of Arg1 has the advantage of minimizing compensatory effects. To exclude potential differences between the two groups due to tamoxifen treatment, WT littermates were also treated with tamoxifen.

The main findings of the study were downregulation of eNOS in the vessel wall, preserved endothelial function and hemodynamics, preserved NO metabolites, and preserved L-arginine bioavailability.

### *5.1.1 Lack of Arg1 does not affect vascular function under basal conditions*

It is well known that eNOS and Arg1 are co-expressed in ECs, and both use L-arginine as a substrate. Thus, Arg1 has often been described to control eNOS activity by limiting the bioavailability of L-arginine for eNOS. Increased activity/expression of Arg1 has been reported to be involved in endothelial dysfunction and hypertension (Caldwell et al., 2018; Mahdi et al., 2020). Taking this into consideration, it was expected that the EC-specific deletion of Arg1 would affect vascular function and systemic hemodynamics. Surprisingly, EC Arg1 KO mice did not show any changes in vascular function, systemic hemodynamics, or levels of NO metabolites in plasma or aorta. The eNOS-dependent response to ACh was fully preserved in both in conductance vessels (aortic rings) and 3<sup>rd</sup> order mesentery arteries (resistance vessels). These findings were in line with the preserved diastolic and systolic BP *in vivo* in EC Arg1 KO mice compared to WT mice. Also, cardiac function was preserved in EC Arg1 KO mice compared to littermate control mice. These data indicate that Arg1 expressed in ECs plays a minor role in the regulation of vascular function under homeostatic conditions.

These findings are supported by a study by another group that generated EC Arg1 KO mice by expression of Cre-recombinase under the control of a constitutive Cdh5-dependent promoter (Bhatta et al., 2017). In this study, it was also shown that ACh-mediated relaxation was preserved in conductance vessels (aorta) and resistance vessels (mesentery arteries) under homeostatic conditions however, in this study eNOS expression and activity were not investigated. Another group generated EC Arg1 KO mice induced by Cre-recombinase under the control of the Tie2 promoter (Chennupati et al., 2018). The difference between this model and ours is that Tie2-Cre is not specific for ECs but is also expressed in hematopoietic cells (Payne et al., 2018). Nevertheless, this study also showed that depletion of Arg1 from ECs did not have any beneficial effect on vascular function in diabetic mice. Taken together, Arg1 expressed in ECs does not affect eNOS-dependent ACh relaxation of the vessel.

## Discussion

EC Arg1 KO mice showed an increased contractile response to PE. Along with these data, EC Arg1 KO mice showed a significant decrease in eNOS expression in the aorta, as shown by RT-qPCR and western blot analyses. Previous studies have already shown that the inhibition of eNOS or its downstream enzyme sGC causes an increased response towards PE in the aortic rings of rats (Silva et al., 2014), which is consistent with the reduced eNOS expression in the aorta in this study. These results suggest that the lack of Arg1 is accompanied by a compensatory downregulation of eNOS that could potentially affect the response to PE.

It is tempting to speculate that the expression of eNOS and Arg1 is coordinated in ECs. A similar coordination by the hypoxia responsive element has been found between iNOS and Arg1 in ECs (Branco-Price et al., 2012). Interestingly, it has been shown that the hypoxic-response element is a promoter of the human eNOS gene, suggesting the potential for coordinated transcriptional regulation of eNOS and Arg1 (Coulet et al., 2003). This relationship requires further investigation.

### *5.1.2 Preserved NO-metabolites and L-arginine bioavailability in EC Arg1 KO mice*

Based on what is discussed in the literature about the relationship between Arg1 and eNOS, removal of Arg1 from EC was expected to result in changes in NO metabolites in the aorta and plasma as well as an increase in global L-arginine bioavailability.

In the present study, no significant changes were observed in the plasma levels of NO metabolites or in the aorta or other tissues. These results can be explained by a compensatory downregulation of eNOS expression in ECs, which is consistent with preserved levels of L-arginine, L-ornithine, and L-citrulline, as well as a preserved global L-arginine bioavailability in plasma. In the body, other compartments express Arg1 at a higher level, such as hepatocytes or other cells surrounding ECs like vascular smooth muscle cells (Ignarro et al., 2001; Caldwell et al., 2018), which may affect the circulating L-arginine level to a greater extent than Arg1 expressed in the ECs.

Furthermore, the expression of Arg1 in vascular smooth muscle cells may have a greater impact on the maintenance of aortic function than EC Arg1. This is in line with the finding that arginase activity is increased in the aorta of EC Arg1 KO mice, showing a compensatory mechanism of vascular smooth muscle cells.

On the other hand, differences in NO-heme levels between the EC Arg1 KO and littermate controls were found in other organs. A significant increase in NO-heme was found in the liver and, in contrast, decreased NO-heme levels in the lung tissues. This finding suggests that EC Arg1 may play a specific role in different organs of the body. This finding is also in line with the different frequencies of EC in the lung and liver (Crapo et al., 1982; Ding et al., 2016; Schupp et al., 2021). The majority of the cellular composition of the liver consists of hepatocytes (70%).

## Discussion

Non-parenchymal cells, including ECs, make up the remaining 30%, with ECs comprising the largest portion at 50%. However, in the lungs, 30% of all cells are ECs. Therefore, they make up a larger percentage of the total cells in the lungs than in the liver. However, these data also suggest that further organ-specific investigation of the role of EC Arg1 needs to be done in the future.

The hypothesis that Arg1 is a counterpart of NOS enzymes is based on cell culture studies investigating the role of arginase inhibition on NOS activity in macrophages (Hecker et al., 1995; Hey et al., 1997; Tenu et al., 1999). A recent study investigated this relationship and found that Arg1 regulates NOS activity in an experimental setup of finite L-arginine supply due to the consumption of L-arginine by both enzymes (Momma et al., 2022). In the second setup, where L-arginine levels remained constant, arginase inhibition did not affect L-citrulline accumulation. They not only tested this concept in macrophages but also in human umbilical artery endothelial cells with a constant supply of L-arginine. Also, in this case they did not find changes in the activity of NOS before and after arginase inhibition. It is tempting to speculate that Arg1 in ECs limits eNOS only in conditions of L-arginine deficiency, such as reduced L-arginine intake or reduced production, and needs further studies. It is tempting to speculate that Arg1 expressed in other compartments has a greater effect on vascular function or circulating NO metabolites than Arg1 expressed in ECs.

### *5.1.3 Conclusion*

To summarize, these data suggest that Arg1 expressed in ECs plays a minor role in regulating vascular function, levels of NO metabolites, and L-arginine bioavailability under homeostatic conditions.

## 5.2 The lack of red cell Arg1 contributes to circulating NO metabolites in plasma but does not improve vascular function or contribute to cardioprotection after I/R

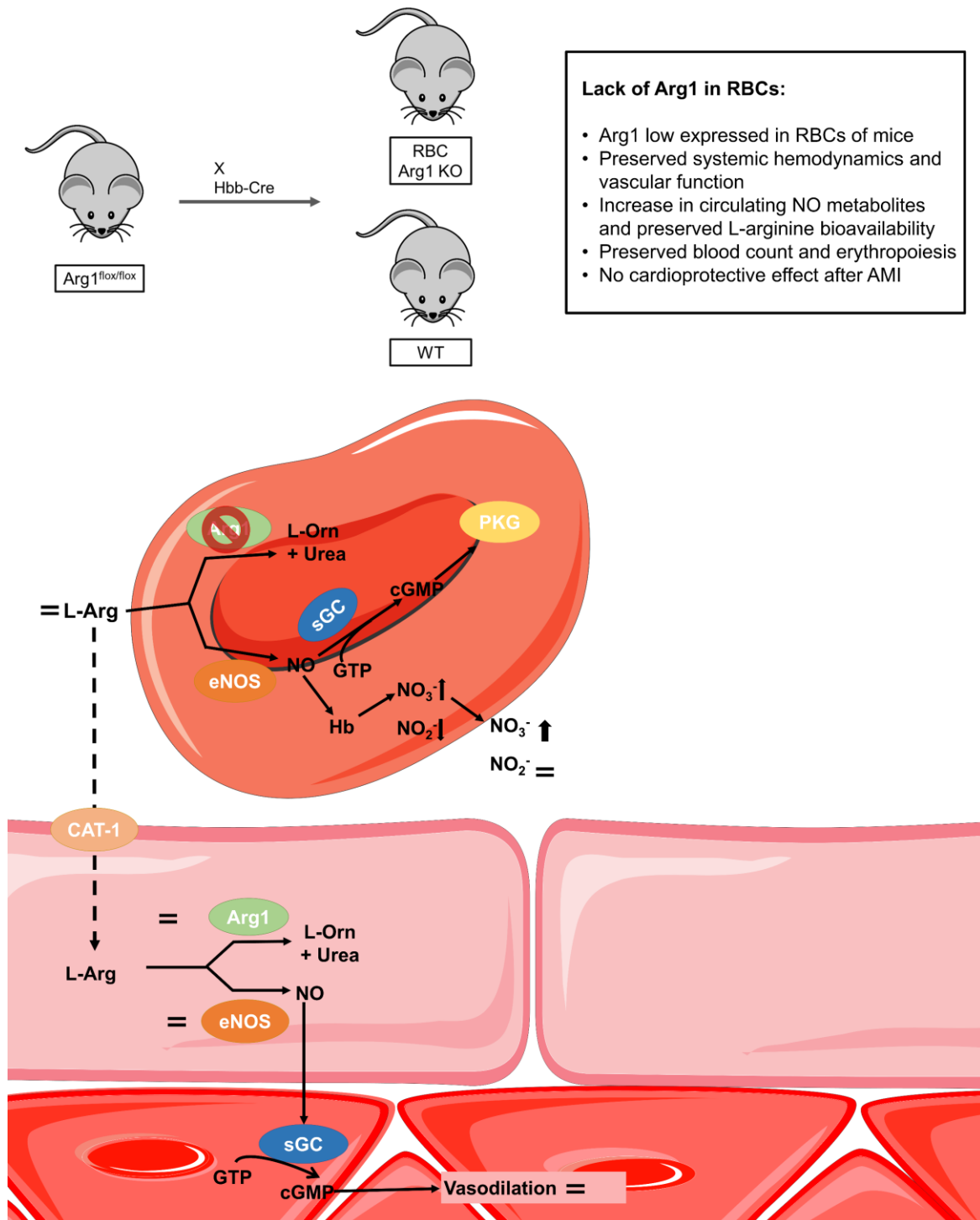


**Figure 23** The lack of red cell Arg1 contributes to circulating nitrate in plasma, but does not improve vascular function or contribute to cardioprotection after I/R. A low expression of Arg1 was found in mouse RBCs as compared to other blood compartments. RBC Arg1 KO mice showed preserved L-arginine bioavailability but an increase in nitrate in plasma, which did not reduce infarct size after I/R injury. Erythroid differentiation was unchanged in RBC Arg1 KO mice compared to WT littermates.

## Discussion

In the second part of the study, RBC-specific Arg1 KO mice were generated by crossing Arg1<sup>flox/flox</sup> mice (El Kasmi et al., 2008) with Hbb-Cre<sup>pos</sup> mice (Peterson et al., 2004), which express Cre-recombinase under the control of the promoter of the human beta hemoglobin chain (Hbb). The Hbb Cre mice generated by Peterson were deeply characterized for their specificity for erythroid cells. The mice carry the LCR- $\beta$ -globin promoter, which restricts the expression of the Cre-recombinase to the erythroid lineage. The specificity of this promoter was investigated using the reporter gene lacZ (Papayannopoulou et al., 2000). So far, this is the most specific Cre-recombinase targeting erythroid cells.

The main finding of this study was that RBCs carry the lowest arginase activity of all blood compartments. Furthermore, RBC Arg1 KO mice showed changes in circulating NO metabolites in plasma but no changes in vascular function or the outcome of I/R injury, as well as no changes in erythroid differentiation.

### *5.2.1 Low Arg1 activity RBCs as compared to WBC and platelets*

This study investigated the role of Arg1 in RBCs. Arginase activity was measured in RBCs and compared to arginase activity in other blood compartments. It was found that RBCs have the lowest arginase activity of all blood cells and that WBC carry the highest arginase activity among blood cells. But also, platelet show a higher arginase activity compared to the RBCs.

Already 40 years ago studies investigating the activity of arginase in RBCs and found high arginase activity in RBCs of humans ( $957 \pm 206 \mu\text{mol urea/g hemoglobin/h}$ ), whereas the activity in rodents was below  $1 \mu\text{mol urea/g hemoglobin/hr}$  (Spector et al., 1985). Later, it was shown that RBCs express Arg1, but not Arg2, and mice express it at a lower level (P. S. Kim et al., 2002; J. Yang et al., 2013).

Previous studies have observed that red cell Arg1 plays a role in sickle cell disease (SCD). An increase in Arg1 activity in RBCs was observed in patients with SCD, which is characterized by a mutation of the  $\beta$ -globin chain that leads to a change in the morphology of RBCs ("sickling"). These RBCs are more fragile (Machogu et al., 2018). Hemolysis in SCD results in the release of free Hb and arginase from RBCs, thus leading to oxidative stress and a decrease in arginine bioavailability due to the consumption of L-arginine by free Arg1. (VanderJagt et al., 1997; Morris et al., 2000; Reiter et al., 2002).

This study showed that the activity of arginase in RBC-ghosts (after leukodepletion and platelet removal) was around the detection limit of the urea assay, which is in line with the early findings of arginase activity in mice (Spector et al., 1985). On the other hand, platelets showed an arginase activity nearly 10 times higher than that found in RBCs, and WBCs showed an even higher activity, around 100 times higher. However, RBC Arg1 KO mice did not show changes in other blood compartments compared to WT controls.

## Discussion

These findings are in line with former studies, showing the expression of Arg1 in macrophages and neutrophils in mice, whereas the expression of Arg1 in humans is limited to neutrophils (Munder et al., 2005). Taken together, these data suggest that Arg1 expression differs between mice and humans. Humans express Arg1 at high levels in RBCs, whereas mice express Arg1 predominantly in WBC and only at low levels in RBCs. Furthermore, it points out the importance of cleaning RBCs from WBC and platelets for the analysis of arginase.

### *5.2.2 L-arginine bioavailability is unchanged but NO metabolites in plasma are changed*

eNOS and Arg1 use L-arginine as a substrate. The bulk of the literature argued that Arg1 in RBCs regulates L-arginine bioavailability and therefore regulates NO biosynthesis from eNOS and regulating nitrate and nitrite levels, similar to what was hypothesized for Arg1 in ECs (Morris et al., 2005; Eligini et al., 2013; J. Yang et al., 2013). In this study, an increase in L-ornithine levels was observed in the plasma of RBC Arg1 KO mice, but no changes in L-arginine, L-citrulline, arginine-ornithine ratio, and L-arginine bioavailability were observed. This indicates that Arg1 from RBCs contributes significantly to the circulating L-ornithine pool. But, it does not have an impact on L-arginine bioavailability.

Interestingly, RBC Arg1 KO mice showed a significant increase in total NO species in plasma and RBC, which is a result of increased nitrate levels. Interestingly, RBC Arg1 KO mice showed a significant decrease in nitrate levels in RBCs, but no changes in nitrite levels in plasma. As shown in the first part of the study, the lack of EC Arg1 did not affect L-arginine bioavailability, but EC Arg1 KO mice also showed downregulation of eNOS in the vessel wall, which makes it complicated to understand the role of EC Arg1 in L-arginine bioavailability.

Previously, the role of Arg1 in RBCs was investigated by using the arginase inhibitor Nor-NOHA and found an increase in nitrate but also in nitrite levels in the supernatant of RBCs (J. Yang et al., 2013).

Notably, a recent study showed that Nor-NOHA can react with riboflavin or H<sub>2</sub>O<sub>2</sub> and release NO-like molecules, such as nitrite (Momma et al., 2020). This shows the limitation of using Nor-NOHA to investigate arginase activity in the presence of riboflavin, which is also present in the plasma and RBCs (Hustad et al., 2002). This would explain the preserved nitrite levels in RBC Arg1 KO mice, but increased nitrite levels after inhibiting arginase in RBCs (J. Yang et al., 2013).

Overall, these data show that the lack of Arg1 in RBCs does not lead to an increase in L-arginine bioavailability but leads to an increase in circulating nitrate.

## Discussion

### 5.2.3 *The lack of Arg1 in RBCs does not affect systemic hemodynamics or vascular function*

Previous studies showed that eNOS expressed in RBC regulates BP independently of eNOS expressed in ECs (Leo et al., 2021). To investigate whether Arg1 from RBCs is involved in the regulation of BP or vascular function, both were analyzed in RBC Arg1 KO mice.

RBC Arg1 KO mice did not show any changes in systemic hemodynamics. In line with this finding, preserved eNOS-dependent vasorelaxation was found, as well as preserved expression of eNOS in the aorta. Furthermore, RBC Arg1 KO mice showed no changes in FMD. These findings are consistent with those of EC Arg1 KO mice, which also did not show changes in eNOS-dependent vasorelaxation or FMD. The preserved vascular function is also in line with the finding of unchanged vascular function in the RBC eNOS KO mice. (Leo et al., 2021). This suggests that Arg1 expressed in RBCs plays a minor role in the regulation of vascular function and regulation of vascular function.

### 5.2.4 *Deletion of Arg1 from RBC is not cardioprotective after AMI*

To investigate whether the deletion of Arg1 from the RBC and the increase in nitrate levels in the plasma affect the outcome of AMI, I/R injury was performed. LV function was measured by echocardiography before and after I/R injury, and the infarct size was analyzed. RBC Arg1 KO mice did not show changes in LV function and infarct size compared to the WT control.

This finding was unexpected. In the past, *ex vivo* studies investigated the role of Arg1 in RBCs in AMI (J. Yang et al., 2013; J. Yang et al., 2018). In this study, blood from humans and mice and RBC suspensions from humans and mice were treated with nor-NOHA, an arginase inhibitor, and the nitrite and nitrate levels in the supernatant were measured. Moreover, they showed in an *ex vivo* myocardial I/R injury model that the inhibition of Arg1 in RBC is cardioprotective by improving LV function.

*Ex vivo* experiments, such as *ex vivo* myocardial ischemia-reperfusion injury models, are highly reproducible and provide information regarding physiological, morphological, and biochemical changes during I/R injury. In the experimental setup, effects from other organs, the systemic circulation, and the nervous system are excluded. This can be seen as an advantage to reveal effects that were covered before, and new potential targets can be found, which need to be tested *in vivo*. *In vivo* I/R injury, on the other hand, also affects other parameters such as CO and systemic hemodynamics. Furthermore, in cases of cell-specific KO models, like shown in this study, the real impact of an enzyme from cell compartment can be investigated with the influence of other organs of the systemic circulation.

Yang et al. showed that arginase inhibition in RBCs led to an increase in nitrate levels in the supernatant of RBCs from mice and an increase in nitrite and nitrate levels in the supernatant



## Discussion

of human RBCs. They hypothesized that the cardioprotective effect is dependent on eNOS and the increase in NO metabolites using eNOS KO mice, which did not show a cardioprotective effect after treatment with Nor-NOHA in RBCs and blood. The cardioprotective effect of eNOS has also been confirmed in RBC eNOS KO and KI mice (Cortese-Krott et al., 2022). In addition, RBC Arg KO mice showed increased nitrate levels.

This study showed that the elevated levels of nitrate in the plasma of RBC Arg1 KO mice did not result in cardioprotection during I/R injury, and the presence of Arg1 in RBCs does not limit the cardioprotective effects of eNOS in RBCs. Additionally, it is important to note that mice have significantly lower arginase activity in RBCs than humans; thus, the lack of cardioprotection in KO mice does not necessarily apply to humans.

### *5.2.5 Arg1 does not play a role in erythroid differentiation*

To investigate whether the lack of Arg1 affects erythroid differentiation, the hematological phenotype was analyzed. RBC Arg1 KO mice did not show any changes in blood count and RBC indices compared to the control. Furthermore, erythroid differentiation in the bone marrow and spleen was preserved, and RBC Arg1 KO mice showed preserved spleen size.

However, the role of Arg1 in erythroid cell differentiation remains largely unknown. It has been demonstrated that the expression of Arg1 is delayed in erythroid progenitors. Its expression is low in proerythroblasts and reaches peak levels in fully developed RBCs (Grzywa et al., 2021). The late expression of Arg1 in erythroid differentiation indicates that Arg1 does not affect erythropoiesis in the early stage of erythroid development, and this study shows that the later stages of erythroid differentiation are not affected by the lack of Arg1 in erythroid cells. Consistent with these findings, L-arginine was shown to be essential for the differentiation of CD34<sup>+</sup> cells into erythroid cells, but not for the survival of erythroid cells (Shima et al., 2006). On the other hand, it was shown that the dose-dependent inhibition of Arg1 in K562 cells by chloroquine or hydroxychloroquine leads to an increase in HbF synthesis (Iyamu et al., 2009).

On the other hand, a decrease in plasma ferritin levels was observed. Ferritin is an indicator of iron status and is essential for erythropoiesis. Reduced ferritin levels are often accompanied by increased transferrin levels. RBC Arg1 KO mice showed preserved transferrin levels. These findings indicate that Arg1 expressed in RBCs somehow affects iron status, but this needs further investigation.

These data suggest that Arg1 expressed in erythroid cells may reduce ferritin levels but does not affect erythroid differentiation under homeostatic conditions.

## Discussion

### 5.2.6 Conclusion

This study revealed that arginase activity in erythrocytes was the lowest among all blood cells, which was an unexpected finding. Moreover, the lack of Arg1 in RBCs led to a decrease in L-ornithine levels in plasma, but did not cause an increase in L-arginine bioavailability. Furthermore, an increase in total NO species was found in RBC and plasma but a decrease in nitrite in RBCs. Contrary to what was expected, the lack of Arg1 did not affect infarct size and LV function after AMI. Additionally, Arg1 is not involved in erythroid differentiation under basal conditions. The regulation of Arg1/eNOS is probably different in RBC, and its expression appears to play a minor role, at least in mice.

### 5.3 Lack of sGC in erythroid cells leads to disrupted erythropoiesis in the bone marrow, which is fully rescued by stress erythropoiesis in the spleen.

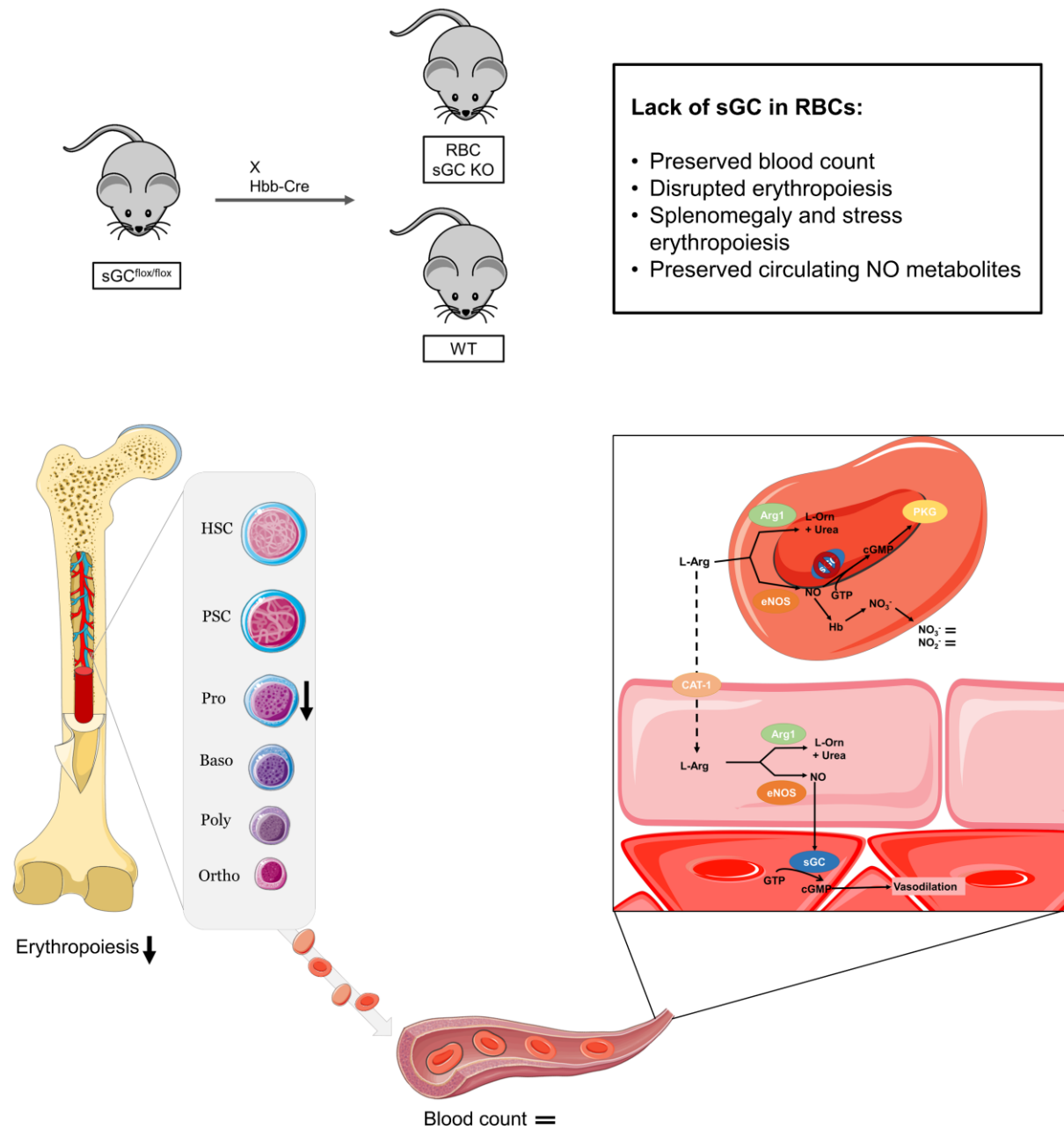


**Figure 24** Lack of sGC in erythroid cells leads to disrupted erythropoiesis in the bone marrow, which is fully rescued by stress erythropoiesis in the spleen. RBC sGC KO mice showed a reduced percentage of proerythroblasts in the bone marrow and reduced BFU-E colonies. Furthermore, splenomegaly and stress erythropoiesis were observed in the spleen of RBC sGC KO mice. Disrupted erythropoiesis in the bone marrow was fully rescued by stress erythropoiesis in the spleen, as shown by the preserved hematocrit.

## Discussion

In the third part of this study, the role of red cell sGC in RBC physiology *in vivo* was investigated. Mice lacking sGC only in RBCs were successfully generated by crossing sGC $\alpha 1^{\text{flox/flox}}$  mice (Mergia et al., 2006) with Hbb-Cre<sup>POS</sup> mice (Peterson et al., 2004). RBC sGC KO mice showed disrupted erythropoiesis in the bone marrow, splenomegaly, stress erythropoiesis in the spleen, and preserved erythrocyte count and hematocrit.

### 5.3.1 sGC in erythroid cells is involved in RBC maturation

The enzyme sGC is expressed in early stage erythroid cells and RBCs (Ikuta et al., 2001; Cortese-Krott et al., 2018), but its function in these cells was largely unknown *in vivo*.

Interestingly, RBC sGC KO mice had a overall decrease in erythropoietic activity in the bone marrow. This phenotype was demonstrated by a decrease in the percentage of erythroid cells counted by Pappenheim-staining of bone marrow specimens and a lower number of proerythroblasts in the bone marrow, as assessed by quantitative analysis of erythroid differentiation by flow cytometry. Moreover, RBC sGC KO mice showed a decrease in BFU-Es in the bone marrow, but all other colonies were unchanged. In these mice, disrupted erythropoiesis was not due to iron deficiency, as transferrin and ferritin levels in plasma were preserved.

Interestingly, no changes in the erythroid differentiation of global sGC KO mice were found, as shown by Pappenheim-staining and flow cytometric analysis of bone marrow cells. The global sGC KO mice did not show changes in BFU-Es, but a significant increase in CFU-GM. To the best of my knowledge, this is the first time an erythroid-specific Cre/LoxP approach has been applied to investigate the role of sGC in erythropoiesis. Previously, studies mainly focused on systemic hemodynamics, platelet activation, and kidney function of global KO models targeting each of the two subunits/isoforms ( $\alpha 1$ ,  $\alpha 2$ ,  $\beta 1$ ) (Mergia et al., 2006; Friebe et al., 2007; Buys et al., 2008). In addition, a cell-specific KO of the  $\beta 1$ -subunit of sGC KO in hematopoietic cells (*Pf4*-Cre recombinase) targeting megakaryocytes and platelets showed the important role of sGC in thrombosis and homeostasis (G. Zhang et al., 2011).

Consistent with these findings, a previous study demonstrated that NO-cGMP signaling promotes erythropoiesis (Ikuta et al., 2016). In this study, mice overexpressing sGC in myeloid and erythroid cells were generated. The mice not only showed an increase in RBCs, hematocrit, and total hemoglobin, but also a decrease in the WBC count. The underlying molecular mechanism involves the activation of lineage-specific transcription factors, such as GATA1 (Ikuta et al., 2016). Furthermore, it was shown that K562 cells show increased expression of  $\gamma$ -globin after treatment with the sGC activator protoporphyrin IX (Ikuta et al., 2001). In addition, they found that erythroid cells expressing  $\gamma$ -globin showed higher sGC activity than cells expressing  $\beta$ -globin. A similar correlation was found in SCD.

## Discussion

Patients with SCD exhibit a notable increase in cGMP in RBCs compared to healthy individuals, which was further increased by treatment with hydroxyurea (Conran et al., 2004). Hydroxyurea is a pharmacological approach to treat SCD by inducing the expression of  $\gamma$ -globin via the activation of sGC in erythroid progenitor cells (Cokic et al., 2008). In addition, the treatment of primary erythroblasts from patients with  $\beta$ -thalassemia with 8-Bromo-cGMP induced an increase in  $\gamma$ -globin (Ikuta et al., 2001).

These findings suggest that sGC expressed in erythroid cells is not only essential for the expression of  $\gamma$ -globin but also for erythroid differentiation in the bone marrow in early stages.

### *5.3.2 Stress erythropoiesis compensates for disrupted erythropoiesis in the bone marrow*

A quite interesting finding was stress erythropoiesis and splenomegaly in RBC sGC KO mice. Specifically, RBCs sGC KO mice showed splenomegaly, which was characterized by an increase in the spleen/body weight ratio. Furthermore, an increase in BFU-E colonies was found in the spleen of RBC sGC KO mice compared to WT controls. Moreover, an increase in nucleate erythroid cells was observed in the spleen of RBC sGC KO mice.

The spleen is an essential organ that filters blood and eliminates dysfunctional RBCs. It also has the ability to produce new RBCs and take over erythropoiesis in cases of blood loss or stress caused by diseases (H. Li et al., 2021). The main causes of splenomegaly in humans are hematological disorders such as leukemia and primary myelofibrosis (O'Reilly, 1998).

In the past, it has been shown that global PKG KO mice show anemia and splenomegaly (Foller et al., 2008). The anemia found in the global PKG KO mouse was characterized by intravascular hemolysis, increased reticulocytes, and an increase in EPO levels. The RBC sGC KO mice generated by us did not show any of these characteristics. However, RBC sGC KO mice showed splenomegaly, which correlated with the observation of stress erythropoiesis in the spleen and a fully preserved hematocrit and RBC count. Thus, the spleen compensates for disrupted erythropoiesis in the bone marrow. In addition, RBC sGC KO mice showed preserved EPO levels in plasma.

In contrast to steady-state erythropoiesis, which is regulated by EPO, stress erythropoiesis is regulated by proteins such as BMP4 and hedgehog, whose expression is induced by hypoxia (Hattangadi et al., 2011; Ji, 2020).

Interestingly, global sGC KO mice did not show changes in the spleen/body weight ratio, as well as no changes in the number of BFU-E colonies in the spleen, but a significant increase in CFU-GM colonies was found in the spleen of global sGC KO mice similar to what was observed in the bone marrow.

## Discussion

Moreover, a blood count in RBC sGC KO mice, global sGC KO mice, and WT littermates was carried out. RBC sGC KO mice did not show any changes in the numbers/indices of RBCs, WBCs, and platelets. In contrast, the lack of sGC in all tissues led to an increase in MCV and a decrease in leukocytes, as well as an increase in neutrophils and monocytes. Furthermore, a preserved reticulocyte count was observed in both mouse lines compared to that in their control groups. This finding indicates that global sGC KO mice show neutrophilia driven by an increase in granulopoiesis, as shown by an increased number of CFU-GM in the bone marrow and spleen. An increase in the neutrophils count can be caused by chronic inflammation or cardiovascular inflammation (Naeim, 2018; Silvestre-Roig et al., 2020). The hematological phenotype displayed by global sGC KO mice appears to be an indication of a chronic inflammation, which covers the real hematological phenotype shown in the RBCs sGC KO mice.

These findings suggest that the regulation of steady-state erythropoiesis differs from that of stress erythropoiesis. While red cell sGC appear to be essential for erythropoiesis in the bone marrow, erythropoiesis in the spleen can occur without the presence of sGC in erythroid cells. As a result, the spleen is capable of entirely compensating for disrupted erythropoiesis in the bone marrow.

### 5.3.3 *The levels of NO metabolites did not change in RBCs and plasma*

Furthermore, NO metabolites in tissues, cells, and plasma of RBC sGC KO mice and WT littermates were measured. Interestingly, RBC sGC KO mice did not show any changes in NO metabolites in RBCs or plasma. RBC eNOS KO mice showed a significant decrease in NO-heme, but no change in RBC nitrite and nitrate. But significant decrease in nitrate and nitrite levels in the plasma of RBC eNOS KO mice (Leo et al., 2021). These findings suggest that NO produced by eNOS in RBCs is converted to NO-heme and plays a major role in the modulation of circulating NO metabolites in the plasma. RBC GC KO mice showed preserved NO metabolites in RBCs and plasma, suggesting that NO generated by eNOS in RBCs is mostly converted into NO-heme in RBC, or nitrate and nitrite, which diffuse into plasma. It is tempting to speculate that sGC in RBC is not the direct target of eNOS from RBCs or that only a minor part of NO produced by eNOS activates sGC. Interestingly, a significant decrease in nitrite levels in the aorta, as well as in the liver was found in RBC sGC KO mice. In contrast, mice showed a significant increase in nitrite levels in the lungs. Indicating that sGC in RBCs may affect NO metabolites production *in vivo*.

### 5.3.4 *Conclusion*

The removal of sGC from RBCs leads to disrupted erythropoiesis in the early stages. This disrupted erythropoiesis is fully compensated by stress erythropoiesis in the spleen, as

## Discussion

reflected by the preserved RBC count and hematocrit. Furthermore, the lack of sGC does not affect circulating NO metabolites. Taken together, sGC in RBCs plays an important role in erythroid differentiation in the bone marrow.

## 6 Summary & perspective

The aim of this study was to investigate the Arg1/eNOS/sGC signaling pathway in RBCs *in vivo* using transgenic mice models. EC and RBC Arg1 KO and RBC sGC KO mice were generated and characterized. This study had three major findings. The analysis of both EC- and RBC Arg1 KO mice showed that the relationship between Arg1 and eNOS in EC and RBCs is different than argued before. Lack of EC Arg1 leads to downregulation of eNOS and increased vascular contractility but does not affect vascular dilation under homeostatic conditions. On the other hand, Arg1 in RBCs showed the lowest activity in all blood compartments and did not affect the regulation of vascular function, L-arginine bioavailability, and erythroid differentiation. In addition, this study demonstrated that sGC plays an important role in erythroid differentiation in the bone marrow and is compensated by stress erythropoiesis in the spleen. Thus, these data indicate that *de novo* synthesis of erythrocytes is differently regulated when it occurs in the bone marrow or spleen, as proerythroblasts are formed in the spleens of RBC sGC KO mice with the same efficiency as in WT mice.

Specifically, EC Arg1 KO mice and RBC Arg1 KO mice showed preserved vascular function and systemic hemodynamics, as well as preserved L-arginine bioavailability. The lack of Arg1 in ECs led to downregulation of eNOS expression in the aorta, which did not affect circulating NO metabolites or eNOS-dependent vasorelaxation. It is tempting to speculate that the downregulation of eNOS is due to a coordinated regulation of Arg1 and eNOS gene expression in ECs, but this must be verified in further studies.

In contrast, the lack of Arg1 in RBC Arg1 KO did not affect the expression of eNOS in the aorta, but led to an increase in nitrate levels in plasma and RBCs and a decrease in nitrite levels in RBCs, with no effect on vascular function. Furthermore, the lack of Arg in RBCs did not affect the outcomes after AMI. It is important to note that this study showed that RBCs exhibit the lowest arginase activity of all blood compartments, different from human RBCs, indicating that Arg1 expressed in RBCs plays a minor role in arginase activity in the blood of mice.

Furthermore, this study investigated the role of the Arg1/eNOS/sGC pathway in erythroid differentiation. The lack of Arg1 in erythroid cells had only a minor effect on erythroid differentiation; only ferritin levels were reduced. On the other hand, the data demonstrated that sGC plays a key role in erythroid differentiation in the bone marrow. RBC sGC KO mice showed reduced BFU-Es and proerythroblasts in the bone marrow, indicating that sGC expressed in erythroid cells is essential in the early stage of steady-state erythropoiesis in the bone marrow. Interestingly, the study showed that RBC sGC KO mice exhibit stress erythropoiesis, which is defined by an increase in spleen size, nucleated erythroid cells, and BFU-Es in the spleen. Stress-erythropoiesis fully compensates for disrupted steady-state



## Summary & perspective

erythropoiesis, as shown by the normal blood count. Therefore, sGC in erythroid cells plays a major role in the regulation of erythropoiesis in the bone marrow, but not in the spleen. This phenotype was not observed in global sGC KO mice.

To the best of my knowledge this is the first study that investigated specifically the role of Arg1 and sGC in RBC using cell-specific KO mice. It is important to note that these findings are limited to rodents and cannot be directly applied to humans.

Cell-specific KO models are state-of-the-art for unmasking the role of enzymes in physiological processes occurring in a specific cell compartment. As shown in the sGC KO models, the effects of sGC on erythropoiesis were compensated/masked by a predominant pro-inflammatory phenotype with increased CFU-GMs. A limitation of our study was the relatively small sample size of global sGC KO mice. Future studies with larger sample sizes are needed to confirm our findings and further elucidate the role of sGC in this pathway.

Further studies on these mouse lines will reveal how the Arg1/eNOS/sGC pathway affects erythropoiesis and cardiovascular hemostasis.

The two Arg1 KO lines offered valuable insights into the function of Arg1 under homeostatic conditions. In particular, the conditional tamoxifen-inducible EC Arg1 KO model may be used to investigate the involvement of Arg1 in different diseases without the influence of a compensatory mechanism from aging or other tissues.

Currently, sGC is used as a target for the treatment of diseases such as heart failure and pulmonary arterial hypertension. The results obtained in RBC sGC KO and others (Ikuta et al., 2016) show a potential new therapeutic use of sGC as a target for anemia, but further human studies are required to confirm the role of sGC in human erythropoiesis.

Overall, the study of the role of signaling pathways in RBCs and their effects on hematology and cardiovascular physiology may reveal new regulatory pathways linking them and pharmacological targets for the cure of these diseases.

## 7 References

- Akashi, K., Traver, D., Miyamoto, T., & Weissman, I. L. (2000). A clonogenic common myeloid progenitor that gives rise to all myeloid lineages. *Nature*, *404*(6774), 193-197. doi:10.1038/35004599
- Angermeier, E., Domes, K., Lukowski, R., Schlossmann, J., Rathkolb, B., Angelis, M. H., & Hofmann, F. (2016). Iron deficiency anemia in cyclic GMP kinase knockout mice. *Haematologica*, *101*(2), e48-51. doi:10.3324/haematol.2015.137026
- Arnold, W. P., Mittal, C. K., Katsuki, S., & Murad, F. (1977). Nitric oxide activates guanylate cyclase and increases guanosine 3':5'-cyclic monophosphate levels in various tissue preparations. *Proc Natl Acad Sci U S A*, *74*(8), 3203-3207. doi:10.1073/pnas.74.8.3203
- Atochin, D. N., Yuzawa, I., Li, Q., Rauwerdink, K. M., Malhotra, R., Chang, J., Brouckaert, P., Ayata, C., Moskowitz, M. A., Bloch, K. D., Huang, P. L., & Buys, E. S. (2010). Soluble guanylate cyclase alpha1beta1 limits stroke size and attenuates neurological injury. *Stroke*, *41*(8), 1815-1819. doi:10.1161/STROKEAHA.109.577635
- Bagnost, T., Ma, L., da Silva, R. F., Rezakhaniha, R., Houdayer, C., Stergiopoulos, N., Andre, C., Guillaume, Y., Berthelot, A., & Demougeot, C. (2010). Cardiovascular effects of arginase inhibition in spontaneously hypertensive rats with fully developed hypertension. *Cardiovasc Res*, *87*(3), 569-577. doi:10.1093/cvr/cvq081
- Beaulieu, M., Levesque, E., Tchernof, A., Beatty, B. G., Belanger, A., & Hum, D. W. (1997). Chromosomal localization, structure, and regulation of the UGT2B17 gene, encoding a C19 steroid metabolizing enzyme. *DNA Cell Biol*, *16*(10), 1143-1154. doi:10.1089/dna.1997.16.1143
- Beltran-Povea, A., Caballano-Infantes, E., Salguero-Aranda, C., Martin, F., Soria, B., Bedoya, F. J., Tejedo, J. R., & Cahuana, G. M. (2015). Role of nitric oxide in the maintenance of pluripotency and regulation of the hypoxia response in stem cells. *World J Stem Cells*, *7*(3), 605-617. doi:10.4252/wjsc.v7.i3.605
- Bhatta, A., Yao, L., Xu, Z., Toque, H. A., Chen, J., Atawia, R. T., Fouda, A. Y., Bagi, Z., Lucas, R., Caldwell, R. B., & Caldwell, R. W. (2017). Obesity-induced vascular dysfunction and arterial stiffening requires endothelial cell arginase 1. *Cardiovasc Res*, *113*(13), 1664-1676. doi:10.1093/cvr/cvx164
- Bloch, W., Fleischmann, B. K., Lorke, D. E., Andressen, C., Hops, B., Hescheler, J., & Addicks, K. (1999). Nitric oxide synthase expression and role during cardiomyogenesis. *Cardiovasc Res*, *43*(3), 675-684. doi:10.1016/s0008-6363(99)00160-1
- Branco-Price, C., Zhang, N., Schnelle, M., Evans, C., Katschinski, D. M., Liao, D., Ellies, L., & Johnson, R. S. (2012). Endothelial cell HIF-1alpha and HIF-2alpha differentially regulate metastatic success. *Cancer Cell*, *21*(1), 52-65. doi:10.1016/j.ccr.2011.11.017

## References

- Bryan, N. S., Rassaf, T., Maloney, R. E., Rodriguez, C. M., Saijo, F., Rodriguez, J. R., & Feelisch, M. (2004). Cellular targets and mechanisms of nitros(yl)ation: an insight into their nature and kinetics in vivo. *Proc Natl Acad Sci U S A*, *101*(12), 4308-4313. doi:10.1073/pnas.0306706101
- Butler, J., Usman, M. S., Anstrom, K. J., Blaustein, R. O., Bonaca, M. P., Ezekowitz, J. A., Freitas, C., Lam, C. S. P., Lewis, E. F., Lindenfeld, J., McMullan, C. J., Mentz, R. J., O'Connor, C., Rosano, G. M. C., Saldarriaga, C. I., Senni, M., Udelson, J., Voors, A. A., & Zannad, F. (2022). Soluble guanylate cyclase stimulators in patients with heart failure with reduced ejection fraction across the risk spectrum. *Eur J Heart Fail*, *24*(11), 2029-2036. doi:10.1002/ejhf.2720
- Buyts, E. S., Sips, P., Vermeersch, P., Raher, M. J., Rogge, E., Ichinose, F., Dewerchin, M., Bloch, K. D., Janssens, S., & Brouckaert, P. (2008). Gender-specific hypertension and responsiveness to nitric oxide in sGC $\alpha$ 1 knockout mice. *Cardiovasc Res*, *79*(1), 179-186. doi:10.1093/cvr/cvn068
- Caldwell, R. W., Rodriguez, P. C., Toque, H. A., Narayanan, S. P., & Caldwell, R. B. (2018). Arginase: A Multifaceted Enzyme Important in Health and Disease. *Physiol Rev*, *98*(2), 641-665. doi:10.1152/physrev.00037.2016
- Chang, C. I., Liao, J. C., & Kuo, L. (1998). Arginase modulates nitric oxide production in activated macrophages. *Am J Physiol*, *274*(1), H342-348. doi:10.1152/ajpheart.1998.274.1.H342
- Chen, L., Wang, J., Liu, J., Wang, H., Hillyer, C. D., Blanc, L., An, X., & Mohandas, N. (2021). Dynamic changes in murine erythropoiesis from birth to adulthood: implications for the study of murine models of anemia. *Blood Adv*, *5*(1), 16-25. doi:10.1182/bloodadvances.2020003632
- Chennupati, R., Meens, M. J., Janssen, B. J., van Dijk, P., Hakvoort, T. B. M., Lamers, W. H., De Mey, J. G. R., & Koehler, S. E. (2018). Deletion of endothelial arginase 1 does not improve vasomotor function in diabetic mice. *Physiol Rep*, *6*(11), e13717. doi:10.14814/phy2.13717
- Cinelli, M. A., Do, H. T., Miley, G. P., & Silverman, R. B. (2020). Inducible nitric oxide synthase: Regulation, structure, and inhibition. *Med Res Rev*, *40*(1), 158-189. doi:10.1002/med.21599
- Cokic, V. P., Andric, S. A., Stojilkovic, S. S., Noguchi, C. T., & Schechter, A. N. (2008). Hydroxyurea nitrosylates and activates soluble guanylyl cyclase in human erythroid cells. *Blood*, *111*(3), 1117-1123. doi:10.1182/blood-2007-05-088732
- Cokic, V. P., Smith, R. D., Beleslin-Cokic, B. B., Njoroge, J. M., Miller, J. L., Gladwin, M. T., & Schechter, A. N. (2003). Hydroxyurea induces fetal hemoglobin by the nitric oxide-

## References

- dependent activation of soluble guanylyl cyclase. *J Clin Invest*, *111*(2), 231-239. doi:10.1172/JCI16672
- Conran, N., Oresco-Santos, C., Acosta, H. C., Fattori, A., Saad, S. T., & Costa, F. F. (2004). Increased soluble guanylate cyclase activity in the red blood cells of sickle cell patients. *Br J Haematol*, *124*(4), 547-554. doi:10.1111/j.1365-2141.2004.04810.x
- Cortese-Krott, M. M., Mergia, E., Kramer, C. M., Luckstadt, W., Yang, J., Wolff, G., Panknin, C., Bracht, T., Sitek, B., Pernow, J., Stasch, J. P., Feelisch, M., Koesling, D., & Kelm, M. (2018). Identification of a soluble guanylate cyclase in RBCs: preserved activity in patients with coronary artery disease. *Redox Biol*, *14*, 328-337. doi:10.1016/j.redox.2017.08.020
- Cortese-Krott, M. M., Suvorava, T., Leo, F., Heuser, S. K., LoBue, A., Li, J., Becher, S., Schneckmann, R., Srivastava, T., Erkens, R., Wolff, G., Schmitt, J. P., Grandoch, M., Lundberg, J. O., Pernow, J., Isakson, B. E., Weitzberg, E., & Kelm, M. (2022). Red blood cell eNOS is cardioprotective in acute myocardial infarction. *Redox Biol*, *54*, 102370. doi:10.1016/j.redox.2022.102370
- Coulet, F., Nadaud, S., Agrapart, M., & Soubrier, F. (2003). Identification of hypoxia-response element in the human endothelial nitric-oxide synthase gene promoter. *J Biol Chem*, *278*(47), 46230-46240. doi:10.1074/jbc.M305420200
- Crapo, J. D., Barry, B. E., Gehr, P., Bachofen, M., & Weibel, E. R. (1982). Cell number and cell characteristics of the normal human lung. *Am Rev Respir Dis*, *126*(2), 332-337. doi:10.1164/arrd.1982.126.2.332
- Ding, C., Li, Y., Guo, F., Jiang, Y., Ying, W., Li, D., Yang, D., Xia, X., Liu, W., Zhao, Y., He, Y., Li, X., Sun, W., Liu, Q., Song, L., Zhen, B., Zhang, P., Qian, X., Qin, J., & He, F. (2016). A Cell-type-resolved Liver Proteome. *Mol Cell Proteomics*, *15*(10), 3190-3202. doi:10.1074/mcp.M116.060145
- El Kasmi, K. C., Qualls, J. E., Pesce, J. T., Smith, A. M., Thompson, R. W., Henao-Tamayo, M., Basaraba, R. J., Konig, T., Schleicher, U., Koo, M. S., Kaplan, G., Fitzgerald, K. A., Tuomanen, E. I., Orme, I. M., Kanneganti, T. D., Bogdan, C., Wynn, T. A., & Murray, P. J. (2008). Toll-like receptor-induced arginase 1 in macrophages thwarts effective immunity against intracellular pathogens. *Nat Immunol*, *9*(12), 1399-1406. doi:10.1038/ni.1671
- Eligini, S., Porro, B., Lualdi, A., Squellerio, I., Veglia, F., Chiorino, E., Crisci, M., Garlasche, A., Giovannardi, M., Werba, J. P., Tremoli, E., & Cavalca, V. (2013). Nitric oxide synthetic pathway in red blood cells is impaired in coronary artery disease. *PLOS ONE*, *8*(8), e66945. doi:10.1371/journal.pone.0066945
- Erkens, R., Kramer, C. M., Luckstadt, W., Panknin, C., Krause, L., Weidenbach, M., Dirzka, J., Krenz, T., Mergia, E., Suvorava, T., Kelm, M., & Cortese-Krott, M. M. (2015). Left

## References

- ventricular diastolic dysfunction in Nrf2 knock out mice is associated with cardiac hypertrophy, decreased expression of SERCA2a, and preserved endothelial function. *Free Radic Biol Med*, 89, 906-917. doi:10.1016/j.freeradbiomed.2015.10.409
- Erkens, R., Suvorava, T., Sutton, T. R., Fernandez, B. O., Mikus-Lelinska, M., Barbarino, F., Flogel, U., Kelm, M., Feelisch, M., & Cortese-Krott, M. M. (2018). Nrf2 Deficiency Unmasks the Significance of Nitric Oxide Synthase Activity for Cardioprotection. *Oxid Med Cell Longev*, 2018, 8309698. doi:10.1155/2018/8309698
- Farah, C., Michel, L. Y. M., & Balligand, J. L. (2018). Nitric oxide signalling in cardiovascular health and disease. *Nat Rev Cardiol*, 15(5), 292-316. doi:10.1038/nrcardio.2017.224
- Ferreira, W. A., Jr., Chweih, H., Lanaro, C., Almeida, C. B., Brito, P. L., Gotardo, E. M. F., Torres, L., Miguel, L. I., Franco-Penteado, C. F., Leonardo, F. C., Garcia, F., Saad, S. T. O., Frenette, P. S., Brockschneider, D., Costa, F. F., Stasch, J. P., Sandner, P., & Conran, N. (2020). Beneficial Effects of Soluble Guanylyl Cyclase Stimulation and Activation in Sickle Cell Disease Are Amplified by Hydroxyurea: In Vitro and In Vivo Studies. *J Pharmacol Exp Ther*, 374(3), 469-478. doi:10.1124/jpet.119.264606
- Foller, M., Feil, S., Ghoreschi, K., Koka, S., Gerling, A., Thunemann, M., Hofmann, F., Schuler, B., Vogel, J., Pichler, B., Kasinathan, R. S., Nicolay, J. P., Huber, S. M., Lang, F., & Feil, R. (2008). Anemia and splenomegaly in cGKI-deficient mice. *Proc Natl Acad Sci U S A*, 105(18), 6771-6776. doi:10.1073/pnas.0708940105
- Frankenreiter, S., Bednarczyk, P., Kniess, A., Bork, N. I., Straubinger, J., Koprowski, P., Wrzosek, A., Mohr, E., Logan, A., Murphy, M. P., Gawaz, M., Krieg, T., Szewczyk, A., Nikolaev, V. O., Ruth, P., & Lukowski, R. (2017). cGMP-Elevating Compounds and Ischemic Conditioning Provide Cardioprotection Against Ischemia and Reperfusion Injury via Cardiomyocyte-Specific BK Channels. *Circulation*, 136(24), 2337-2355. doi:10.1161/CIRCULATIONAHA.117.028723
- Friebe, A., Mergia, E., Dangel, O., Lange, A., & Koesling, D. (2007). Fatal gastrointestinal obstruction and hypertension in mice lacking nitric oxide-sensitive guanylyl cyclase. *Proc Natl Acad Sci U S A*, 104(18), 7699-7704. doi:10.1073/pnas.0609778104
- Furchgott, R. F., Cherry, P. D., Zawadzki, J. V., & Jothianandan, D. (1984). Endothelial cells as mediators of vasodilation of arteries. *J Cardiovasc Pharmacol*, 6 Suppl 2, S336-343. doi:10.1097/00005344-198406002-00008
- Furchgott, R. F., & Zawadzki, J. V. (1980). The obligatory role of endothelial cells in the relaxation of arterial smooth muscle by acetylcholine. *Nature*, 288(5789), 373-376. doi:10.1038/288373a0
- Ghofrani, H. A., Galie, N., Grimminger, F., Grunig, E., Humbert, M., Jing, Z. C., Keogh, A. M., Langleben, D., Kilama, M. O., Fritsch, A., Neuser, D., Rubin, L. J., & Group, P.-S.

## References

- (2013). Riociguat for the treatment of pulmonary arterial hypertension. *N Engl J Med*, 369(4), 330-340. doi:10.1056/NEJMoa1209655
- Godecke, A., Decking, U. K., Ding, Z., Hirchenhain, J., Bidmon, H. J., Godecke, S., & Schrader, J. (1998). Coronary hemodynamics in endothelial NO synthase knockout mice. *Circ Res*, 82(2), 186-194. doi:10.1161/01.res.82.2.186
- Gogiraju, R., Renner, L., Bochenek, M. L., Zifkos, K., Molitor, M., Danckwardt, S., Wenzel, P., Munzel, T., Konstantinides, S., & Schafer, K. (2022). Arginase-1 Deletion in Erythrocytes Promotes Vascular Calcification via Enhanced GSNOR (S-Nitrosoglutathione Reductase) Expression and NO Signaling in Smooth Muscle Cells. *Arterioscler Thromb Vasc Biol*, 42(12), e291-e310. doi:10.1161/ATVBAHA.122.318338
- Gotting, M., & Nikinmaa, M. (2015). More than hemoglobin - the unexpected diversity of globins in vertebrate red blood cells. *Physiol Rep*, 3(2)doi:10.14814/phy2.12284
- Grzywa, T. M., Nowis, D., & Golab, J. (2021). The role of CD71(+) erythroid cells in the regulation of the immune response. *Pharmacol Ther*, 228, 107927. doi:10.1016/j.pharmthera.2021.107927
- Hattangadi, S. M., Wong, P., Zhang, L., Flygare, J., & Lodish, H. F. (2011). From stem cell to red cell: regulation of erythropoiesis at multiple levels by multiple proteins, RNAs, and chromatin modifications. *Blood*, 118(24), 6258-6268. doi:10.1182/blood-2011-07-356006
- Hecker, M., Nematollahi, H., Hey, C., Busse, R., & Racke, K. (1995). Inhibition of arginase by NG-hydroxy-L-arginine in alveolar macrophages: implications for the utilization of L-arginine for nitric oxide synthesis. *FEBS Lett*, 359(2-3), 251-254. doi:10.1016/0014-5793(95)00039-c
- Heuser, S. K., LoBue, A., Li, J., Zhuge, Z., Leo, F., Suvorava, T., Olsson, A., Schneckmann, R., Guimaraes Braga, D. D., Srivastava, T., Montero, L., Schmitz, O. J., Schmitt, J. P., Grandoch, M., Weitzberg, E., Lundberg, J. O., Pernow, J., Kelm, M., Carlstrom, M., & Cortese-Krott, M. M. (2022). Downregulation of eNOS and preserved endothelial function in endothelial-specific arginase 1-deficient mice. *Nitric Oxide*, 125-126, 69-77. doi:10.1016/j.niox.2022.06.004
- Hevel, J. M., White, K. A., & Marletta, M. A. (1991). Purification of the inducible murine macrophage nitric oxide synthase. Identification as a flavoprotein. *J Biol Chem*, 266(34), 22789-22791.
- Hey, C., Boucher, J. L., Vadon-Le Goff, S., Ketterer, G., Wessler, I., & Racke, K. (1997). Inhibition of arginase in rat and rabbit alveolar macrophages by N omega-hydroxy-D,L-indospicine, effects on L-arginine utilization by nitric oxide synthase. *Br J Pharmacol*, 121(3), 395-400. doi:10.1038/sj.bjp.0701143

## References

- Hu, J., Liu, J., Xue, F., Halverson, G., Reid, M., Guo, A., Chen, L., Raza, A., Galili, N., Jaffray, J., Lane, J., Chasis, J. A., Taylor, N., Mohandas, N., & An, X. (2013). Isolation and functional characterization of human erythroblasts at distinct stages: implications for understanding of normal and disordered erythropoiesis in vivo. *Blood*, *121*(16), 3246-3253. doi:10.1182/blood-2013-01-476390
- Hustad, S., McKinley, M. C., McNulty, H., Schneede, J., Strain, J., Scott, J. M., & Ueland, P. M. (2002). Riboflavin, Flavin Mononucleotide, and Flavin Adenine Dinucleotide in Human Plasma and Erythrocytes at Baseline and after Low-Dose Riboflavin Supplementation. *Clinical Chemistry*, *48*(9), 1571-1577. doi:10.1093/clinchem/48.9.1571
- Ignarro, L. J., Buga, G. M., Wei, L. H., Bauer, P. M., Wu, G., & del Soldato, P. (2001). Role of the arginine-nitric oxide pathway in the regulation of vascular smooth muscle cell proliferation. *Proc Natl Acad Sci U S A*, *98*(7), 4202-4208. doi:10.1073/pnas.071054698
- Ignarro, L. J., Buga, G. M., Wood, K. S., Byrns, R. E., & Chaudhuri, G. (1987). Endothelium-derived relaxing factor produced and released from artery and vein is nitric oxide. *Proc Natl Acad Sci U S A*, *84*(24), 9265-9269. doi:10.1073/pnas.84.24.9265
- Ikuta, T., Ausenda, S., & Cappellini, M. D. (2001). Mechanism for fetal globin gene expression: role of the soluble guanylate cyclase-cGMP-dependent protein kinase pathway. *Proc Natl Acad Sci U S A*, *98*(4), 1847-1852. doi:10.1073/pnas.98.4.1847
- Ikuta, T., Sellak, H., Odo, N., Adekile, A. D., & Gaensler, K. M. (2016). Nitric Oxide-cGMP Signaling Stimulates Erythropoiesis through Multiple Lineage-Specific Transcription Factors: Clinical Implications and a Novel Target for Erythropoiesis. *PLOS ONE*, *11*(1), e0144561. doi:10.1371/journal.pone.0144561
- Iyamu, E., Perdew, H., & Woods, G. (2009). Growth inhibitory and differentiation effects of chloroquine and its analogue on human leukemic cells potentiate fetal hemoglobin production by targeting the polyamine pathway. *Biochem Pharmacol*, *77*(6), 1021-1028. doi:10.1016/j.bcp.2008.11.016
- Jelkmann, W. (2016). Erythropoietin. *Front Horm Res*, *47*, 115-127. doi:10.1159/000445174
- Ji, P. (2020). Finding erythroid stress progenitors: cell surface markers revealed. *Haematologica*, *105*(11), 2499-2501. doi:10.3324/haematol.2020.262493
- Johnstone, S. R., Kroncke, B. M., Straub, A. C., Best, A. K., Dunn, C. A., Mitchell, L. A., Peskova, Y., Nakamoto, R. K., Koval, M., Lo, C. W., Lampe, P. D., Columbus, L., & Isakson, B. E. (2012). MAPK phosphorylation of connexin 43 promotes binding of cyclin E and smooth muscle cell proliferation. *Circ Res*, *111*(2), 201-211. doi:10.1161/CIRCRESAHA.112.272302

## References

- Kim, J. H., Bugaj, L. J., Oh, Y. J., Bivalacqua, T. J., Ryoo, S., Soucy, K. G., Santhanam, L., Webb, A., Camara, A., Sikka, G., Nyhan, D., Shoukas, A. A., Ilies, M., Christianson, D. W., Champion, H. C., & Berkowitz, D. E. (2009). Arginase inhibition restores NOS coupling and reverses endothelial dysfunction and vascular stiffness in old rats. *J Appl Physiol (1985)*, *107*(4), 1249-1257. doi:10.1152/jappphysiol.91393.2008
- Kim, P. S., Iyer, R. K., Lu, K. V., Yu, H., Karimi, A., Kern, R. M., Tai, D. K., Cederbaum, S. D., & Grody, W. W. (2002). Expression of the liver form of arginase in erythrocytes. *Molecular genetics and metabolism*, *76*(2), 100-110. doi:10.1016/s1096-7192(02)00034-3
- Kleinbongard, P., Schulz, R., Rassaf, T., Lauer, T., Dejam, A., Jax, T., Kumara, I., Gharini, P., Kabanova, S., Ozuyaman, B., Schnurch, H. G., Godecke, A., Weber, A. A., Robenek, M., Robenek, H., Bloch, W., Rosen, P., & Kelm, M. (2006). Red blood cells express a functional endothelial nitric oxide synthase. *Blood*, *107*(7), 2943-2951. doi:10.1182/blood-2005-10-3992
- Kucukkaya, B., Ozturk, G., & Yalcintepe, L. (2006). Nitric oxide levels during erythroid differentiation in K562 cell line. *Indian J Biochem Biophys*, *43*(4), 251-253.
- Lee, J., Dey, S., Rajvanshi, P. K., Merling, R. K., Teng, R., Rogers, H. M., & Noguchi, C. T. (2023). Neuronal nitric oxide synthase is required for erythropoietin stimulated erythropoiesis in mice. *Front Cell Dev Biol*, *11*, 1144110. doi:10.3389/fcell.2023.1144110
- Lenox, L. E., Perry, J. M., & Paulson, R. F. (2005). BMP4 and Madh5 regulate the erythroid response to acute anemia. *Blood*, *105*(7), 2741-2748. doi:10.1182/blood-2004-02-0703
- Lenox, L. E., Shi, L., Hegde, S., & Paulson, R. F. (2009). Extramedullary erythropoiesis in the adult liver requires BMP-4/Smad5-dependent signaling. *Exp Hematol*, *37*(5), 549-558. doi:10.1016/j.exphem.2009.01.004
- Leo, F., Suvorava, T., Heuser, S. K., Li, J., LoBue, A., Barbarino, F., Piragine, E., Schneckmann, R., Hutzler, B., Good, M. E., Fernandez, B. O., Vornholz, L., Rogers, S., Doctor, A., Grandoch, M., Stegbauer, J., Weitzberg, E., Feelisch, M., Lundberg, J. O., Isakson, B. E., Kelm, M., & Cortese-Krott, M. M. (2021). Red Blood Cell and Endothelial eNOS Independently Regulate Circulating Nitric Oxide Metabolites and Blood Pressure. *Circulation*, *144*(11), 870-889. doi:10.1161/CIRCULATIONAHA.120.049606
- Li, H., Liu, Z. L., Lu, L., Buffet, P., & Karniadakis, G. E. (2021). How the spleen reshapes and retains young and old red blood cells: A computational investigation. *PLoS Comput Biol*, *17*(11), e1009516. doi:10.1371/journal.pcbi.1009516



## References

- Li, W., Guo, R., Song, Y., & Jiang, Z. (2020). Erythroblastic Island Macrophages Shape Normal Erythropoiesis and Drive Associated Disorders in Erythroid Hematopoietic Diseases. *Front Cell Dev Biol*, *8*, 613885. doi:10.3389/fcell.2020.613885
- Liao, C., Hardison, R. C., Kennett, M. J., Carlson, B. A., Paulson, R. F., & Prabhu, K. S. (2018). Selenoproteins regulate stress erythroid progenitors and spleen microenvironment during stress erythropoiesis. *Blood*, *131*(23), 2568-2580. doi:10.1182/blood-2017-08-800607
- Liu, J., Zhang, J., Ginzburg, Y., Li, H., Xue, F., De Franceschi, L., Chasis, J. A., Mohandas, N., & An, X. (2013). Quantitative analysis of murine terminal erythroid differentiation in vivo: novel method to study normal and disordered erythropoiesis. *Blood*, *121*(8), e43-49. doi:10.1182/blood-2012-09-456079
- Livak, K. J., & Schmittgen, T. D. (2001). Analysis of relative gene expression data using real-time quantitative PCR and the 2<sup>-</sup>(Delta Delta C(T)) Method. *Methods*, *25*(4), 402-408. doi:10.1006/meth.2001.1262
- Lundberg, J. O., & Weitzberg, E. (2022). Nitric oxide signaling in health and disease. *Cell*, *185*(16), 2853-2878. doi:10.1016/j.cell.2022.06.010
- Machogu, E. M., & Machado, R. F. (2018). How I treat hypoxia in adults with hemoglobinopathies and hemolytic disorders. *Blood*, *132*(17), 1770-1780. doi:10.1182/blood-2018-03-818195
- Mahdi, A., Kovamees, O., & Pernow, J. (2020). Improvement in endothelial function in cardiovascular disease - Is arginase the target? *Int J Cardiol*, *301*, 207-214. doi:10.1016/j.ijcard.2019.11.004
- Mayer, B., John, M., & Bohme, E. (1990). Purification of a Ca<sup>2+</sup>/calmodulin-dependent nitric oxide synthase from porcine cerebellum. Cofactor-role of tetrahydrobiopterin. *FEBS Lett*, *277*(1-2), 215-219. doi:10.1016/0014-5793(90)80848-d
- McCann Haworth, S. M., Zhuge, Z., Nihlen, C., Von Rosen, M. F., Weitzberg, E., Lundberg, J. O., Krmar, R. T., Nasiell, J., & Carlstrom, M. (2021). Red blood cells from patients with pre-eclampsia induce endothelial dysfunction. *J Hypertens*, *39*(8), 1628-1641. doi:10.1097/HJH.0000000000002834
- Mergia, E., Friebe, A., Dangel, O., Russwurm, M., & Koesling, D. (2006). Spare guanylyl cyclase NO receptors ensure high NO sensitivity in the vascular system. *J Clin Invest*, *116*(6), 1731-1737. doi:10.1172/JCI27657
- Mergia, E., Russwurm, M., Zoidl, G., & Koesling, D. (2003). Major occurrence of the new alpha2beta1 isoform of NO-sensitive guanylyl cyclase in brain. *Cell Signal*, *15*(2), 189-195. doi:10.1016/s0898-6568(02)00078-5
- Mergia, E., Thieme, M., Hoch, H., Daniil, G., Hering, L., Yakoub, M., Scherbaum, C. R., Rump, L. C., Koesling, D., & Stegbauer, J. (2018). Impact of the NO-Sensitive Guanylyl

## References

- Cyclase 1 and 2 on Renal Blood Flow and Systemic Blood Pressure in Mice. *Int J Mol Sci*, 19(4)doi:10.3390/ijms19040967
- Miki, N., Kawabe, Y., & Kuriyama, K. (1977). Activation of cerebral guanylate cyclase by nitric oxide. *Biochem Biophys Res Commun*, 75(4), 851-856. doi:10.1016/0006-291x(77)91460-7
- Mohan, S., Reddick, R. L., Musi, N., Horn, D. A., Yan, B., Prihoda, T. J., Natarajan, M., & Abboud-Werner, S. L. (2008). Diabetic eNOS knockout mice develop distinct macro- and microvascular complications. *Lab Invest*, 88(5), 515-528. doi:10.1038/labinvest.2008.23
- Momma, T. Y., & Ottaviani, J. I. (2020). Arginase inhibitor, N(omega)-hydroxy-L-norarginine, spontaneously releases biologically active NO-like molecule: Limitations for research applications. *Free Radic Biol Med*, 152, 74-82. doi:10.1016/j.freeradbiomed.2020.02.033
- Momma, T. Y., & Ottaviani, J. I. (2022). There is no direct competition between arginase and nitric oxide synthase for the common substrate L-arginine. *Nitric Oxide*, 129, 16-24. doi:10.1016/j.niox.2022.09.002
- Moncada, S., Palmer, R. M., & Higgs, E. A. (1991). Nitric oxide: physiology, pathophysiology, and pharmacology. *Pharmacol Rev*, 43(2), 109-142.
- Monticelli, L. A., Buck, M. D., Flamar, A. L., Saenz, S. A., Tait Wojno, E. D., Yudanin, N. A., Osborne, L. C., Hepworth, M. R., Tran, S. V., Rodewald, H. R., Shah, H., Cross, J. R., Diamond, J. M., Cantu, E., Christie, J. D., Pearce, E. L., & Artis, D. (2016). Arginase 1 is an innate lymphoid-cell-intrinsic metabolic checkpoint controlling type 2 inflammation. *Nat Immunol*, 17(6), 656-665. doi:10.1038/ni.3421
- Moretti, C., Zhuge, Z., Zhang, G., Haworth, S. M., Paulo, L. L., Guimaraes, D. D., Cruz, J. C., Montenegro, M. F., Cordero-Herrera, I., Braga, V. A., Weitzberg, E., Carlstrom, M., & Lundberg, J. O. (2019). The obligatory role of host microbiota in bioactivation of dietary nitrate. *Free Radic Biol Med*, 145, 342-348. doi:10.1016/j.freeradbiomed.2019.10.003
- Morris, C. R., Kato, G. J., Poljakovic, M., Wang, X., Blackwelder, W. C., Sachdev, V., Hazen, S. L., Vichinsky, E. P., Morris, S. M., Jr., & Gladwin, M. T. (2005). Dysregulated arginine metabolism, hemolysis-associated pulmonary hypertension, and mortality in sickle cell disease. *JAMA*, 294(1), 81-90. doi:10.1001/jama.294.1.81
- Morris, C. R., Kuypers, F. A., Larkin, S., Vichinsky, E. P., & Styles, L. A. (2000). Patterns of arginine and nitric oxide in patients with sickle cell disease with vaso-occlusive crisis and acute chest syndrome. *J Pediatr Hematol Oncol*, 22(6), 515-520. doi:10.1097/00043426-200011000-00009
- Munder, M., Mollinedo, F., Calafat, J., Canchado, J., Gil-Lamaignere, C., Fuentes, J. M., Luckner, C., Doschko, G., Soler, G., Eichmann, K., Muller, F. M., Ho, A. D., Goerner,

## References

- M., & Modolell, M. (2005). Arginase I is constitutively expressed in human granulocytes and participates in fungicidal activity. *Blood*, *105*(6), 2549-2556. doi:10.1182/blood-2004-07-2521
- Naeim, F. (2018). *Atlas of hematopathology : morphology, immunophenotype, cytogenetics, and molecular approaches* (2nd edition. edn). Waltham, MA: Elsevier.
- Nagasaka, Y., Buys, E. S., Spagnolli, E., Steinbicker, A. U., Hayton, S. R., Rauwerdink, K. M., Brouckaert, P., Zapol, W. M., & Bloch, K. D. (2011). Soluble guanylate cyclase-alpha1 is required for the cardioprotective effects of inhaled nitric oxide. *Am J Physiol Heart Circ Physiol*, *300*(4), H1477-1483. doi:10.1152/ajpheart.00948.2010
- Nimmegeers, S., Sips, P., Buys, E., Brouckaert, P., & Van de Voorde, J. (2007). Functional role of the soluble guanylyl cyclase alpha(1) subunit in vascular smooth muscle relaxation. *Cardiovasc Res*, *76*(1), 149-159. doi:10.1016/j.cardiores.2007.06.002
- Nobes, P. R., & Carter, A. B. (1990). Reticulocyte counting using flow cytometry. *J Clin Pathol*, *43*(8), 675-678. doi:10.1136/jcp.43.8.675
- O'Reilly, R. A. (1998). Splenomegaly in 2,505 patients in a large university medical center from 1913 to 1995. 1913 to 1962: 2,056 patients. *West J Med*, *169*(2), 78-87.
- Old, J. (2013). Hemoglobinopathies and Thalassemias. In D. Rimoin, R. Pyeritz, & B. Korf (Eds.), *Emery and Rimoin's Principles and Practice of Medical Genetics*, (pp. 1-44). Oxford: Academic Press.
- Palis, J. (2014). Primitive and definitive erythropoiesis in mammals. *Front Physiol*, *5*, 3. doi:10.3389/fphys.2014.00003
- Palis, J., Robertson, S., Kennedy, M., Wall, C., & Keller, G. (1999). Development of erythroid and myeloid progenitors in the yolk sac and embryo proper of the mouse. *Development*, *126*(22), 5073-5084. doi:10.1242/dev.126.22.5073
- Papayannopoulou, T., Priestley, G. V., Rohde, A., Peterson, K. R., & Nakamoto, B. (2000). Hemopoietic lineage commitment decisions: in vivo evidence from a transgenic mouse model harboring micro LCR-beta<sub>pro</sub>-LacZ as a transgene. *Blood*, *95*(4), 1274-1282.
- Paulson, R. F., Hariharan, S., & Little, J. A. (2020). Stress erythropoiesis: definitions and models for its study. *Exp Hematol*, *89*, 43-54 e42. doi:10.1016/j.exphem.2020.07.011
- Payne, S., De Val, S., & Neal, A. (2018). Endothelial-Specific Cre Mouse Models. *Arterioscler Thromb Vasc Biol*, *38*(11), 2550-2561. doi:10.1161/ATVBAHA.118.309669
- Perry, J. M., Harandi, O. F., & Paulson, R. F. (2007). BMP4, SCF, and hypoxia cooperatively regulate the expansion of murine stress erythroid progenitors. *Blood*, *109*(10), 4494-4502. doi:10.1182/blood-2006-04-016154
- Perry, J. M., Harandi, O. F., Porayette, P., Hegde, S., Kannan, A. K., & Paulson, R. F. (2009). Maintenance of the BMP4-dependent stress erythropoiesis pathway in the murine

## References

- spleen requires hedgehog signaling. *Blood*, 113(4), 911-918. doi:10.1182/blood-2008-03-147892
- Perutz, M. F. (1960). Structure of hemoglobin. *Brookhaven Symp Biol*, 13, 165-183.
- Peterson, K. R., Fedosyuk, H., Zelenchuk, L., Nakamoto, B., Yannaki, E., Stamatoyannopoulos, G., Ciciotte, S., Peters, L. L., Scott, L. M., & Papayannopoulou, T. (2004). Transgenic Cre expression mice for generation of erythroid-specific gene alterations. *Genesis*, 39(1), 1-9. doi:10.1002/gene.20020
- Pollock, J. S., Forstermann, U., Mitchell, J. A., Warner, T. D., Schmidt, H. H., Nakane, M., & Murad, F. (1991). Purification and characterization of particulate endothelium-derived relaxing factor synthase from cultured and native bovine aortic endothelial cells. *Proc Natl Acad Sci U S A*, 88(23), 10480-10484. doi:10.1073/pnas.88.23.10480
- Reiter, C. D., Wang, X., Tanus-Santos, J. E., Hogg, N., Cannon, R. O., 3rd, Schechter, A. N., & Gladwin, M. T. (2002). Cell-free hemoglobin limits nitric oxide bioavailability in sickle-cell disease. *Nat Med*, 8(12), 1383-1389. doi:10.1038/nm1202-799
- Russwurm, M., Behrends, S., Harteneck, C., & Koesling, D. (1998). Functional properties of a naturally occurring isoform of soluble guanylyl cyclase. *Biochem J*, 335 ( Pt 1)(Pt 1), 125-130. doi:10.1042/bj3350125
- Schupp, J. C., Adams, T. S., Cosme, C., Jr., Raredon, M. S. B., Yuan, Y., Omote, N., Poli, S., Chioccioli, M., Rose, K. A., Manning, E. P., Sauler, M., Deluliis, G., Ahangari, F., Neumark, N., Habermann, A. C., Gutierrez, A. J., Bui, L. T., Lafyatis, R., Pierce, R. W., Meyer, K. B., Nawijn, M. C., Teichmann, S. A., Banovich, N. E., Kropski, J. A., Niklason, L. E., Pe'er, D., Yan, X., Homer, R. J., Rosas, I. O., & Kaminski, N. (2021). Integrated Single-Cell Atlas of Endothelial Cells of the Human Lung. *Circulation*, 144(4), 286-302. doi:10.1161/CIRCULATIONAHA.120.052318
- Shima, Y., Maeda, T., Aizawa, S., Tsuboi, I., Kobayashi, D., Kato, R., & Tamai, I. (2006). L-arginine import via cationic amino acid transporter CAT1 is essential for both differentiation and proliferation of erythrocytes. *Blood*, 107(4), 1352-1356. doi:10.1182/blood-2005-08-3166
- Silva, B. R., Pernomian, L., Grando, M. D., & Bendhack, L. M. (2014). Phenylephrine activates eNOS Ser 1177 phosphorylation and nitric oxide signaling in renal hypertensive rat aorta. *Eur J Pharmacol*, 738, 192-199. doi:10.1016/j.ejphar.2014.05.040
- Silvestre-Roig, C., Braster, Q., Ortega-Gomez, A., & Soehnlein, O. (2020). Neutrophils as regulators of cardiovascular inflammation. *Nat Rev Cardiol*, 17(6), 327-340. doi:10.1038/s41569-019-0326-7
- Singh, R. P., Grinenko, T., Ramasz, B., Franke, K., Lesche, M., Dahl, A., Gassmann, M., Chavakis, T., Henry, I., & Wielockx, B. (2018). Hematopoietic Stem Cells but Not Multipotent Progenitors Drive Erythropoiesis during Chronic Erythroid Stress in EPO

## References

- Transgenic Mice. *Stem Cell Reports*, 10(6), 1908-1919. doi:10.1016/j.stemcr.2018.04.012
- Sorensen, I., Adams, R. H., & Gossler, A. (2009). DLL1-mediated Notch activation regulates endothelial identity in mouse fetal arteries. *Blood*, 113(22), 5680-5688. doi:10.1182/blood-2008-08-174508
- Spector, E. B., Rice, S. C., Kern, R. M., Hendrickson, R., & Cederbaum, S. D. (1985). Comparison of arginase activity in red blood cells of lower mammals, primates, and man: evolution to high activity in primates. *Am J Hum Genet*, 37(6), 1138-1145.
- Stauss, H. M., Godecke, A., Mrowka, R., Schrader, J., & Persson, P. B. (1999). Enhanced blood pressure variability in eNOS knockout mice. *Hypertension*, 33(6), 1359-1363. doi:10.1161/01.hyp.33.6.1359
- Stephenson, J. R., Axelrad, A. A., McLeod, D. L., & Shreeve, M. M. (1971). Induction of colonies of hemoglobin-synthesizing cells by erythropoietin in vitro. *Proc Natl Acad Sci U S A*, 68(7), 1542-1546. doi:10.1073/pnas.68.7.1542
- Suresh, S., Rajvanshi, P. K., & Noguchi, C. T. (2019). The Many Facets of Erythropoietin Physiologic and Metabolic Response. *Front Physiol*, 10, 1534. doi:10.3389/fphys.2019.01534
- Tejedo, J. R., Tapia-Limonchi, R., Mora-Castilla, S., Cahuana, G. M., Hmadcha, A., Martin, F., Bedoya, F. J., & Soria, B. (2010). Low concentrations of nitric oxide delay the differentiation of embryonic stem cells and promote their survival. *Cell Death Dis*, 1(10), e80. doi:10.1038/cddis.2010.57
- Tenu, J. P., Lepoivre, M., Moali, C., Brollo, M., Mansuy, D., & Boucher, J. L. (1999). Effects of the new arginase inhibitor N(omega)-hydroxy-nor-L-arginine on NO synthase activity in murine macrophages. *Nitric Oxide*, 3(6), 427-438. doi:10.1006/niox.1999.0255
- Toque, H. A., Nunes, K. P., Rojas, M., Bhatta, A., Yao, L., Xu, Z., Romero, M. J., Webb, R. C., Caldwell, R. B., & Caldwell, R. W. (2013). Arginase 1 mediates increased blood pressure and contributes to vascular endothelial dysfunction in deoxycorticosterone acetate-salt hypertension. *Front Immunol*, 4, 219. doi:10.3389/fimmu.2013.00219
- Tsiftoglou, A. S. (2021). Erythropoietin (EPO) as a Key Regulator of Erythropoiesis, Bone Remodeling and Endothelial Transdifferentiation of Multipotent Mesenchymal Stem Cells (MSCs): Implications in Regenerative Medicine. *Cells*, 10(8)doi:10.3390/cells10082140
- VanderJagt, D. J., Kanellis, G. J., Isichei, C., Patuszyn, A., & Glew, R. H. (1997). Serum and urinary amino acid levels in sickle cell disease. *J Trop Pediatr*, 43(4), 220-225. doi:10.1093/tropej/43.4.220
- Waugh, R. E., McKenney, J. B., Bauserman, R. G., Brooks, D. M., Valeri, C. R., & Snyder, L. M. (1997). Surface area and volume changes during maturation of reticulocytes in the

## References

- circulation of the baboon. *J Lab Clin Med*, 129(5), 527-535. doi:10.1016/s0022-2143(97)90007-x
- Wood, K. C., Cortese-Krott, M. M., Kovacic, J. C., Noguchi, A., Liu, V. B., Wang, X., Raghavachari, N., Boehm, M., Kato, G. J., Kelm, M., & Gladwin, M. T. (2013). Circulating blood endothelial nitric oxide synthase contributes to the regulation of systemic blood pressure and nitrite homeostasis. *Arterioscler Thromb Vasc Biol*, 33(8), 1861-1871. doi:10.1161/ATVBAHA.112.301068
- Yang, J., Gonon, A. T., Sjoquist, P. O., Lundberg, J. O., & Pernow, J. (2013). Arginase regulates red blood cell nitric oxide synthase and export of cardioprotective nitric oxide bioactivity. *Proc Natl Acad Sci U S A*, 110(37), 15049-15054. doi:10.1073/pnas.1307058110
- Yang, J., Zheng, X., Mahdi, A., Zhou, Z., Tratsiakovich, Y., Jiao, T., Kiss, A., Kovamees, O., Alvarsson, M., Catrina, S. B., Lundberg, J. O., Brismar, K., & Pernow, J. (2018). Red Blood Cells in Type 2 Diabetes Impair Cardiac Post-Ischemic Recovery Through an Arginase-Dependent Modulation of Nitric Oxide Synthase and Reactive Oxygen Species. *JACC Basic Transl Sci*, 3(4), 450-463. doi:10.1016/j.jacbts.2018.03.006
- Yang, Y. M., Huang, A., Kaley, G., & Sun, D. (2009). eNOS uncoupling and endothelial dysfunction in aged vessels. *Am J Physiol Heart Circ Physiol*, 297(5), H1829-1836. doi:10.1152/ajpheart.00230.2009
- Yao, L., Bhatta, A., Xu, Z., Chen, J., Toque, H. A., Chen, Y., Xu, Y., Bagi, Z., Lucas, R., Huo, Y., Caldwell, R. B., & Caldwell, R. W. (2017). Obesity-induced vascular inflammation involves elevated arginase activity. *Am J Physiol Regul Integr Comp Physiol*, 313(5), R560-R571. doi:10.1152/ajpregu.00529.2016
- Zhang, C., Hein, T. W., Wang, W., Chang, C. I., & Kuo, L. (2001). Constitutive expression of arginase in microvascular endothelial cells counteracts nitric oxide-mediated vasodilatory function. *FASEB J*, 15(7), 1264-1266. doi:10.1096/fj.00-0681fje
- Zhang, G., Xiang, B., Dong, A., Skoda, R. C., Daugherty, A., Smyth, S. S., Du, X., & Li, Z. (2011). Biphasic roles for soluble guanylyl cyclase (sGC) in platelet activation. *Blood*, 118(13), 3670-3679. doi:10.1182/blood-2011-03-341107
- Zhang, H., Wang, S., Liu, D., Gao, C., Han, Y., Guo, X., Qu, X., Li, W., Zhang, S., Geng, J., Zhang, L., Mendelson, A., Yazdanbakhsh, K., Chen, L., & An, X. (2021). EpoR-tdTomato-Cre mice enable identification of EpoR expression in subsets of tissue macrophages and hematopoietic cells. *Blood*, 138(20), 1986-1997. doi:10.1182/blood.2021011410
- Zhang, H. D., Ma, Y. J., Liu, Q. F., Ye, T. Z., Meng, F. Y., Zhou, Y. W., Yu, G. P., Yang, J. P., Jiang, H., Wang, Q. S., Li, G. P., Ji, Y. Q., Zhu, G. L., Du, L. T., & Ji, K. M. (2018).

## References

- Human erythrocyte lifespan measured by Levitt's CO breath test with newly developed automatic instrument. *J Breath Res*, 12(3), 036003. doi:10.1088/1752-7163/aaacf1
- Zimring, J. C. (2020). Turning over a new leaf on turning over RBCs. *Blood*, 136(14), 1569-1570. doi:10.1182/blood.2020008463

## 8 Acknowledgment

My first and big thanks go to Prof. Dr. Miriam Cortese-Krott, who made this dissertation possible for me. She not only trusted me with this project but also gave me the opportunity to follow my ideas, encouraged me to develop my scientific thinking, and supported me in the face of challenges. She always had an open ear, helped me with any challenges I faced, and helped me solve them with her scientific and personal experience. She also gave me the opportunity to present my research at international conferences, where I gained valuable experience for my life.

I also want to thank Prof. Dr. Axel Gödecke for his mentorship and revision of my doctoral thesis. I want to thank him as the speaker of the IRTG1902. The IRTG1902 gave me the opportunity to meet other Ph.D. students and to start with collaborations. It supported scientific exchange and enabled me to participate in training courses from HHU and abroad. Dr. Sandra Berger was always available and ready to help with any problems.

Furthermore, I would like to thank Prof. Matthias Carlström, PhD, and his entire lab for supporting this thesis by performing the experiments. Especially Zhengbing Zhuge, PhD, for performing myography, and Annika Olsson to perform Arginase ELISA in the Aorta.

Furthermore, I would like to thank Dr. Tatsiana Suvorava, Dr. Francesca Leo, Julia Hocks and Stefanie Becher for the performance of I/R injury, measurement of systemic hemodynamics and caring out echocardiography.

I also want to thank Prof. Brant E. Isakson PhD, from the university of Virginia for carrying out the TEM-imaging.

Furthermore, thanks go to Prof. Dr. Germing and Ron-Patrick Cadeddu from the Department of Hematology at the UKD. For the stimulating discussions and the support in understanding the hematological phenotypes. I would like to thank Birgitte Kalmutzke for the Pappenheim-staining analysis.

I would like to thank my two colleagues, Anthea Lo Bue M. Sc. and Dr. Junjie Li. They have not only helped me on the scientific side, in measuring NO metabolites and L-arginine metabolites and carrying out western blots, and in the discussions on results, but they have also always been very good friends by my side. They have been emotional support all the years, with whom I could share any problems and fears, who have always been by my side and supported me in every way, and with whom even stressful days ended with a smile. You have made this a great, funny, and unforgettable time.

Finally, I would like to thank my family and friends.



## Acknowledgment

I would like to thank my friends, who were by my side all the time, listening to my conversations about my research or just having a beer with me after long days, and my boyfriend, who motivated me all the time.

My greatest thanks go to my family. Without the support of my parents and sister, I would not be where I am now. They have always supported me and believed in me when I couldn't do it myself. With them on my side, I know I can achieve anything I want in my life.

## 9 Publication & Manuscripts

Parts of this dissertation were already published in peer-reviewed scientific journals and presented on scientific conferences

### Original publications:

1. Zhuge Z, McCann Haworth S, Nihlen C, Carvalho L, **Heuser SK**, Kleschyov AL, Nasiell J, Cortese-Krott MM, Weitzberg E, Lundberg JO, et al. Red blood cells from endothelial nitric oxide synthase-deficient mice induce vascular dysfunction involving oxidative stress and endothelial arginase I. *Redox Biol.* 2023;60:102612. doi: 10.1016/j.redox.2023.102612

Contribution: executed experiments, calculated results, drafted figure.

2. **Heuser SK**, LoBue A, Li J, Zhuge Z, Leo F, Suvorava T, Olsson A, Schneckmann R, Guimaraes Braga DD, Srivastava T, et al. Downregulation of eNOS and preserved endothelial function in endothelial-specific arginase 1-deficient mice. *Nitric Oxide.* 2022;125-126:69-77. doi: 10.1016/j.niox.2022.06.004

Contribution: Executed experiments, calculated results, prepared figure, wrote manuscript.

3. Cortese-Krott MM, Suvorava T, Leo F, **Heuser SK**, LoBue A, Li J, Becher S, Schneckmann R, Srivastava T, Erkens R, et al. Red blood cell eNOS is cardioprotective in acute myocardial infarction. *Redox Biol.* 2022;54:102370. doi: 10.1016/j.redox.2022.102370

Contribution: Executed experiments, calculated results, prepared figure, edited manuscript.

4. Leo\* F, Suvorava\* T, **Heuser SK**, Li J, LoBue A, Barbarino F, Piragine E, Schneckmann R, Hutzler B, Good ME, et al. Red blood cell and endothelial eNOS independently regulate circulating nitric oxide metabolites and blood pressure. *Circulation.* 2021;144:870-889. doi: 10.1161/CIRCULATIONAHA.120.049606

Contribution: Executed experiments, calculated results, prepared figure, edited manuscript.

**Reviews:**

1. Li J, LoBue A, **Heuser SK**, Cortese-Krott MM. Determination of Nitric Oxide and Its Metabolites in Biological Tissues Using Ozone-Based Chemiluminescence Detection: A State-of-the-Art Review. *Antioxidants (Basel)*. 2024;13. doi: 10.3390/antiox1302017

Contribution: Writing one chapter of the manuscript, supporting correction and revision of the text

2. LoBue A, **Heuser SK**, Lindemann M, Li J, Rahman M, Kelm M, Stegbauer J, Cortese-Krott MM. Red blood cell eNOS: a major player in regulating cardiovascular health. *British Journal of Pharmacology*.n/a. doi: <https://doi.org/10.1111/bph.16230>

Contribution: Writing one chapter of the manuscript, supporting correction and revision of the text

3. Li\* J, LoBue\* A, **Heuser SK**, Leo F, Cortese-Krott MM. Using diaminofluoresceins (DAFs) in nitric oxide research. *Nitric Oxide*. 2021;115:44-54. doi: 10.1016/j.niox.2021.07.002

Contribution: Writing subchapter, correction and revision of the text

## 10 Curriculum Vitae

### Personal Characteristics

---

First Name	Sophia Katharina
Family Name	Heuser
Date of Birth	October 2 <sup>th</sup> , 1994
Place of Birth	Bonn
Nationality	Germany

### Education

---

02/2019	<b>PhD candidate at Heinrich-Heine-University, Düsseldorf</b>  Clinic of Cardiology, Polemology and angiology  Myocardial Infarction Research Laboratory  Title of PhD thesis:  The role of the Arg1/eNOS/sGC pathway in red blood cell physiology in vivo
04/2022-present	Membership of iGRAD – Interdisciplinary Graduate and Research Academy Düsseldorf
05/2021--present	Associated Member of IRTG 1902
12/2019	License to practice as a pharmacist
05/2019-10/2019	6-month research practicum in the Wich research lab, University of New South Wales, Sydney, Australia (practical year)
11/2018-04/2019	6-month practicum in the Hecht Apotheke, Mainz, Germany
2013-2018	Study of Pharmacy, Faculty of Pharmacy, Johanne-Gutenberg-University, Mainz, Germany
2005-2013	Rodenkirchen Gymnasium, Cologne, Germany

### Supervision of graduated students and teaching responsibilities

---

2019	Supervision of an exchange student from America founded by the DAAD-RISE program
------	--

## Curriculum Vitae

From 2019                      Teacher/Lecturer “Arginases and arginase Assay” in Master Module “Pharmaceutical biotechnology” and Molecular Oncology of the Master in Molecular Medicine, Medical Faculty, HHU

### Participation in international conferences

---

12-17.02.2023                      Ventura, US: Gordon Research Conference: Nitric Oxide  
  
Oral presentation: Erythroid specific knock out of soluble guanylate cyclase leads to disrupted erythropoiesis, anemia and splenomegaly in mice

11.-12.02.2023                      Ventura, US. Gordon Research Seminar: Nitric Oxide  
  
Poster Presentation: Erythroid specific knock out of soluble guanylate cyclase leads to disrupted erythropoiesis, anemia and splenomegaly in mice

28.10.-01.11.2022                      Sendai, Japan: Redox Week 2022  
  
Oral Presentation: Erythroid specific knock out of soluble guanylate cyclase leads to disrupted erythropoiesis, anemia and splenomegaly in mice

01-02.06.2021                      Düsseldorf, Germany: Cardiovascular Disease (CaVaD) Symposium 2021  
  
Poster Presentation: Lack of sGC in erythrocytes is leading to anemia and cardiac dysfunction

### Honors

---

2022                                      Travel Award for the Nitric Oxid Week in Sendai for the Raising star session

2023                                      Short Talk Award Gordon Research Conference – Nitric Oxid